Northumbria Research Link

Citation: El, Gennady (2021) Soliton gas in integrable dispersive hydrodynamics. Journal of Statistical Mechanics: Theory and Experiment, 2021 (11). p. 114001. ISSN 1742-5468

Published by: IOP Publishing

URL: https://doi.org/10.1088/1742-5468/ac0f6d <https://doi.org/10.1088/1742-5468/ac0f6d>

This version was downloaded from Northumbria Research Link: https://nrl.northumbria.ac.uk/id/eprint/46877/

Northumbria University has developed Northumbria Research Link (NRL) to enable users to access the University's research output. Copyright © and moral rights for items on NRL are retained by the individual author(s) and/or other copyright owners. Single copies of full items can be reproduced, displayed or performed, and given to third parties in any format or medium for personal research or study, educational, or not-for-profit purposes without prior permission or charge, provided the authors, title and full bibliographic details are given, as well as a hyperlink and/or URL to the original metadata page. The content must not be changed in any way. Full items must not be sold commercially in any format or medium without formal permission of the copyright holder. The full policy is available online: http://nrl.northumbria.ac.uk/policies.html

This document may differ from the final, published version of the research and has been made available online in accordance with publisher policies. To read and/or cite from the published version of the research, please visit the publisher's website (a subscription may be required.)

Northumbria University NEWCASTLE

UniversityLibrary

Journal of Statistical Mechanics:
Theory and Experiment

SISSA

PAPER • OPEN ACCESS

Soliton gas in integrable dispersive hydrodynamics

To cite this article: Gennady A El *J. Stat. Mech.* (2021) 114001

View the article online for updates and enhancements.

You may also like

- Towards thermodynamics of solitons: cooling
Soeren Rutz and Fedor Mitschke
- Integrability and nonlinear phenomena
David Gómez-Ullate, Sara Lombardo, Manuel Mañas et al.
- Statistical equilibrium of the Korteweg–de Vries and Benjamin–Ono unidirectional soliton models
Brett Altschul

IOP ebooks™

Bringing together innovative digital publishing with leading authors from the global scientific community.

Start exploring the collection–download the first chapter of every title for free.

This content was downloaded from IP address 212.219.26.61 on 25/11/2021 at 15:23

OPEN ACCESS

Journal of Statistical Mechanics: Theory and Experiment
An IOP and SISSA journal

PAPER: Generalized Hydrodynamics

Soliton gas in integrable dispersive hydrodynamics

Gennady A El*

Department of Mathematics, Physics and Electrical Engineering, Northumbria University, Newcastle upon Tyne, NE1 8ST, United Kingdom
E-mail: gennady.el@northumbria.ac.uk

Received 9 April 2021
Accepted for publication 20 June 2021
Published 2 November 2021

Online at stacks.iop.org/JSTAT/2021/114001
https://doi.org/10.1088/1742-5468/ac0f6d

Abstract. We review the spectral theory of soliton gases in integrable dispersive hydrodynamic systems. We first present a phenomenological approach based on the consideration of phase shifts in pairwise soliton collisions and leading to the kinetic equation for a non-equilibrium soliton gas. Then, a more detailed theory is presented in which soliton gas dynamics are modelled by a thermodynamic type limit of modulated finite-gap spectral solutions of the Korteweg–de Vries and the focusing nonlinear Schrödinger (NLS) equations. For the focusing NLS equation the notions of soliton condensate and breather gas are introduced that are related to the phenomena of spontaneous modulational instability and the rogue wave formation. The integrability properties of the kinetic equation for soliton gas are discussed and some physically relevant solutions are presented and compared with direct numerical simulations of dispersive hydrodynamic systems.

Keywords: nonlinear dynamics, classical integrability, non-linear Schroedinger equation

*Author to whom any correspondence should be addressed.

Original content from this work may be used under the terms of the Creative Commons Attribution 4.0 licence. Any further distribution of this work must maintain attribution to the author(s) and the title of the work, journal citation and DOI.

© 2021 The Author(s).
Published on behalf of SISSA Medialab srl by IOP Publishing Ltd

1742-5468/21/114001+69$33.00

Contents

J. Stat. Mech. (2021) 114001

1. Introduction

1.1. Integrable turbulence and soliton gas

Random nonlinear dispersive waves have been the subject of active research in nonlinear physics for more than five decades, most notably in the context of water wave dynamics. A significant portion of the work in this direction has been centred around weak wave turbulence [1]. The wave turbulence theory deals with out of equilibrium statistics of incoherent, weakly nonlinear dispersive waves in non-integrable systems. One of the early and most significant results of the wave turbulence theory was the analytical determination by Zakharov [2] of the analogs of the Kolmogorov spectra describing energy flux through scales in dissipative hydrodynamic turbulence. These spectra, called the Kolmogorov–Zakharov spectra, were obtained as solutions of the kinetic equations for the evolution of the Fourier spectra of random weakly nonlinear dispersive waves in multidimensional non-integrable systems.

More recently, a new theme in turbulence theory has emerged in connection with the dynamics of strongly nonlinear random waves described by one-dimensional integrable systems, such as the Korteweg–de Vries (KdV) and 1D nonlinear Schrödinger (NLS) equations. This kind of random wave motion in nonlinear conservative systems, dubbed 'integrable turbulence' [3], has attracted significant attention from both the fundamental and applied perspectives. The interest in integrable turbulence is motivated by the complexity of many natural or experimentally observed nonlinear wave phenomena often requiring a statistical description, even though the underlying physical model is, in principle, amenable to the well-established mathematical techniques of integrable systems theory, such as the inverse scattering transform (IST) or finite-gap theory [4–6]. Indeed, integrable systems are known to capture the essential properties of many wave processes occurring in real-world systems [7]. The integrable turbulence framework is particularly pertinent to the description of modulationally unstable systems, whose solutions, under the effect of random noise, can exhibit highly complex nonlinear behaviour that can be adequately described in terms of the turbulence theory concepts, such as probability distribution functions, ensemble averages, power spectra, etc [8–10]. We stress that the term 'turbulence' in this context is understood as complex spatiotemporal dynamics

J. Stat. Mech. (2021) 114001

that require probabilistic description and are not related to the energy cascades through scales, the prime feature of hydrodynamic and weak turbulence.

Localised nonlinear solitary waves are a ubiquitous feature of nonlinear dispersive wave propagation, whose discovery dates back to shallow water wave observations by John Scott Russell in 1845 [11]. If the wave dynamics are described by one of the completely integrable equations, the solitary waves exhibit particle-like properties, such as elastic, pairwise interactions accompanied by certain phase/position shifts. Such solitary waves are called solitons [12] and have been extensively studied, both theoretically [4, 13, 14] and experimentally [15]. The main tool for the analysis of integrable nonlinear dispersive PDEs is the IST [16] based on the reformulation of a nonlinear PDE as a compatibility condition of two *linear* problems: a stationary spectral (scattering) problem and the evolution problem for the same auxiliary function. Within the scattering problem, solitons are associated with discrete values of the spectrum, while the integrable evolution preserves these spectral values in time.

Solitons can form ordered macroscopic coherent structures, such as modulated soliton trains and dispersive shock waves [17, 18]. Furthermore, solitons can form *irregular*, statistical ensembles that can be interpreted as soliton gases. The nonlinear wave field in such gases represents a particular case of integrable turbulence, often called soliton turbulence (with the caveat that the latter term has also been used in the context of non-integrable wave dynamics, see e.g. [19, 20]). Generally, soliton gas and soliton turbulence represent two complementary aspects of the same physical object, the natural counterparts of the wave-particle duality of a single soliton. In the soliton-gas description, the focus is on the collective dynamics/kinetics of solitons as interacting (quasi)particles characterised by certain amplitude (or velocity) distribution function, while the soliton turbulence description emphasises the characteristics of the random nonlinear wave field associated with the soliton gas, such as probability density function, power spectrum, etc. The observations and analysis of irregular soliton complexes in the ocean have been reported in [21, 22]. Recent laboratory experiments on the generation of shallow-water and deep water soliton gases were reported in [23, 24], respectively. It has also been demonstrated that the soliton gas dynamics in the focusing NLS equation enables a remarkably accurate description of the statistical properties of the nonlinear stage of noise-induced modulational instability [25], as well as provides important insights into the dynamical and statistical mechanisms of the spontaneous formation of rogue waves [26, 27].

Analytical description of soliton gases in nonlinear dispersive wave systems was initiated in Zakharov's 1971 paper [28], where a spectral kinetic equation for KdV solitons was introduced using an IST-based phenomenological 'flea gas' reasoning, enabling the evaluation of an effective adjustment to the soliton's velocity in a *rarefied gas* due to the interactions (collisions) between individual solitons, accompanied by the well-defined phase-shifts. The kinetic equation for a rarefied soliton gas describes the evolution of the distribution function of the solitons with respect to the spectral parameter and the

J. Stat. Mech. (2021) 114001

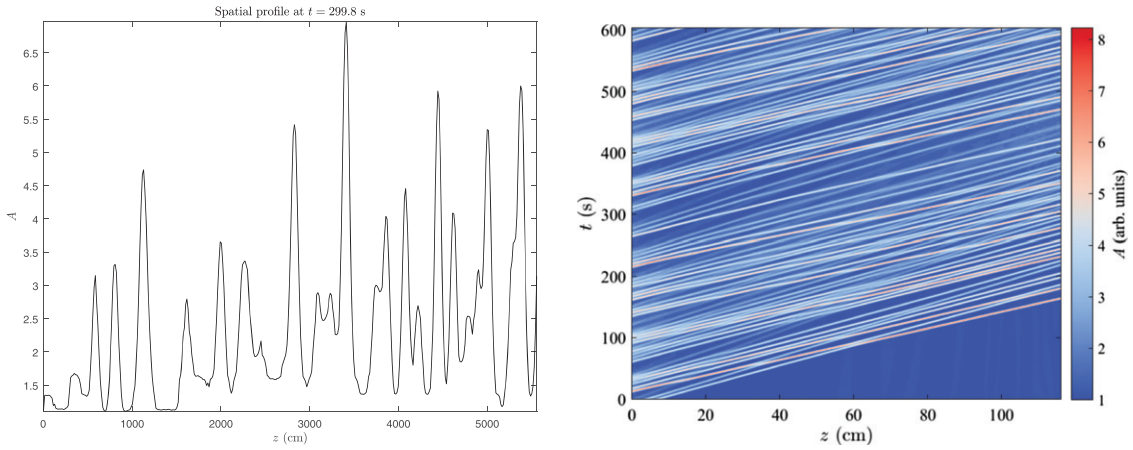

Figure 1. Soliton gas in dispersive hydrodynamics. (Left) Experimentally measured profile of the nonlinear wave field of a dense soliton gas in a viscous fluid conduit. (Right) x, t-contour image. The images are courtesy of the Dispersive Hydrodynamics Laboratory, Boulder, Colorado.

positions of soliton centres, i.e. the *density of states* (DOS). In a *dense gas*, however, the solitons exhibit significant overlap and, as a result, are continuously involved in a strong nonlinear interaction with each other. This can be seen in figure 1, displaying a laboratory realisation of a dense soliton gas in a viscous fluid conduit [29], a versatile fluid dynamics platform enabling high precision experiments on the generation and interaction of solitary waves that exhibit nearly elastic collisions [30, 31]. One can appreciate that, for a dense gas the particle interpretation of individual solitons becomes less transparent and the wave aspect of the collective soliton dynamics comes to the foreground. Indeed, a consistent generalisation of Zakharov's kinetic equation for KdV solitons to the case of a dense soliton gas has been achieved in [32] in the framework of the nonlinear wave modulation (Whitham) theory [33]. It was proposed in [32, 34] that soliton gas can be modelled by the thermodynamic type solitonic limit of the spectral finite-gap KdV solutions and their modulations [35]. The resulting kinetic equation has the form of a nonlinear integro-differential equation for the DOS in the IST spectral phase space. The structure of the kinetic equation obtained in [32] suggested that, remarkably, in a dense gas the net effect of soliton interactions can be formally evaluated using the same phase-shift argument that was used in the rarefied gas theory [28]. This observation, termed the collision rate assumption, has enabled an effective phenomenological theory of a dense soliton gas for the focusing NLS equation [36] and more recently, for the defocusing and resonant NLS equations [37]. The phenomenological theory of soliton gas for the focusing NLS equation proposed in [36] has been confirmed and substantially extended in [38] within the framework of the thermodynamic limit of spectral finite-gap solutions of the focusing NLS equation and their modulations. This latter work has revealed a number of new soliton gas phenomena due to a very different structure of

J. Stat. Mech. (2021) 114001

the spectral phase space of the focusing NLS equation compared to the KdV equation. In particular, the generalisation of soliton gas, termed *breather gas*, was introduced by considering a special family of focusing NLS solitonic solutions called breathers. Such a breather gas represents an intriguing type of integrable turbulence observed in the ocean [39] and realised numerically [40].

The mathematical properties of the kinetic equation for soliton gas were studied in [41, 42] where it was proved that it admits an infinite series of integrable linearly degenerate hydrodynamic reductions obtained by a multi-component delta-function ansatz for the DOS. A further study of the classical integrability properties of the soliton gas kinetic equation was undertaken in [43]. A very recent paper [44] presents rigorous results for the uniqueness, existence and non-negativity of the solutions to the integral equations for the DOS in the spectral kinetic theory for KdV and focusing NLS soliton gases [32, 38].

Apart from the above line of research on soliton gases inspired by Zakharov's 1971 work there have been many other developments—analytical, numerical and experimental—exploring various aspects of soliton gas/soliton turbulence dynamics in both integrable and nonintegrable classical wave systems (see e.g. [45–54]). Additionally, there has been a recent surge of related activity in generalised hydrodynamics (GHD) (see [55–57] and references therein), where the equations analogous to those arising in the soliton gas theory became pivotal for the understanding of large-scale, hydrodynamic properties of integrable quantum many-body systems.

1.2. Dispersive hydrodynamics

This review considers classical soliton gases from the perspective of dispersive hydrodynamics modelled by hyperbolic or elliptic conservation laws regularized by small conservative, dispersive corrections [58], the KdV equation $u_t + 6uu_x + u_{xxx} = 0$ being the simplest example. The smallness of the dispersive term is understood in the sense that the typical coherence length of the medium—determined by a balance between nonlinear and dispersive effects—is much less than the scale of initial, boundary, or intermediate flow conditions where long wavelength, nonlinear, hydrodynamic effects dominate. This distinguishes dispersive hydrodynamic problems from typical formulations in classical soliton theory, which usually involve variations of the wave field on the scale of the coherence length. The dispersive hydrodynamic framework arises naturally in the description of problems related to the large-scale dynamics of shallow water or internal waves, but also proved extremely useful in the modelling of various phenomena in nonlinear optics including the 'atom optics' of quantum fluids, such as Bose–Einstein condensates.

In the scalar case general dispersive hydrodynamics are described by the equations of the form

$$u_t + F(u)_x = (D[u])_x, \tag{1.1}$$

where $F(u)$ is the nonlinear hyperbolic flux and $D[u]$ is a differential (generally integro-differential) operator, possibly nonlinear, that gives rise to a real-valued dispersion relation $\omega = \omega_0(k)$ for linearised waves.

J. Stat. Mech. (2021) 114001

Scalar integrable dispersive hydrodynamics of the form (1.1), such as the KdV, modified KdV, Camassa–Holm or Benjamin–Ono equations often arise as small-amplitude, 'unidirectional' approximations of more general Eulerian bidirectional systems (see [33])

$$\begin{aligned} \rho_t + (\rho u)_x &= (D_1[\rho, u])_x, \\ (\rho u)_t + \left(\rho u^2 + \sigma P(\rho)\right)_x &= (D_2[\rho, u])_x, \qquad \sigma = \pm 1, \end{aligned} \tag{1.2}$$

where $D_{1,2}[\rho, u]$ are conservative, dispersive operators, ρ and u are interpreted as a mass density and fluid velocity, respectively, and $\sigma P(\rho)$, where $P(\rho) > 0$ is the pressure law. For $\sigma = +1$ this class of equations generalises the shallow water and isentropic gas dynamics equations, while encompassing many of the integrable dispersive hydrodynamic models, such as the Kaup–Boussinesq system [59], the hydrodynamic form of the defocusing NLS equation [60], the Calogero–Sutherland system describing the dispersive hydrodynamics of quantum many-body systems [61] and many others. For $\sigma = -1$ equations (1.2) describe 'elliptic' dispersive hydrodynamics, the most prominent example being the focusing NLS equation describing, in particular, the evolution of weakly nonlinear narrow-band wave packets on deep water and the propagation of light in optical media in the self-focusing, cubic nonlinearity regime.

The integrability of dispersive hydrodynamics (1.1) is understood as the existence of the Lax pair, a system of linear differential equations for an auxiliary (generally vector-valued) function $\psi(x, t; \lambda)$:

$$\mathcal{L}\psi = \lambda\psi, \qquad \psi_t = \mathcal{A}\psi, \tag{1.3}$$

where $\mathcal{L}$ and $\mathcal{A}$ are linear differential operators depending on $u(x, t)$ and its derivatives, and λ is a spectral parameter so that equation (1.1) can be written in the operator form $\mathcal{L}_t + (\mathcal{L}\mathcal{A} - \mathcal{A}\mathcal{L}) = 0$ under the additional requirement of *isospectrality*, $\lambda_t = 0$. For sufficiently rapidly decaying fields, $u(x, t) \to 0$ as $|x| \to \pm\infty$, the spectrum of the operator $\mathcal{L}$, often called the Lax spectrum, consists of two components: discrete and continuous. The points of the discrete spectrum correspond to solitons in the asymptotic solution at $t \gg 1$, while the continuous spectrum corresponds to dispersive radiation. The solutions whose spectrum consists of N discrete points only are called N-soliton solutions.

A prominent example of a multiscale nonlinear wave structure supported by dispersive hydrodynamics is the dispersive shock wave exhibiting coherence at both microscopic (soliton) and macroscopic (wave modulation) scales [18]. Contrastingly, soliton gas as a dispersive hydrodynamic structure exhibits coherence at the microscopic scale while being macroscopically incoherent, in the sense that the values of the wave field at two points separated by a distance much larger than the intrinsic dispersive length of the system (the soliton width) are not dynamically related. The source of randomness in dispersive hydrodynamics is typically related to some sort of stochastic large-scale initial or boundary conditions, although one can envisage dynamical mechanisms of the effective randomization of the wave field and the soliton gas generation [62, 63]. In particular,

J. Stat. Mech. (2021) 114001

statistical soliton ensembles can be naturally generated from both non-vanishing deterministic (e.g. quasiperiodic) and random initial conditions via the processes of soliton fission [64, 65] or modulational instability [25].

The inherent scale separation in dispersive hydrodynamic flows suggests the use of asymptotic methods for their description. One such method, the Whitham modulation theory [33] proved particularly effective and has been extensively developed in the contexts of both integrable and nonintegrable systems. Within the Whitham theory the dispersive hydrodynamic system is asymptotically reduced to a system of quasilinear equations, which describe large-scale variations of the wave's modulation parameters, such as the amplitude, the wavenumber, the mean, etc. The Whitham hydrodynamic equations can be derived by applying a multiple-scale singular perturbation theory or, equivalently, by averaging the dispersive hydrodynamic conservation laws over rapid oscillations. Although the Whitham method does not rely on integrability, the presence of integrable structure in the original dispersive hydrodynamic system greatly enhances the structure of the modulation system as well. The inherited integrability of the Whitham modulation equations is realised via the generalised hodograph transform [66, 67].

Importantly, the Whitham theory for integrable dispersive PDEs admits spectral formulation within the extension of IST called the finite-gap theory [4, 5]. The finite-gap theory describes an important class of periodic or quasiperiodic (multiphase) solutions to integrable systems, whose Lax spectrum (the set of admissible values of the spectral parameter λ in (1.3) corresponding to L^2 eigenfunctions ψ) lies in the *finite* union of disjoint bands. In 1980 Flaschka, Forest and McLaughlin showed that the Whitham equations obtained via multiphase averaging of the KdV equation describe the slow evolution of the band spectrum of the finite-gap Lax operator $\mathcal{L}$ [35]. It has then been shown by Lax and Levermore [68] that the spectral Whitham equations derived in [35] also describe the weak, distribution limits of dispersive conservation laws obtained in the limit of small dispersion.

It has been noted by Lax in [69] that the Whitham modulation equations can be viewed as certain analogs of the moment equations in classical statistical fluid mechanics [70]. This observation, combined with the spectral formulation of the Whitham theory [35] and the ideas of Venakides on the continuum limit of theta-functions [71], has enabled the development of the spectral theory of soliton gas [32, 34, 38] providing the justification of the phenomenological approach of [36] and a general mathematical framework for the study of soliton gases/soliton turbulence in classical integrable dispersive hydrodynamic systems.

The structure of the review is as follows. In section 2, we present a phenomenological theory of soliton gas in unidirectional and bidirectional systems of integrable dispersive hydrodynamics using the KdV and NLS equations as the prototype examples. The main result is the construction of the kinetic equation describing the evolution of the DOS in a non-equilibrium soliton gas. In the bi-directional case, we identify two different types of soliton gases: isotropic and anisotropic, differing in the properties of overtaking and head-on soliton collisions. In section 3, we develop a detailed spectral theory of soliton gas for the KdV equation and of soliton and breather gases for the focusing NLS equations. This is done by applying a special thermodynamic type limit

J. Stat. Mech. (2021) 114001

to the spectral finite-gap solutions and their modulations described by the appropriate Whitham equations. For the focusing NLS equation, we introduce the notion of soliton condensate and also consider three distinct types of 'rogue wave' breather gases. In section 4, hydrodynamic reductions of the spectral kinetic equation are derived by employing a multi-component delta-function ansatz for the DOS and their integrability is investigated. In section 5, we apply the hydrodynamic reductions to consider a canonical Riemann problem describing the collision of two multi-component soliton gases. Finally, the conclusion provides a brief summary and outlines some directions of future research.

2. Kinetic equation for soliton gas: phenomenological construction

We first introduce soliton gas phenomenologically, as an infinite ensemble of interacting solitons randomly distributed on the line with non-zero density. This intuitive definition lacks precision but it is sufficient for the purposes of this section. A more elaborate mathematical model of a soliton gas will be described in section 3.

2.1. Unidirectional soliton gas

It is convenient to introduce the basic ideas of soliton gas theory using the KdV equation as a prototype model of nonlinear dispersive wave propagation in a broad variety of physical systems. We consider the KdV equation in the form

$$u_t + 6uu_x + u_{xxx} = 0. \tag{2.1}$$

The KdV equation (2.1) belongs to the family of completely integrable equations. For a broad class of initial conditions its integrability is realised via the IST method [4]. The inverse scattering theory associates the soliton of the KdV equation (2.1) with a point of discrete spectrum λ_n, of the Schrödinger operator, which is the Lax operator for the KdV equation (cf (1.3)),

$$\mathcal{L} = -\partial_{xx}^2 - u(x,t) \tag{2.2}$$

Assuming $u \to 0$ as $x \to \pm\infty$, the KdV soliton solution corresponding to $\lambda_i = -\eta_i^2$, $\eta_i > 0$, is given by

$$u_{\rm s}(x,t;\eta_i) = 2\eta_i^2 \,\mathrm{sech}^2[\eta_i(x - 4\eta_i^2 t - x_i^0)], \tag{2.3}$$

where the soliton amplitude $a_i = 2\eta_i^2$, the speed $s_i = 4\eta_i^2$ and x_i^0 is the initial position or 'phase'. Along with the simplest single-soliton solution, the KdV equation supports N-soliton solutions $u_N(x,t)$ characterised by N discrete spectral parameters $\eta_1 < \eta_2 < \cdots < \eta_N$ and the set of initial positions $\{x_i^0 | i = 1, \cdots, N\}$. Since the discrete spectrum of the (self-adjoint) Schrödinger operator (2.2) is non-degenerate (i.e. $\eta_i \neq \eta_j \Leftrightarrow i \neq j$) all solitons in the N-soliton solution have different velocities and the long-time

J. Stat. Mech. (2021) 114001

asymptotic solution assumes the form of a rank-ordered soliton train,

$$t \gg 1: \quad u_N(x,t) \sim \sum_{j=1}^{N} 2\eta_i^2 \operatorname{sech}^2[\eta_i(x - 4\eta_i^2 t - x_i^0 + \Delta_i)], \tag{2.4}$$

where the phase (position) shifts Δ_i occur due to the interaction of individual solitons at the initial stage of the evolution [4, 72]. These phase shifts play an important role in our consideration as detailed below.

The integrable structure of the KdV equation has profound implications for the soliton interaction dynamics:

(a) The KdV evolution preserves the IST spectrum, $\partial_t \eta_j = 0$, implying that solitons retain their 'identity' (amplitude, speed) upon interactions.

(b) The collision of two solitons with spectral parameters η_i and η_j, $i \neq j$ results in their phase (position) shifts given by

$$\Delta_{ij} \equiv \Delta(\eta_i, \eta_j) = \frac{\sigma_{ij}}{\eta_i} \ln \left| \frac{\eta_i + \eta_j}{\eta_i - \eta_j} \right|, \qquad \sigma_{ij} = \operatorname{sgn}(\eta_i - \eta_j), \tag{2.5}$$

so that the taller soliton acquires shift forward and the smaller one—shift backwards;

(c) Solitons interact pairwise, i.e. the resulting, accumulated phase shift Δ_i of a given soliton with spectral parameter η_i after its interaction with M solitons with parameters η_j, $j \neq i$, is equal to the sum of the individual phase shifts,

$$\Delta_i = \sum_{j=1, j\neq i}^{M} \Delta_{ij}. \tag{2.6}$$

It is important to stress that the collision phase shifts are the far-field effects and mathematically, the artefacts of the asymptotic representation of the exact two-soliton solution of the KdV equation in the form of a sum of two individual solitons: $u_2(x,t;\eta_1,\eta_2) \simeq u_s(x + \Delta_{12}, t; \eta_1) + u_s(x + \Delta_{21}, t; \eta_2)$, which is only valid if solitons are sufficiently separated (the long-time asymptotics). The interaction of solitons is a complex nonlinear process [73] and the resulting wave field in the interaction region cannot be represented as a linear superposition of the phase-shifted one-soliton solutions.

Motivated by the above properties of N-soliton solutions, we now introduce a rarefied soliton gas by generalising the asymptotic soliton train solution (2.4) in the following way. We let $N \to \infty$ in (2.4) and introduce the DOS $f(\eta, x, t)$ defined such that $f(\eta_0, x_0, t_0)\mathrm{d}\eta\,\mathrm{d}x$ is the number of solitons found at $t = t_0$ in the element $[\eta_0, \eta_0 + \mathrm{d}\eta] \times [x_0, x_0 + \mathrm{d}x]$ of the phase space $\mathfrak{S} = \Gamma \times \mathbb{R}$. Here, $\Gamma = [\eta_{\min}, \eta_{\max}] \subset \mathbb{R}^+$ is the spectral support of DOS, without loss of generality one can assume $\Gamma = [0, 1]$. The parameter controlling the total spatial density of the soliton gas is then

$$\beta = \int_0^1 f(\eta)\mathrm{d}\eta. \tag{2.7}$$

J. Stat. Mech. (2021) 114001

For a rarefied gas $\beta \ll 1$.

We further assume (to be validated later) the Poisson distribution with density β for the soliton centres $x_j \in \mathbb{R}$, so that the distances $d_k = x_k - x_{k-1}$ between solitons are independent random values distributed with probability density $\mathcal{P}(d) = \beta \exp(-\beta d)$. We thus arrive at a 'stochastic soliton lattice'

$$u_\infty(x,t) \sim \sum_{i=1}^{\infty} 2\eta_i^2 \operatorname{sech}^2[\eta_i(x - 4\eta_i^2 t - x_i^0)], \quad \eta_i \in \Gamma,\ x_i \in \mathbb{R},\ \beta \ll 1, \tag{2.8}$$

that can be viewed as an approximate model of a rarefied soliton gas.

Each realisation of the random process $u_\infty(x,t)$ (2.8) satisfies the KdV equation (2.1) almost everywhere in $x \in \mathbb{R}$. Due to the small spatial density β, the individual solitons in a soliton gas overlap only in the regions of their exponential tails, except for the rare events of their collisions where a complex nonlinear interaction occurs [73] affecting the statistical characteristics of the random field (2.8) [74].

We first look at the equilibrium, or uniform, soliton gas for which $\partial f/\partial x = 0$. In view of the isospectrality of the KdV evolution, the spatially independent DOS $f(\eta)$ at $t = 0$ implies that $\partial f/\partial t = \partial f/\partial x = 0\ \forall\ t > 0$.

Consider the propagation of a 'tracer' soliton with the spectral parameter $\eta = \eta_1 \in [0,1]$ in a uniform soliton gas with a given DOS $f(\eta)$, $\eta \in [0,1]$ and assume that the gas is rarefied, $\int_0^1 f(\eta)\mathrm{d}\eta \ll 1$. Due to the collisions of the tracer 'η_1-soliton' with the 'μ-solitons' ($\mu \neq \eta_1$) in the gas, each collision leading to the phase shift (2.5), the effective (mean) velocity of the trial soliton is approximately evaluated as

$$s(\eta_1) \ \approx\ 4\eta_1^2 + \frac{1}{\eta_1}\int_0^1 \ln\left|\frac{\eta_1+\mu}{\eta_1-\mu}\right| f(\mu)[4\eta_1^2 - 4\mu^2]\,\mathrm{d}\mu. \tag{2.9}$$

The integral correction term in (2.9) follows from the continuum limit of equation (2.6) assuming that in a rarefied gas $s(\eta_1) = 4\eta_1^2$ to leading order. Then, the total spatial shift of the η_1-soliton over the time interval $\mathrm{d}t$ due to the interactions with μ-solitons, $\mu \in [0,1]$, is given by $\Delta_1 = [\int_0^1 \Delta(\eta_1,\mu)\Xi(\eta_1,\mu)\mathrm{d}\mu]\mathrm{d}t$, where $\Xi(\eta_1,\mu_0)\mathrm{d}\mu \approx |4\eta_1^2 - 4\mu_0^2| f(\mu_0)\mathrm{d}\mu$ is the average collision rate of η_1-soliton with μ-solitons with the spectral parameter $\mu \in [\mu_0,\ \mu_0 + \mathrm{d}\mu]$. Then using expression (2.5) for the KdV phase shift, we obtain (2.9). The effective velocity $s(\eta_1)$ has a natural interpretation of the transport velocity in soliton gas.

We note that the spectral parameter η_1 of the 'special' soliton should not necessarily belong to the support $\Gamma = [0,1]$ of $f(\eta)$. If $\eta_1 \notin \Gamma$, we shall call such a soliton a 'trial' soliton. The important distinction between tracer and trial solitons will become more transparent later. The modification of the 'free' velocity of a trial soliton due its propagation through a uniform soliton gas is illustrated in figure 2.

We now consider a non-equilibrium (non-uniform) soliton gas with $f(\eta) \equiv f(\eta,x,t)$, $s(\eta) \equiv s(\eta,x,t)$ so that spatiotemporal variations of f and s occur on scales much larger than those associated with variations of the nonlinear wave field $u(x,t)$ in (2.8). The isospectrality of the KdV dynamics implies the conservation equation for the density in the phase space $\mathfrak{S}$ (i.e. DOS),

$$f_t + (sf)_x = 0, \tag{2.10}$$

J. Stat. Mech. (2021) 114001

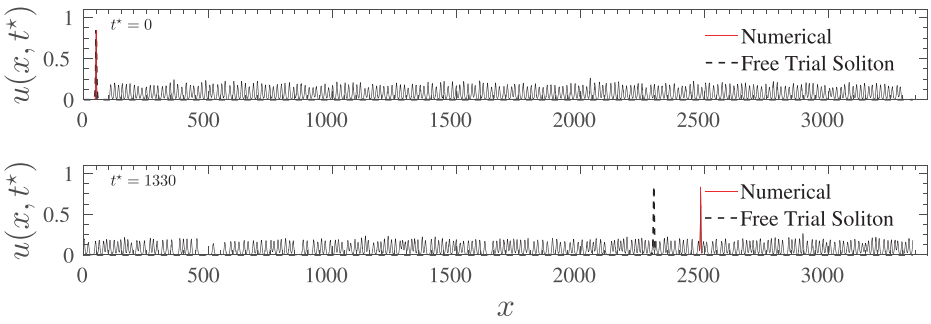

Figure 2. Comparison for the propagation of a free soliton with the spectral parameter $\eta = \eta_1$ in a void (black dashed line) with the propagation of the trial soliton with the same spectral parameter η_1 (red solid line) through a one-component rarefied KdV soliton gas with the DOS $f_0\delta(\eta - \eta_0)$. Parameters used in the numerical simulations are: $\eta_1 = 0.65$, $\eta_0 = 0.3$ and density $f_0 = 0.048$. One can see that the trial soliton propagates faster in the gas due to the interactions with smaller solitons. Reproduced from [75]. Copyright © EPLA, 2016. All rights reserved.

which, together with expression (2.9) for the effective transport velocity $s(\eta)$ can be viewed as a kinetic equation for rarefied soliton gas first introduced by Zakharov in 1971 [28]. As we mentioned, x and t in (2.10) are 'slow' variables compared to x and t in the KdV equation (2.1). Thus, the kinetic equations (2.9) and (2.10) can be viewed as a modulation equation for the soliton gas (2.8). We shall see later that this analogy has a more precise meaning, with a hierarchy of spatiotemporal scales involved.

Zakharov's approximate equation (2.9) for the effective transport velocity in a soliton gas was generalised in [32] to the case of dense ($\beta = \mathcal{O}(1)$) gas. This was done by evaluating the thermodynamic limit of the nonlinear dispersion relations associated with the spectral finite-gap solutions of the KdV equation (2.1) (see section 3.2 below). The result has the form of a linear integral equation

$$s(\eta) = 4\eta^2 + \frac{1}{\eta}\int_0^1 \ln\left|\frac{\eta+\mu}{\eta-\mu}\right| f(\mu)[s(\eta) - s(\mu)]\mathrm{d}\mu, \tag{2.11}$$

which essentially provides the relation between the spectral flux density $v = fs$ and the DOS f in the transport equation (2.10) and so can be viewed as the equation of state of the soliton gas. Expression (2.9) for the effective soliton velocity in a rarefied soliton gas represents an approximate first order solution of the equation of state (2.11) obtained by assuming that the integral term is a small correction to the free soliton velocity $4\eta^2$.

One can notice that equation (2.11) can be formally written down by utilising the same phase-shift argument used in the derivation of the approximate expression (2.9), i.e. by a formal replacement in (2.9) of the leading order value $4\eta^2$ for the soliton velocity with its effective value $s(\eta)$. The validity of this replacement in the KdV equation case suggests the general *collision rate assumption*, whereby the total position shift of the soliton with $\eta = \eta_1$ due to soliton collisions in a gas with DOS $f(\mu)$ over the time interval

J. Stat. Mech. (2021) 114001

dt is given by

$$\Delta_1 = \left[\int_\Gamma \Delta(\eta_1,\mu)|s(\eta_1)-s(\mu)|f(\mu)\mathrm{d}\mu\right]\mathrm{d}t, \tag{2.12}$$

where Γ is the spectral support of the DOS $f(\eta)$. This assumption was used in [36] for the construction of the kinetic equation for the dense soliton gas for the focusing NLS equation (see section 2.2.2 below). We note that in a different context, the collision rate assumption is at the heart of the GHD, the theory for the large-scale dynamics of quantum many-body integrable systems. In GHD, the point-like quasiparticles are subject to the instantaneous velocity-dependent spatial shifts upon colliding (see [55–57, 76–78] and references therein). It is important to stress, however, that the validity of (2.12) in the context of classical soliton gases, although intuitively suggestive, is far from obvious. Indeed, as we have already mentioned, the very notion of the phase shift in soliton theory is only applicable in the context of the long-time asymptotics, i.e. when solitons have sufficient time to separate from each other after the interaction, which can only happen in a rarefied gas. The fact that, in a dense gas, where solitons experience significant overlap and continual interaction, the net effect of soliton collisions on the mean velocity is expressed in the same way as in the rarefied gas is quite remarkable.

Along with the notion of the phase shift, the phenomenological definition of the DOS $f(\eta)$ introduced above for a rarefied gas also requires a more careful treatment as the procedure of identifying individual solitons within a dense soliton gas is not obvious (as a matter of fact, the dense soliton gas is no longer described by an approximate 'soliton lattice' expression (2.8)). This issue can be partially addressed by assuming that for any sufficiently broad interval $x \in [x_0, x_0+L]$, $L \gg 1$ the soliton gas can be approximated by an exact N-soliton solution and then using the 'windowing' procedure introduced in [37] to 'release' the solitons contained within this interval and identify them when they get sufficiently separated. This procedure will be described in section 2.3. Later, in section 3, the DOS for dense soliton gases for the KdV and focusing NLS equations will be introduced in a more mathematically satisfactory way via the thermodynamic limit of the finite-gap spectra of nonlinear multiphase solutions.

With all of the above caveats, the equation of state for a general unidirectional soliton gas can be formulated. Let the soliton solution of integrable dispersive hydrodynamics be characterised by the value $\lambda = \lambda_i$ of the discrete spectrum of the Lax operator, and the position shift in the overtaking two-soliton collisions be $\Delta(\lambda,\ \mu) = \ \mathrm{sgn}(\lambda - \ \mu)G(\lambda,\ \mu)$, where $G(\lambda,\ \mu) > 0$. Then we obtain upon using (2.12),

$$s(\lambda,x,t) = s_0(\lambda) + \int_\Gamma G(\lambda,\mu)f(\mu,x,t)[s(\lambda,x,t)-s(\mu,x,t)]\mathrm{d}\mu \tag{2.13}$$

under the additional assumption $s'(\lambda) > 0$ (to be verified in concrete cases). Here, $s_0(\lambda)$ is the velocity of a free soliton and Γ is the support of the DOS $f(\lambda)$. We use the general notation λ for the spectral parameter in (2.13) with the understanding that it could be some function of the eigenvalue of the Lax operator (as is the case for the KdV equation, cf (2.2) and (2.3)).

J. Stat. Mech. (2021) 114001

By re-arranging the integral equation (2.13), a useful representation for $s(\lambda)$ can be obtained

$$s(\lambda) = \frac{s_0(\lambda) - \int_\Gamma G(\lambda,\mu) f(\mu) s(\mu) \mathrm{d}\mu}{1 - \int_\Gamma G(\lambda,\mu) f(\mu) \mathrm{d}\mu}. \tag{2.14}$$

Although the equation of state (2.13), as written, implies that $s(\lambda)$ is defined for $\lambda \in \Gamma$, its consequence (2.14) can be used to find the speed $s(\lambda_1)$ of the 'trial' soliton with $\lambda = \lambda_1 \notin \Gamma$ propagating through the soliton gas with a given DOS $f(\lambda)$ and transport velocity $s(\lambda)$, $\lambda \in \Gamma$. This extension can be readily justified by formally replacing $f(\lambda) \to f(\lambda) + w\delta(\lambda - \lambda_1)$, $w > 0$, in (2.13) and subsequently letting $w \to 0$.

The representation (2.14) suggests that the case of soliton gas with $f(\lambda)$, $s(\lambda)$ satisfying

$$\int_\Gamma G(\lambda,\mu) f(\mu) \mathrm{d}\mu = 1, \qquad \int_\Gamma G(\lambda,\mu) f(\mu) s(\mu) \mathrm{d}\mu = s_0(\lambda) \tag{2.15}$$

is special. Indeed, this case corresponds to the peculiar type of soliton gas termed *soliton condensate* [38]. Soliton condensate will be considered in section 3.3.4 in the context of the focusing NLS equation.

2.2. Bidirectional soliton gas

In this section, following [37], we will derive the kinetic equation for integrable bidirectional Eulerian dispersive hydrodynamics (1.2) using the phenomenological construction outlined in the previous section. For convenience, we reproduce system (1.2) here in a slightly simplified form covering majority of dispersive hydrodynamic systems arising in applications:

$$\begin{aligned} &\rho_t + (\rho u)_x = 0, \\ &(\rho u)_t + \left(\rho u^2 + \sigma P(\rho)\right)_x = (D[\rho,u])_x, \qquad \sigma = \pm 1, \end{aligned} \tag{2.16}$$

where $D[\rho,u])$ is the dispersion operator that gives rise to a real-valued dispersion relation $\omega = \omega_0(k)$ for linearised solutions. The bidirectionality of (2.16) implies that the linear dispersion relation has two branches: $\omega_0^-(k)$ and $\omega_0^+(k)$—corresponding to slow and fast waves respectively, i.e. the phase velocities are ordered as $\omega_0^-(k)/k < \omega_0^+(k)/k$ in the long wavelength limit $k \to 0$.

Suppose that system (2.16) supports a family of bidirectional soliton solutions that bifurcate from the two branches of the linear wave spectrum $\omega = \omega_0^\pm(k)$. We denote the corresponding soliton families $(\rho_\mathrm{s}^-, u_\mathrm{s}^-)$ and $(\rho_\mathrm{s}^+, u_\mathrm{s}^+)$. Let these soliton solutions be parametrised by a real-valued spectral (IST) parameter λ so that $\lambda \in \Gamma_+$ for the 'fast' branch and $\lambda \in \Gamma_-$ for the 'slow' branch, where $\Gamma_\pm$ are simply-connected subsets of $\mathbb{R}$ with one intersection point at most. Let the respective soliton velocities be $c_\pm(\lambda)$. For convenience, we assume that $c_\pm'(\lambda) > 0$, and $c_-(\lambda_1) < c_+(\lambda_2)$ if $\lambda_1 \in \Gamma_-$ and $\lambda_2 \in \Gamma_+$, $\lambda_1 \neq \lambda_2$. If $\Gamma_- \cap \Gamma_+ = \{\lambda_*\}$ we assume $c_-(\lambda_*) = c_+(\lambda_*)$. The generalisation to the case $c_\pm'(\lambda) < 0$, $c_-(\lambda_1) > c_+(\lambda_2)$ will be straightforward.

One can distinguish between the two types of pairwise collisions in a bidirectional soliton gas: the overtaking collisions between solitons belonging to the same spectral

J. Stat. Mech. (2021) 114001

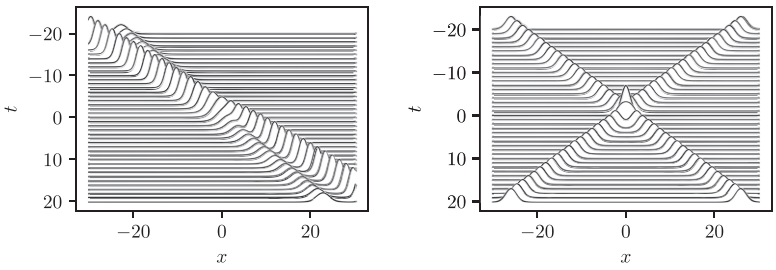

Figure 3. Soliton collisions in a bidirectional shallow-water soliton gas: (a) overtaking; (b) head-on.

branch and characterised by the position shifts Δ_{++} and Δ_{--}, respectively, and the head-on collisions between solitons of different branches, characterized by the position shifts Δ_{+-} and Δ_{-+}. Let $\lambda \neq \mu$, and $\Delta_{\pm\pm}(\lambda, \mu)$ and $\Delta_{\pm\mp}(\lambda, \mu)$ denote the position shifts of a λ-soliton due to its collision with a μ-soliton, with the first and the second signs $\pm$ in the subscript indicating the branch correspondence of the λ-soliton and the μ-soliton, respectively: e.g. $\Delta_{-+}(\lambda, \mu)$ is the position shift of a λ-soliton with $\lambda \in \Gamma_-$ in a collision with a μ-soliton with $\mu \in \Gamma_+$. The typical wave patterns in the overtaking and head-on soliton interactions in a bidirectional shallow-water soliton gas are shown in figure 3.

2.2.1. Isotropic and anisotropic soliton gases. We call the bidirectional soliton gas *isotropic* if the position shifts for the overtaking and head-on collisions between λ- and μ-solitons satisfy the following sign conditions:

$$\operatorname{sgn}[\Delta_{++}] = \operatorname{sgn}[\Delta_{+-}], \qquad \operatorname{sgn}[\Delta_{--}] = \operatorname{sgn}[\Delta_{-+}], \tag{2.17}$$

i.e. the λ-soliton experiences a shift of a certain sign, say shift forward (and the μ-soliton—the shift of an opposite sign) irrespective of the type of the collision—overtaking or head-on. If conditions (2.17) are not satisfied, i.e. the sign of the phase shift depends on the type of the collision, we shall call the corresponding soliton gas *anisotropic*. The difference between the phase shifts in isotropic and anisotropic collisions is illustrated in figure 5 using concrete examples.

Following the construction for unidirectional soliton gas outlined in section 2.1, we now consider bidirectional soliton gases for integrable Eulerian dispersive hydrodynamics (2.16). We introduce two separate DOS's $f_-(\lambda, x, t)$ and $f_+(\lambda, x, t)$ for the populations of solitons whose spectral parameters belong to the slow (Γ_-) and fast (Γ_+) branches of the spectral set Γ, respectively. The isospectrality of the integrable evolution now implies two separate conservation laws:

$$(f_-)_t + (s_- f_-)_x = 0, \qquad (f_+)_t + (s_+ f_+)_x = 0, \tag{2.18}$$

where $s_-(\lambda, x, t)$ and $s_+(\lambda, x, t)$ are the transport velocities associated with the slow and fast spectral branches Γ_- and Γ_+, respectively.

We derive the equations of state for $s_\pm$ by extending the phenomenological approach of section 2.1 based on the collision rate assumption. Consider a λ-soliton from the slow branch, $\lambda \in \Gamma_-$, and compute its displacement in a gas over a 'mesoscopic' time interval

J. Stat. Mech. (2021) 114001

$\mathrm{d}t$, sufficiently large to incorporate a large number of collisions, but sufficiently small to ensure that the spatiotemporal field $f_\pm(\lambda, x, t)$ is stationary over $\mathrm{d}t$ and approximately constant on a typical spatial scale $c_\pm(\lambda)\mathrm{d}t$. Having this in mind, we drop the (x, t)-dependence for convenience. Each overtaking collision with a μ-soliton of the same branch, $\mu \in \Gamma_-$, shifts the λ-soliton by the distance $\Delta_{--}(\lambda,\ \mu)$. Then, invoking the collision rate assumption (2.12) the displacement of the λ-soliton over the time $\mathrm{d}t$ due to the overtaking collisions with μ-solitons, where $\mu \in [\mu_0,\ \mu_0 + \mathrm{d}\mu]$, is given by $\int_{\Gamma_-} \Delta_{--}(\lambda, \mu) f_-(\mu)|s_-(\lambda) - s_-(\mu)|\mathrm{d}t\,\mathrm{d}\mu$. Additionally, each head-on collision with a fast soliton, $\mu \in \Gamma_+$, shifts the slow λ-soliton with $\lambda \in \Gamma_-$ by $\Delta_{-+}(\lambda,\ \mu)$, and the resulting displacement after a time $\mathrm{d}t$ is given $\int_{\Gamma_+} \Delta_{-+}(\lambda, \mu) f_+(\mu)|s_+(\lambda) - s_-(\mu)|\mathrm{d}t\,\mathrm{d}\mu$. A similar consideration is applied to the fast soliton branch, $\lambda \in \Gamma_+$. Equating the total displacements of the slow and fast λ-solitons to $s_-(\lambda)\mathrm{d}t$ and $s_+(\lambda)\mathrm{d}t$, respectively, we obtain the equation of state of a bidirectional gas in the form of two coupled linear integral equations:

$$\begin{aligned} s_-(\lambda) &= c_-(\lambda) + \int_{\Gamma_-} \Delta_{--}(\lambda, \mu) f_-(\mu)|s_-(\lambda) - s_-(\mu)|\mathrm{d}\mu \\ &\quad + \int_{\Gamma_+} \Delta_{-+}(\lambda, \mu) f_+(\mu)|s_-(\lambda) - s_+(\mu)|\mathrm{d}\mu, \quad \lambda \in \Gamma_-, \\ s_+(\lambda) &= c_+(\lambda) + \int_{\Gamma_+} \Delta_{++}(\lambda, \mu) f_+(\mu)|s_+(\lambda) - s_+(\mu)|\mathrm{d}\mu \\ &\quad + \int_{\Gamma_-} \Delta_{+-}(\lambda, \mu) f_-(\mu)|s_+(\lambda) - s_-(\mu)|\mathrm{d}\mu, \quad \lambda \in \Gamma_+. \end{aligned} \tag{2.19}$$

If the spectral support $\Gamma = \Gamma_- \cup \Gamma_+ \subset \mathbb{R}$ is a simply connected set and the gas is isotropic, the distinction between the fast and slow branches becomes unnecessary and the kinetic equations (2.18) and (2.19) for bidirectional soliton gas is naturally reduced to the unidirectional gas equations (2.10) and (2.13) for a single DOS $f(\lambda)$ defined on the entire set Γ. It was shown in [37] that the dynamics governed by the kinetic equations (2.10), (2.13), (2.18) and (2.19) are in a very good agreement with the results of direct numerical simulations of isotropic and anisotropic bidirectional soliton gases, respectively.

2.2.2. Kinetic equations for soliton gas in NLS dispersive hydrodynamics. As a representative example of bidirectional integrable dispersive hydrodynamics (2.16), we consider the system

$$\begin{gathered} \rho_t + (\rho u)_x = 0, \\ (\rho u)_t + \left(\rho u^2 + \sigma\frac{\rho^2}{2}\right)_x = \frac{\mu}{4}[\rho(\ln\,\rho)_{xx}]_x, \qquad \sigma = \pm 1, \qquad \mu = \pm 1. \end{gathered} \tag{2.20}$$

For $\mu = 1$, system (2.20) is equivalent to the NLS equation:

$$i\psi_t + \frac{1}{2}\psi_{xx} - \sigma|\psi|^2\psi = 0, \tag{2.21}$$

J. Stat. Mech. (2021) 114001

with the mapping between the two representations being realised by the so-called Madelung transform:

$$\psi = \sqrt{\rho}\,\exp\left(\mathrm{i}\phi\right), \qquad \phi_x = u. \tag{2.22}$$

The case $\sigma = +1$ in (2.21) corresponds to the defocusing NLS equation describing the propagation of light beams through optical fibres in the regime of normal dispersion, as well as nonlinear matter waves in quasi-1D repulsive Bose–Einstein condensates (see for instance [79]). If $\sigma = -1$, equation (2.21) is the focusing NLS equation, which is a canonical model for the description of modulationally unstable wave systems, such as deep water waves or the propagation of light in optical fibres in the regime of anomalous dispersion.

For $\sigma = +1$, the $\mu = -1$ system (2.21) is equivalent to the NLS equation in a 'quantum potential', also known as the resonant NLS equation [80, 81],

$$i\psi_t + \frac{1}{2}\psi_{xx} - |\psi|^2\psi = |\psi|_{xx}\psi/|\psi|. \tag{2.23}$$

This equation, in particular, describes long magneto-acoustic waves in a cold plasma propagating across the magnetic field [82]. It is also directly related to the Kaup–Boussinesq system, an integrable model for bidirectional shallow water waves [59] (see [37] for the transformation between the resonant NLS and the Kaup–Boussinesq system).

We now look at the soliton gas descriptions for each of the above NLS systems

(a) *Defocusing NLS equation*

The inverse scattering theory of the defocusing NLS equation was constructed in [83]. It was shown that the defocusing NLS equation supports a family of dark (or gray) soliton solutions on the finite background, which, up to the initial position and phase, can be most conveniently represented in terms of the hydrodynamic variables ρ, u as

$$\rho_{\mathrm{s}}^{\pm} = 1 - (1-\lambda^2)\mathrm{sech}^2\left[\sqrt{1-\lambda^2}(x - c_{\pm}t)\right], \quad u_{\mathrm{s}}^{\pm} = \lambda\left(1 - \frac{1}{\rho_{\mathrm{s}}^{\pm}(x,t)}\right), \quad c_{\pm} = \lambda \in \Gamma_{\pm}, \tag{2.24}$$

where $\lambda \in \mathbb{R}$ is the discrete spectral parameter in the linear scattering problem associated with the defocusing NLS equation [83], $\Gamma_- = (-1, 0]$ for the slow soliton branch and $\Gamma_+ = [0, +1)$ for the fast soliton branch; note that solutions $(\rho_{\mathrm{s}}^+, u_{\mathrm{s}}^+)$ and $(\rho_{\mathrm{s}}^-, u_{\mathrm{s}}^-)$ have the same analytical expression. Also, despite the same analytical expression for the soliton velocities c_+ and c_- in the defocusing NLS case, we keep the formal notational distinction to retain the connection with the general equation of state (2.19) for bidirectional gas, where the expressions for $c_+(\lambda)$ and $c_-(\lambda)$ can be, in principle, different. Additionally, without loss of generality we assumed in (2.24) the unit density background.

Typical dark soliton solutions for ρ and u are displayed in figure 4(a). The position shifts in the defocusing NLS overtaking and head-on soliton collisions are

J. Stat. Mech. (2021) 114001

given by the same analytical expression, $\Delta_{\pm\pm}(\lambda,\ \mu) = \Delta_{\pm\mp}(\lambda,\ \mu) \equiv \Delta(\lambda,\ \mu)$, where

$$\Delta(\lambda,\mu) = \frac{\mathrm{sgn}(\lambda-\mu)}{2\sqrt{1-\lambda^2}}\ \ln\frac{(\lambda-\mu)^2+\left(\sqrt{1-\lambda^2}+\sqrt{1-\mu^2}\right)^2}{(\lambda-\mu)^2+\left(\sqrt{1-\lambda^2}-\sqrt{1-\mu^2}\right)^2} \equiv \mathrm{sgn}(\lambda-\mu)G_1(\lambda,\mu), \tag{2.25}$$

for all $\lambda,\ \mu \in (-1,1)$. Expressions (2.25) were obtained in [83]. Note that, unlike in the KdV equation, one needs to distinguish between the position and phase shifts for soliton collisions in the NLS dispersive hydrodynamics. The expressions for the phase shifts can also be found in [83] but we do not consider them here.

One can readily verify that the soliton position shifts given by (2.25) satisfy the isotropy conditions (2.17). The variation of $\Delta(\lambda,\ \mu)$ with respect to μ for a fixed λ is displayed in figure 5(a). One can see that the position shifts for the two head-on and overtaking collisions lie on the same curve with $\Delta(\lambda,\ \mu)$ being continuous at $\lambda = 0$, the point of intersection of Γ_- and Γ_+. Due to the isotropic nature of the defocusing NLS soliton interactions, the coupled kinetic equations (2.18) and (2.19) for the bidirectional defocusing NLS gas reduce to the single spectral transport equation (2.10) with the equation of state

$$s(\lambda,x,t) = \lambda + \int_{-1}^{+1} G_1(\lambda,\mu) f(\mu,x,t)[s(\lambda,x,t)-s(\mu,x,t)]\mathrm{d}\mu, \quad \lambda \in (-1,1). \tag{2.26}$$

One can verify by direct computation that the condition $s'(\lambda) > 0$ necessary for the validity of (2.26) is satisfied.

(b) *Resonant NLS equation*

The resonant NLS equation (2.23) is reducible to the well-known integrable Kaup–Boussinesq system for shallow water waves for which the inverse spectral theory was constructed in [59]. It is not difficult to show that the resonant NLS equation has a family of spectral anti-dark soliton solutions given by [81]

$$\rho_{\mathrm{s}}^{\pm} = 1 + (\lambda^2-1)\mathrm{sech}^2\left[\sqrt{\lambda^2-1}(x-c_{\pm}t)\right], \quad u_{\mathrm{s}}^{\pm} = \lambda\left(1-\frac{1}{\rho_{\mathrm{s}}^{\pm}(x,t)}\right), \quad c_{\pm} = \lambda \in \Gamma_{\pm}. \tag{2.27}$$

Typical anti-dark soliton solutions of the resonant NLS are displayed in figure 4(b). In contrast with the defocusing NLS system, the admissible spectral set Γ of the resonant NLS solitons is spanned by two disconnected subsets: $\Gamma_- = (-\infty,-1]$ for slow solitons and $\Gamma_+ = [+1,+\infty)$. The position shifts in the head-on and overtaking collisions of the resonant NLS solitons are given by the same analytical expression $\Delta_{\pm\pm}(\lambda,\ \mu) = \Delta_{\pm\mp}(\lambda,\ \mu) \equiv \Delta(\lambda,\ \mu)$, where

J. Stat. Mech. (2021) 114001

$$\Delta(\lambda,\mu)=\frac{\operatorname{sgn}(\lambda-\mu)}{2\sqrt{\lambda^2-1}}\ln\frac{(\lambda-\mu)^2-\left(\sqrt{\lambda^2-1}+\sqrt{\mu^2-1}\right)^2}{(\lambda-\mu)^2-\left(\sqrt{\lambda^2-1}-\sqrt{\mu^2-1}\right)^2}\equiv\operatorname{sgn}(\lambda-\mu)G_2(\lambda,\mu). \tag{2.28}$$

However, now one can verify that, unlike in the defocusing NLS case, the isotropy condition (2.17) is not satisfied. Indeed, it follows from (2.28) that $\operatorname{sgn}[\Delta_{\pm\pm}(\lambda,\ \mu)]=\ \operatorname{sgn}(\lambda-\mu)$, whereas $\operatorname{sgn}[\Delta_{\pm\mp}(\lambda,\ \mu)]=-\operatorname{sgn}(\lambda-\mu)$, that is in a head-on collision between a λ-soliton and a μ-soliton with $\lambda>\mu$, the λ-soliton's position is now shifted backwards. The variation of $\Delta_{\pm\pm}(\lambda,\ \mu)$ for the resonant NLS equation is shown in figure 5(b). One can see that it is qualitatively different from the variation of $\Delta_{\pm\mp}(\lambda,\ \mu)$ for the defocusing NLS equation (figure 5(a)).

The kinetic equation for the anisotropic resonant NLS soliton gas then takes the form of two continuity equation (2.18) complemented by the coupled equations of state

$$\begin{aligned}
s_-(\lambda)&=\lambda+\int_{-\infty}^{-1}G_2(\lambda,\mu)f_-(\mu)(s_-(\lambda)-s_-(\mu))\mathrm{d}\mu\\
&\quad+\int_{+1}^{\infty}G_2(\lambda,\mu)f_+(\mu)(s_-(\lambda)-s_+(\mu))\mathrm{d}\mu,\quad \lambda\in(-\infty,1]\\
s_+(\lambda)&=\lambda+\int_{+1}^{+\infty}G_2(\lambda,\mu)f_+(\mu)(s_+(\lambda)-s_+(\mu))\mathrm{d}\mu\\
&\quad+\int_{-\infty}^{-1}G_2(\lambda,\mu)f_-(\mu)(s_+(\lambda)-s_-(\mu))\mathrm{d}\mu,\quad \lambda\in[1,+\infty)
\end{aligned} \tag{2.29}$$

assuming that $s'_\pm(\lambda)>0$ and $s_+>s_-$ (verified by direct computation).

(c) *Focusing NLS equation*

The case of the focusing NLS equation (equation (2.21) with $\sigma=-1$) is special as it represents an example of the *focusing* dispersive hydrodynamics, where the long-wave, 'hydrodynamic' motion is described by an elliptic system. The focusing NLS equation is a canonical model for the description of modulationally unstable systems in fluid dynamics and nonlinear optics. Nevertheless, the focusing NLS equation supports stable soliton solutions that can propagate in both directions so the focusing NLS soliton gas should be classified as bidirectional.

We consider the focusing NLS equation in the following normalisation:

$$i\psi_t+\psi_{xx}+2|\psi|^2\psi=0, \tag{2.30}$$

which is standard in the context of the IST analysis. The IST for the focusing NLS equation was introduced in the celebrated paper of Zakharov and Shabat [84], where it was shown that the spectral problem associated with (2.30) has the form

$$\mathcal{L}Y=\lambda Y,\qquad \mathcal{L}=\begin{pmatrix}-i\partial_x & \psi\\ \overline{\psi} & i\partial_x\end{pmatrix}, \tag{2.31}$$

J. Stat. Mech. (2021) 114001

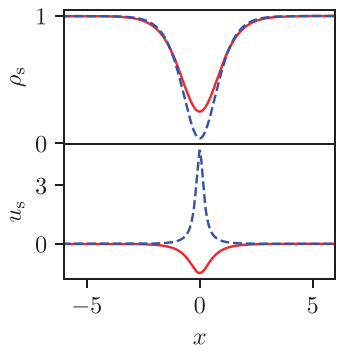

(a) Dark soliton solutions of the defocusing NLS equation (2.24): $\lambda = +0.5, -0.2$.

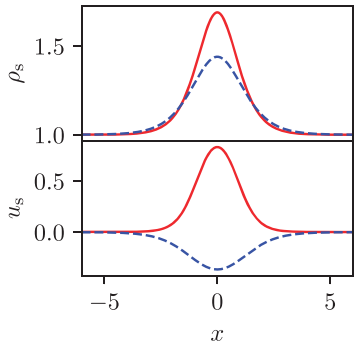

(b) Anti-dark soliton solutions of the resonant NLS equation (2.27): $\lambda = +1.3, -1.2$.

Figure 4. Soliton solutions: solid lines correspond to the fast branch solutions (ρ_s^+, u_s^+) and dashed lines to the slow branch solutions (ρ_s^-, u_s^-).

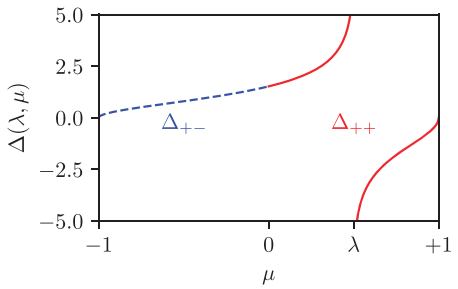

(a) Defocusing NLS (λ, μ)-interaction with $\lambda = 1/2$.

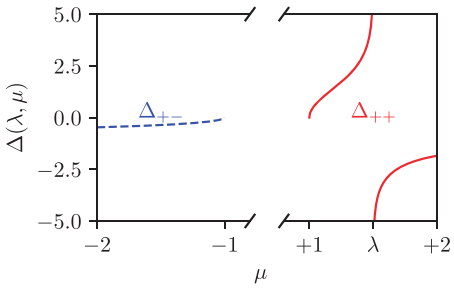

(b) Resonant NLS (λ, μ)-interaction with $\lambda = 3/2$.

Figure 5. Variation of the phase shifts in the isotropic (a) and anisotropic (b) interactions of solitons with spectral parameters λ and μ; λ is fixed and belongs to the 'fast' spectral branch Γ_+.

where λ is the spectral parameter and $Y = Y(x, t, \lambda)$ is a vector; $\overline{\psi}$ denotes the complex conjugate. The Lax operator $\mathcal{L}$ in (2.31) is often called the Zakharov–Shabat operator. The main difference of the Zakharov–Shabat operator from the Lax operators for the KdV, defocusing and resonant NLS equations is that it is not self-adjoint, implying that the spectral parameter λ is complex, $\lambda \in \mathbb{C}$.

A single-soliton solution of equation (2.30) is characterised by a pair of discrete complex eigenvaules, $\lambda_1 = a + ib$ and c.c., of the Zakharov–Shabat operator and is given by

$$\psi_S(x,t) = 2ib\,\mathrm{sech}[2b(x + 4at - x_0)]\mathrm{e}^{-2\mathrm{i}(ax+2(a^2-b^2)t)+\mathrm{i}\phi_0}, \tag{2.32}$$

https://doi.org/10.1088/1742-5468/ac0f6d

J. Stat. Mech. (2021) 114001

where x_0 is the initial position of the soliton and ϕ_0 is the initial phase. One can see that the focusing NLS soliton represents a localised wavepacket with the envelope propagating with the group velocity $c_g = -4a = -4\,\mathrm{Re}\,\lambda_1$ and the carrier wave having the phase velocity $c_p = (b^2 - a^2)/a = -2\,\mathrm{Re}(\lambda_1^2)/\mathrm{Re}\,\lambda_1$. Also, similar to the defocusing and resonant NLS equations, and in contrast with KdV equation, the amplitude and velocity of the focusing NLS soliton are two independent parameters. We identify the two families $(\pm)$ of solitons according to the sign of their group velocity, $\mathrm{sgn}(c_g) = -\mathrm{sgn}(\mathrm{Re}\,\lambda)$.

Similar to other integrable NLS models, the solitons of the focusing NLS equation interact pairwise and experience both position and phase shifts upon the interaction. The position shifts in the focusing NLS overtaking and head-on soliton collisions are given by the same expression, $\Delta_{\pm\pm}(\lambda,\ \mu) = \Delta_{\pm\mp}(\lambda,\ \mu) \equiv \Delta(\lambda,\ \mu)$, where [84]

$$\Delta(\lambda,\mu) = \frac{\mathrm{sgn}[\mathrm{Re}(\mu-\lambda)]}{\mathrm{Im}\,\lambda}\,\ln\left|\frac{\mu-\bar{\lambda}}{\mu-\lambda}\right|. \tag{2.33}$$

One can see that the position shifts (2.33) satisfy conditions (2.17), so we classify the focusing NLS soliton collisions as isotropic.

The DOS $f(\lambda)$ of the focusing NLS soliton gas is generally supported on some compact Schwarz symmetric 2D sets $\Lambda \subset \mathbb{C}$, so it is sufficient to consider only the upper half plane part Λ^+. Here, Schwarz symmetry means that if $\lambda \in \mathbb{C}$ is a point of the spectrum then so is the c.c. point $\bar{\lambda}$. The kinetic equation for the focusing NLS soliton gas then assumes the form [36]

$$\begin{aligned} &f_t + (fs)_x = 0,\\ &s(\lambda,x,t) = -4\,\mathrm{Re}\,\lambda + \frac{1}{\mathrm{Im}\,\lambda}\iint_{\Lambda^+} \ln\left|\frac{\mu-\bar{\lambda}}{\mu-\lambda}\right| [s(\lambda,x,t) - s(\mu,x,t)] f(\mu,x,t)\mathrm{d}\xi\,\mathrm{d}\zeta, \end{aligned} \tag{2.34}$$

where $\mu = \xi + i\zeta$ and $\Lambda^+ \subset \mathbb{C}^+ \setminus i\mathbb{R}^+$.

The case $\Lambda^+ \subset i\mathbb{R}^+$ requires a separate consideration. Solitons of the focusing NLS equation can form stationary complexes described by the special N-soliton solutions, called bound states, for which all discrete spectrum points are located on the imaginary axis [84]. Since for the corresponding bound state soliton gas $\mathrm{Re}\,\lambda = 0$ the equation of state in (2.34) immediately yields $s(\lambda) = 0$ resulting in the equilibrium DOS, $f_t = 0$. It was shown in [25] that the turbulent wave field $\psi(x,t)$ associated with the DOS $f(\lambda)$ in a dense bound state soliton gas exhibits very peculiar statistical properties, shedding light on the fundamental phenomenon of spontaneous modulational instability. This special soliton gas will be considered in section 3.3.4.

2.3. Ensemble averages and modulation equations for soliton turbulence

Within the spectral kinetic description of soliton gas, the solitons are viewed as quasiparticles moving with the speeds determined by the nonlocal equation of state (2.13). The DOS $f(\lambda)$ in this description represents a comprehensive spectral characteristics of soliton gas. However, of ultimate interest in dispersive hydrodynamics is the description of the turbulent nonlinear wave field $u(x,t)$ associated with the underlying spectral

J. Stat. Mech. (2021) 114001

soliton gas dynamics. A natural question arises then: how to solve the inverse scattering problem, i.e. how to 'translate' the spectral characterisation of soliton gas (i.e. the DOS) into the statistical characterisation (ensemble averages, probability density function, correlations, etc) of the associated nonlinear random wave field $u(x,t)$ satisfying an integrable dispersive hydrodynamic equation, e.g. the KdV equation?

Within the classical, deterministic IST setting, the inverse spectral problem is solved via the Gelfand–Levitan–Marchenko equation (see e.g. [4, 72, 85]) or utilising the Riemann–Hilbert problem approach (see e.g. [86]). While the construction of a comprehensive extension of the IST for random potentials seems to be far away at present (see e.g. [87, 88] for some of the important developments), some valuable quantitative results can be obtained by elementary means. We shall describe some of these results using the KdV equation as the simplest accessible example, the generalisation to other integrable unidirectional and bidirectional dispersive hydrodynamic equations being straightforward.

As is well known (see e.g. [1, 70]), a turbulent wave field is characterised by the moments $\langle u^n\rangle$ over the statistical ensemble, which, assuming ergodicity, can be computed as spatial averages $\overline{u^n} = \frac{1}{\ell}\int_0^\ell u^n(\tilde{x},t)\mathrm{d}\tilde{x}$, over a sufficiently large 'mesoscopic' interval $l \ll \ell \ll L$, where l is the typical scale for spatial variations of $u(x,t)$ in a soliton gas, i.e. the typical soliton width, and L is the typical scale for spatial variations of the DOS $f(\lambda,x,t)$ in the non-uniform soliton gas. One of the fundamental properties of integrable dispersive hydrodynamics is the availability of an infinite set of local conservation laws

$$(P_i)_t + (Q_i)_x = 0, \quad i = 1,2,\cdots, \tag{2.35}$$

where P_i and Q_i are functions of the field variable u and its derivatives. For decaying initial data, the integrals $\int_{-\infty}^{\infty} P_i\,\mathrm{d}x$ are conserved in time. For the KdV equation the existence of an infinite series of local polynomial conservation laws was established in [89]. Their conserved densities, sometimes called Kruskal integrals, can be deduced from the Lax pair via appropriate expansions for large values of the spectral parameter (see [4, 90]), e.g. for KdV (2.1) $P_1 = u$, $P_2 = u^2$, $P_3 = \frac{u_x^2}{2} + u^3$. Here, we describe a simple heuristic approach proposed in [37] that enables one to link the spectral DOS $f(\lambda)$ of a soliton gas with the ensemble averages of P_i of the integrable dispersive hydrodynamic system (1.1). We describe the general principle using the KdV equation as a prototype example.

Consider a uniform KdV soliton gas, i.e. a gas whose statistical properties, particularly the DOS $f(\eta)$, do not depend on x,t (we return to the conventional use of the spectral variable $\eta = \sqrt{-\lambda}$ in the context of the KdV solitons, see section 2.1). We now make a natural assumption that the nonlinear wave field in a homogeneous soliton gas represents an ergodic random process, both in x and t (we note in passing that ergodicity is inherent in the spectral model of soliton gas that will be presented in section 3). The ergodicity property implies that the ensemble-averages $\langle P_i[u]\rangle$ in the soliton gas can be replaced by the corresponding spatial averages. Generally, for any functional $H[u(x,t)]$

J. Stat. Mech. (2021) 114001

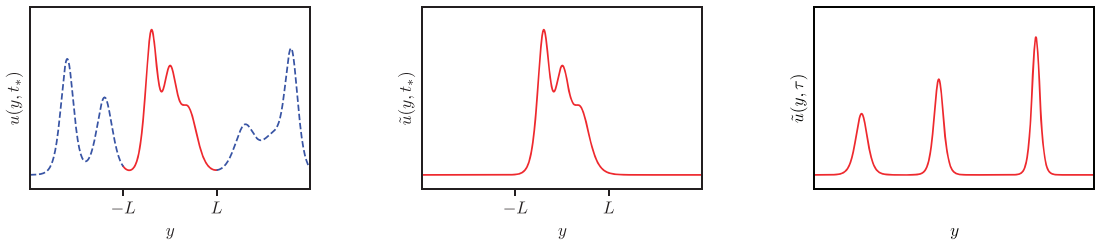

(a) Typical distribution $u(y,t_*)$ for a KdV soliton gas.

(b) Truncation of the distribution $u(y,t_*)$ for $y \in (-L,L)$.

(c) Variation of the truncated distribution $\tilde{u}(y,\tau)$ at time $\tau \gg t_*$.

Figure 6. Schematic for the evaluation of the integral (2.37) in soliton gas using the 'windowing' procedure.

we have

$$\langle H[u]\rangle = \lim_{L\to\infty}\frac{1}{2L}\int_{x-L}^{x+L} H[u(y,t)]\mathrm{d}y \tag{2.36}$$

for a single representative realisation of soliton gas. We define

$$I_j = \int_{x-L}^{x+L} P_j[u(y,t)]\mathrm{d}y, \quad j=1,2,\cdots, \tag{2.37}$$

where $P_j[u]$ is the conserved density and $L \gg 1$. Then $\langle P_j[u]\rangle = I_1/(2L) + \mathcal{O}(L^{-1})$.

Let $u(y,t)$ be a representative realization of a soliton gas and let $\tilde{u}(y,t)$ be defined in such a way that for some $t=t_*$ one has $\tilde{u}(y,t_*) = u(y,t_*)$ for $y \in (x-L, x+L)$ and $\tilde{u}(y,t_*) = 0$ outside of this interval so that the conserved densities $P_i[\tilde{u}(y,t_*)]$ and respective fluxes $Q_i[\tilde{u}(y,t_*)]$ also vanish outside $(x-L, x+L)$. To avoid complications, we assume that the transition between the two behaviors is smooth but sufficiently rapid so that such a 'windowed' portion of soliton gas (see figures 6(a) and (b)) can be approximated by the spectral N-soliton solution for some $N \gg 1$, with the discrete IST spectrum points $\eta_i, i=1,\cdots,N$ being distributed on $\Gamma = [0,1]$ with density $\varphi(\eta) \approx 2Lf(\eta)$ (recall the definition of DOS in section 1).

The integrals (2.37) then can be rewritten as

$$I_j = \int_{-\infty}^{+\infty} P_j[\tilde{u}(y,t)]\mathrm{d}y. \tag{2.38}$$

Since the integrals (2.38) do not depend on time, they can be computed at $t=\tau \gg t_*$ when the 'windowed' solution $\tilde{u}(x,t)$ gets resolved into a train of N well-separated solitons $u_s(x,t;\eta_i), i=1,\cdots,N$ (see figure 6(c)). Assuming that the overlap between the (exponentially decaying) solitons in the train becomes negligible as $t\to\infty$, the integral (2.38) can be represented as a sum of integrals over the individual soliton solutions,

$$I_j = \sum_{j=1}^{N} m_j(\eta), \qquad m_j = \int_{-\infty}^{+\infty} P_j[u_s(y,t;\eta_i)]\mathrm{d}y, \tag{2.39}$$

J. Stat. Mech. (2021) 114001

e.g. for the KdV equation the two first integrals in (2.39) are readily evaluated using the one-soliton solution (2.3) to give:

$$m_1(\eta) = \int_{-\infty}^{+\infty} u_{\rm s}(y,t;\eta)\mathrm{d}y = 4\eta, \qquad m_2(\eta) = \int_{-\infty}^{+\infty} u_{\rm s}^2(y,t;\eta)\mathrm{d}y = \frac{16}{3}\eta^3. \tag{2.40}$$

These are the 'spectral mass' and 'spectral momentum' of the η-soliton, respectively. Now, using (2.3) and taking the continuous limit as $N \to \infty$ in (2.39) according to $\sum_i F(\eta_i) \to \int_\Gamma F(\eta)\varphi(\eta)\mathrm{d}\eta$, we obtain the expressions for the first two statistical moments in the KdV soliton turbulence defined according to (2.36):

$$\langle u\rangle = 4\int_0^1 \eta f(\eta)\,\mathrm{d}\eta, \qquad \langle u^2\rangle = \frac{16}{3}\int_0^1 \eta^3 f(\eta)\,\mathrm{d}\eta. \tag{2.41}$$

One fundamental restriction imposed on the distribution function $f(\eta)$ follows from non-negativity of the variance,

$$\mathcal{A}^2 = \langle u^2\rangle \ - \ \langle u\rangle^2 \ \geqslant \ 0. \tag{2.42}$$

Some consequences of this restriction have been explored in [91]. In particular, considering the 'cold' soliton gas characterised by the Dirac delta-function DOS, $f(\eta) = w\delta(\eta - \eta_0)$ we obtain from (2.41) $\langle u\rangle = 4\eta_0 w$, $\langle u^2\rangle = \frac{16}{3}(\eta_0)^3 w$. Then, the condition (2.42) yields the constraint

$$w \leqslant \frac{\eta_0}{3}. \tag{2.43}$$

We note that the method presented here only requires one to integrate the single-soliton solution and thus can be readily applied to any integrable dispersive hydrodynamic system supporting the soliton resolution scenario. In particular, the ensemble averages for the density $\langle\rho\rangle$, velocity $\langle u\rangle$ and momentum $\langle\rho u\rangle$ in the bidirectional soliton gases for the defocusing and resonant NLS equations were obtained in [37]. Next, we note that the above simple derivation implies that expressions (2.41) apply to both dense and rarefied gas. Indeed, the same expressions were obtained in [50] for a rarefied KdV gas (see also [92] for the similar modified KdV equation results). In section 3, we will show how these expressions follow from the general spectral construction of soliton gas, not invoking the heuristic 'windowing' procedure.

In the above consideration of homogeneous soliton gases, the ensemble averages (2.36) are constant. For a weakly non-uniform (non-equilibrium) gas the DOS is a slowly varying function of x, t and so are the ensemble averages that now need to be interpreted as 'local averages' in the spirit of modulation theory [33]. Essentially, one invokes the 'mesoscopic' scale $l \ll \ell \ll L$ so that the DOS is approximately constant on any interval $(x-\ell, x+\ell)$. Then, the constant ensemble averages (2.36) are replaced by the slowly varying quantities:

$$\langle H[u]\rangle_\ell(x,t) = \frac{1}{2\ell}\int_{x-\ell}^{x+\ell} H[u(y,t)]\mathrm{d}y. \tag{2.44}$$

The 'local' averages $\langle H[u]\rangle_\ell$ do not depend on ℓ at leading order, and their spatiotemporal variations occur on x, t-scales that correspond to the scales associated with variations

J. Stat. Mech. (2021) 114001

of $f(\eta)$ and are much larger than typical (fast) variation scales of the nonlinear wave field $u(x,t)$. Using the scale separation and applying the ensemble averaging to the infinite set of conservation laws for integrable dispersive hydrodynamics, we obtain the modulation system for soliton gas:

$$\frac{\partial}{\partial t}\langle P_i[u]\rangle + \frac{\partial}{\partial x}\langle Q_i[u]\rangle = 0, \quad i = 1, 2, \cdots \tag{2.45}$$

Equation (2.45) can be viewed as a 'stochastic' version of the Whitham modulation equations [33], first discussed in [69]. Equation (2.45) can also be viewed as the integrable turbulence counterpart of the moment equations in the classical hydrodynamic turbulence theory [70]. As a matter of fact, the infinite-component stochastic modulation system (2.45) is consistent with the integro-differential kinetic equations (2.10) and (2.11). We note that the local ensemble averages of the infinite set of conserved densities $\langle P_i[u]\rangle(x,t)$ satisfying system (2.45) can be evaluated in terms of the spectral moments of the DOS $\int_0^1 \eta^{2n+1} f(\eta, x, t)\mathrm{d}\eta$, $n = 0, 1, 2, \cdots$, where $f(\eta, x, t)$ is a relevant solution of the kinetic equations (2.10) and (2.11).

3. Nonlinear spectral theory of soliton gas

The phenomenological kinetic theory of soliton gas described in the previous section is essentially based on the interpretation of solitons as quasi-particles experiencing short-range pairwise interactions accompanied by well-defined phase/position shifts. As was already stressed, although this theoretical framework is justifiable in the case of a rarefied gas, it is not quite satisfactory for a dense gas where solitons experience significant overlap and continual nonlinear interactions so that they could become indistinguishable as separate entities. Clearly it would be desirable to have a more mathematically robust approach to the description of a general, dense soliton gas that would, in particular, provide a formal justification of the collision rate assumption (2.12) and, consequently, of the equation of state (2.13), at least in some concrete cases of integrable dispersive hydrodynamics.

The above discussion strongly suggests that we need to look at the wave side of the soliton's 'dual identity'. As we already mentioned, there are insightful parallels between kinetic theory of soliton gas and the nonlinear wave modulation theory introduced by Whitham in 1965 [33, 93], just before the discovery of the IST method. The Whitham theory describes slow evolution (modulation) of the parameters characterising nonlinear periodic and quasiperiodic waves, such as amplitude, wavenumber, frequency, mean, etc. For integrable equations, such as the KdV and NLS equations, there is an elegant and powerful spectral approach to the derivation of the modulation equations first developed by Flaschka, Forest and McLaughlin for the KdV equation [35] and then extended to other integrable equations, such as the NLS, Benjamin–Ono, sine-Gordon equations, etc, by various authors. The spectral modulation theory is based on the extension of the IST method called the finite-gap theory [4, 5]. In this section, we will show how the finite-gap theory and modulation equations can be used to construct a mathematical model of soliton gas and justify the kinetic equation (2.10), equation (2.11) for the soliton gas

J. Stat. Mech. (2021) 114001

of the KdV equation and, further, equation (2.34) for the soliton gas of the focusing NLS equation.

3.1. The big picture

We start with a high-level description of the spectral theory of soliton gas based on properties of the so-called finite-gap modulated solutions of integrable dispersive hydrodynamic equations. For simplicity we shall refer to the scalar dispersive hydrodynamics (1.1), although the general principles are equally applicable to the vector, bidirectional case. Our qualitative description will be substantiated in the following sections by considering the examples of the KdV and the focusing NLS equations. As we have seen in section 2, the description of soliton gas includes two aspects: (i) the 'microscopic' structure of an equilibrium (uniform) gas, characterised by the equation of state (2.13); (ii) the slow evolution of the non-equilibrium (non-uniform) soliton gas' parameters described by the spectral transport equation (2.10). This setting bears a strong resemblance to the Whitham modulation theory in which the local microscopic structure is given by an exact periodic or quasiperiodic solution of a dispersive hydrodynamic equation, while the slow evolution is described by the modulation equations obtained via some period-averaging procedure or formal multiple scales analysis.

3.1.1. Spectral modulation theory of multiphase waves. The simplest yet most instructive example of modulation theory arises when considering the evolution of linear modulated waves in dispersive media, the so-called kinematic wave theory [33]. Dispersive hydrodynamics (1.1) upon linearisation about an equilibrium $u = u_0$ admit harmonic multiperiodic solutions in the form of a finite Fourier series

$$\tilde{u} = \sum_{j=1}^{N} a_j \, \mathrm{e}^{\mathrm{i}(k_j x - \omega_j t + \theta_j^0)}, \quad N \in \mathbb{N}, \tag{3.1}$$

where $\tilde{u} = u - u_0$, a_j are the amplitudes of the Fourier modes, $\boldsymbol{k} = (k_1, k_2, \cdots, k_N)$ and $\boldsymbol{\omega} = (\omega_1, \omega_2, \cdots, \omega_N)$ are the wavenumber and frequency vectors, respectively, and $\boldsymbol{\theta}^0 = (\theta_1^0, \cdots, \theta_N^0)$ is the initial phase vector. The frequency components in (3.1) satisfy the linear dispersion relation of (1.1), i.e. $\omega_j = \omega_0(k_j)$. Assuming non-commensurability of the components k_j and ω_j of the respective wavenumber and frequency vectors in (3.1), this solution is defined on N-dimensional 2π-torus,

$$\boldsymbol{\theta} = \boldsymbol{k}x - \boldsymbol{\omega}t + \boldsymbol{\theta}^0 \in [0, 2\pi) \times [0, 2\pi) \times \cdots \times [0, 2\pi) = \mathbb{T}^N. \tag{3.2}$$

For a modulated linear wave, all parameters in the Fourier series (3.1) become slow functions of x, t. To capture the modulations, one introduces a small parameter $\varepsilon \ll 1$ and writes an approximate solution as $\tilde{u}(\boldsymbol{\theta}, X, T) \sim \sum_{j=1}^{N} a_j(X, T) \mathrm{e}^{\mathrm{i}\theta_j(x,t)}$, where $X = \varepsilon x, T = \varepsilon t$ are the slow x and t variables, respectively, and $\theta_j(x, t) = \varepsilon^{-1} S_j(X, T)$ are the fast generalised phases. We now define the local wavenumbers and frequencies by

$$k_j(X, T) := \partial_x \theta_j = \partial_X S, \qquad \omega_j(X, T) := -\partial_t \theta_j = -\partial_T S(X, T), \tag{3.3}$$

J. Stat. Mech. (2021) 114001

so that in the absence of modulations the approximate solution reduces to the exact one (3.1). The phase consistency conditions $\partial_{xt}\theta_j = \partial_{tx}\theta_j$ then yield N wave conservation laws,

$$\boldsymbol{k}_T + \boldsymbol{\omega}_X = 0, \qquad \omega_j = \omega_0(k_j), \quad j = 1, \cdots, N. \tag{3.4}$$

System (3.4) represents the simplest example of modulation system. We note that the second part of (3.4) implies that, despite the slow x, t-variations, the components of the frequency vector remain locally (on the typical scale of the fast oscillations in θ) related to the wavenumber vector components by the same linear dispersion relations as in the non-modulated wave (3.1). This result is non-trivial and is established by a multiple scales analysis of the linearised dispersive hydrodynamics with the approximate solution $\tilde{u}(\boldsymbol{\theta}, X, T)$ as the leading order term in the perturbation series in ε. This analysis also yields the modulation equations for the amplitudes $a_j(X, T)$, which we do not consider here. We also note that the initial phases θ_j^0 can be viewed as independent random values, each uniformly distributed on $[0, 2\pi)$. Then, solution (3.1) becomes a random process, whose slow modulations are described by equation (3.4) complemented by the appropriate amplitude modulation equations.

We now turn to the nonlinear analogue of the multiphase solution (3.1). The one-phase nonlinear periodic solutions are quite common in dispersive hydrodynamics and describe travelling waves. However, the existence of *nonlinear multiphase, quasiperiodic* solutions is an exceptional feature of integrable PDEs. Let the integrable dispersive hydrodynamics (1.1) admit multiphase solutions

$$u(x,t) = F_N(\theta_1, \cdots, \theta_N), \qquad \theta_j = k_j x - \omega_j t + \theta_j^0, \tag{3.5}$$

so that

$$F_N(\theta_1, \cdots, \theta_j + 2\pi, \cdots, \theta_N) = F_N(\theta_1, \cdots, \theta_j, \cdots, \theta_N), \quad j = 1, 2, \cdots, N, \tag{3.6}$$

i.e. $\boldsymbol{\theta} = (\theta_1, \theta_2, \cdots, \theta_N) \in \mathbb{T}^N$. The quasiperiodic solution (3.5) can be viewed as a nonlinear analogue of the linearised Fourier solution (3.1).

The existence and properties of nonlinear multiphase solutions to the KdV equation were established in 1970s in a series of pioneering works [94–97] where the finite-gap theory, a nontrivial extension of the IST to periodic and quasiperiodic potentials, was developed (see also the monographs [4, 5] and a historical review [98]). It was shown that the most natural parametrisation of the multiphase solutions (3.5) is achieved in terms of the spectrum of the corresponding Lax operator. For the preliminary discussion of this section it is convenient to assume that the Lax operator is self-adjoint so that its spectrum is real-valued. This is the case for the (unidirectional) KdV and (bidirectional) defocusing NLS equations. The case of complex band spectrum arises for the focusing NLS equation, and this case will be considered separately in section 3.3. The fundamental result of the finite gap theory is that the Lax spectrum $\mathscr{S}_N$ of the N-phase solution (3.5) lies in the union of $N+1$ disjoint bands $\gamma_j = [\lambda_{2j-1}, \lambda_{2j}]$ (one of which could be semi-infinite, then $\gamma_{N+1} = [\lambda_{2N+1}, +\infty)$) separated by N finite gaps $c_j = (\lambda_{2j}, \lambda_{2j+1})$,

$$\lambda \in \mathscr{S}_N \equiv \cup_{i=1}^{N+1} \gamma_i \subset \mathbb{R}, \quad \gamma_i \cap \gamma_j = \emptyset, \ i \neq j. \tag{3.7}$$

J. Stat. Mech. (2021) 114001

For that reason multiphase solutions of integrable equations are often called finite-gap potentials (we recall that the Lax spectrum of a general periodic potential consists of an infinite number of bands and has an even more complicated structure for almost periodic potentials [99]). Thus, the real spectrum of a finite-gap potential is fully parametrised by the state vector $\boldsymbol{\lambda} = (\lambda_1, \lambda_2, \cdots, \lambda_{\mathcal{D}})$, where $\mathcal{D} = 2N + 1$ or $\mathcal{D} = 2N + 2$ depending on the presence or absence of a semi-infinite band.

One of the outcomes of the finite-gap theory are the nonlinear dispersion relations linking the physical parameters of the multiphase solution (3.5) such as the wavenumbers, frequencies, mean, etc, with the components of the $\mathcal{D}$-dimensional spectral state vector $\boldsymbol{\lambda}$. In particular, for the N-component wavenumber and frequency vectors $\boldsymbol{k}$ and $\boldsymbol{\omega}$ in (3.5), we have

$$k_j = K_j(\boldsymbol{\lambda}), \qquad \omega_j = \Omega_j(\boldsymbol{\lambda}), \quad j = 1, \cdots, N, \tag{3.8}$$

e.g. for the KdV equation the nonlinear dispersion relations (3.8) have the form (3.26).

By manipulating the endpoints of spectral bands λ_j, one can modify the waveform of the solution (3.5). Two limiting configurations are of particular interest.

(a) *Harmonic (linear wave) limit*. Achieved by collapsing spectral *gaps*, $|c_j| \equiv \lambda_{2j+1} - \lambda_{2j} \to 0$. In this limit the N-gap solution converts into the linear quasiperiodic solution (3.1), and the nonlinear dispersion relations (3.8) into the dispersion relation $\omega_j = \omega_0(k_j)$ for linearised wave modes. This is not surprising as the inverse scattering theory, including its finite-gap extension, essentially represents a nonlinear analogue of the Fourier method [85].

(b) *Solitonic limit*. In this limit, the N-gap quasiperiodic solution (3.5) transforms into the N-soliton solution exponentially decaying as $|x| \to \infty$ [94] (see also monograph [4]). Spectrally, the solitonic limit is realised by collapsing all finite *bands* into double points, $|\gamma_j| \equiv \lambda_{2j} - \lambda_{2j-1} \to 0$, more precisely, one requires vanishing of the band/gap ratio, $r_j = |\gamma_j|/|c_j| \to 0$. The collapsed bands correspond to the discrete spectrum points in the traditional IST for decaying potentials. On the other hand, the spectral limit $r_j \to 0$ implies vanishing of the corresponding wavenumber, $k_j \to 0$, which is another, physically suggestive way to describe the solitonic limit of finite-gap potentials, particularly useful in the context of soliton gases.

As a simple example illustrating the harmonic and solitonic limits in finite-gap potentials, we consider the one-gap (single-phase) KdV solution. For $N = 1$ the KdV Lax spectrum $\mathscr{S}_1 = [\lambda_1, \lambda_2] \cup [\lambda_3, \infty)$, and the corresponding KdV solution (3.5) assumes the form of a 'cnoidal wave' (see e.g. [72]); without loss of generality, we set $\lambda_3 = 0$,

$$u(x,t) = F_1(\theta; \boldsymbol{\lambda}) = \lambda_2 - \lambda_1 - 2\lambda_2 \operatorname{cn}^2\left(\frac{K(m)}{\pi}\theta; m\right), \tag{3.9}$$

where $\operatorname{cn}[\cdot]$ is the Jacobi elliptic function, $m = \lambda_2/\lambda_1$ is the modulus, $K(m)$ is the complete elliptic integral of the first kind, and $\theta = kx - \omega t + \theta^0$ is the phase with the wavenumber k and the frequency ω given by the nonlinear dispersion relations (cf (3.8))

$$k = \frac{\pi\sqrt{-\lambda_1}}{K(m)}, \qquad \omega = -2k(\lambda_1 + \lambda_2). \tag{3.10}$$

J. Stat. Mech. (2021) 114001

The band/gap ratio in the one-gap solution is given by $r = (\lambda_2 - \lambda_1)/(-\lambda_2)$. The solitonic limit $r \to 0$ ($\lambda_2, \lambda_1 \to -\eta^2$) of (3.9) and (3.10) is then evaluated using the asymptotic behaviour of elliptic functions for $1 - m \sim r \ll 1$ [100],

$$r \to 0: \quad k \sim \frac{1}{\ln \frac{1}{r}} \to 0, \qquad \frac{\omega}{k} \to 4\eta^2, \qquad \mathrm{cn} \to \mathrm{sech}^2, \tag{3.11}$$

so that solution (3.9) takes the form of a soliton (2.3),

$$u(x,t) = u_{\mathrm{s}}(x,t;\eta) = 2\eta^2 \,\mathrm{sech}^2[\eta(x - 4\eta^2 t - x^0)]. \tag{3.12}$$

The opposite, harmonic limit of the cnoidal wave solution (3.9) is realised by closing the spectral gap (i.e. letting $m \to 0$), but we do not consider this limit here as it does not play a role in the soliton gas construction.

The above consideration provides a good intuition for what happens in the general case $N > 1$. Indeed, as shown in [6, 101], a N-gap KdV solution can be represented as a nonlinear superposition of N cnoidal waves with the interaction between the nonlinear modes described by the so-called Riemann period matrix B (see equation (3.25) below). In the N-soliton limit ($r_j \to 0 \ \forall \ j = 1, 2, \cdots, N$), one has (see e.g. [6, 98])

$$k_j \to 0, \quad B_{jj} \to \infty, \qquad B_{ij} \to \frac{i}{\pi} \ln \left| \frac{\eta_i + \eta_j}{\eta_i - \eta_j} \right|, \quad i \neq j, \ i, j = 1, 2 \cdots, N, \tag{3.13}$$

so that the off-diagonal elements of the interaction matrix transform into the normalised two-soliton phase shifts (cf (2.5)).

Modulation theory of nonlinear multiphase waves $F_N(\boldsymbol{\theta}; \boldsymbol{\lambda})$ describes slow evolution of the endpoints of the band spectrum, $\boldsymbol{\lambda} = \boldsymbol{\lambda}(X, T)$, where $X = \varepsilon x$, $T = \varepsilon t$, $\varepsilon \ll 1$ [35, 67]. Similar to the linear modulation theory, slow modulations necessitate the introduction of the generalised phase vector $\boldsymbol{\theta} = \boldsymbol{S}(X, T)/\varepsilon$ so that the local wavenumber and local frequency vectors are defined by (cf (3.3))

$$\boldsymbol{k}(X,T) := \boldsymbol{\theta}_x = \boldsymbol{S}_X, \qquad \boldsymbol{\omega}(X,T) := -\boldsymbol{\theta}_t = -\boldsymbol{S}_T. \tag{3.14}$$

The consistency condition $\boldsymbol{\theta}_{xt} = \boldsymbol{\theta}_{tx}$ then leads to the system of N wave conservation equations, an analogue of the kinematic equation (3.4) for linear waves with an important difference that, instead of the linear dispersion relation $\omega = \omega_0(k)$ linking the components of the frequency and wavenumber vectors, it now includes the nonlinear dispersion relations (3.8) for finite-gap potentials,

$$\boldsymbol{k}_T + \boldsymbol{\omega}_X = 0, \qquad \boldsymbol{k} = \boldsymbol{K}[\boldsymbol{\lambda}(X,T)], \quad \boldsymbol{\omega} = \boldsymbol{\Omega}[\boldsymbol{\lambda}(X,T)]. \tag{3.15}$$

Importantly, the kinematic modulation system (3.15) for a general case of multiphase nonlinear waves is not closed since $\dim(\boldsymbol{\lambda}) = \mathcal{D} > N$. Indeed, the full modulation system contains $\mathcal{D}$ equations for $\lambda_j(X, T)$, and the wave conservation equations are always consistent with (but not equivalent to) the full system (see [35] for the complete description of the KdV spectral modulation theory). However, in the harmonic and soliton limits corresponding to the collapsed spectral gaps or bands, the dimension $\mathcal{D}$ of the state vector $\boldsymbol{\lambda}$ decreases, enabling the necessary closure for the system of wave conservation laws in (3.15) under the additional constraint of constant background (see [17, 102] for

J. Stat. Mech. (2021) 114001

the relevant theory of the dynamic wave-mean flow interaction showing how the effects of nonconstant background can be included). In particular, in the harmonic limit system (3.15) transforms into the kinematic system (3.4). The solitonic limit is a singular one and requires a more delicate treatment.

3.1.2. Thermodynamic limit of finite-gap spectral solutions. The main idea of the spectral construction of soliton gas is to simultaneously take the solitonic limit and the limit $N \to \infty$ of N-gap potential in such a way that

$$k_1, \cdots, k_N \to 0, \quad N \to \infty \text{ but } \lim_{N\to\infty} \sum_{j=1}^{N} k_j = 2\pi\beta = \mathcal{O}(1), \tag{3.16}$$

with a similar behaviour for the frequency components ω_j. The limit (3.16) is the thermodynamic type limit for nonlinear multiphase waves (as we shall see, β in (3.1.2) agrees with the soliton gas density introduced earlier in (2.7)). This limit suggests the following scaling for the wavenumbers and frequencies:

$$k_j \sim \omega_j \sim \frac{1}{N}, \quad N \gg 1. \tag{3.17}$$

Analysis of the nonlinear dispersion relations (3.8) for the KdV and NLS equations yields the asymptotic structure of the spectral set $\mathscr{S}_N$ compatible with the thermodynamic scaling (3.17). It turns out that the large N behaviour (3.17) of k_j, ω_j can be achieved by introducing the special distribution of spectral bands γ_j and gaps c_j on a fixed spectral interval $\Gamma = [\lambda_1, \lambda_{\mathcal{D}}]$ (an arc in the complex plane for the focusing NLS), such that

$$|c_j| \sim -\ln^{-1}|\gamma_j| \sim \frac{1}{N}, \quad N \gg 1, \tag{3.18}$$

i.e. by making the bands exponentially narrow compared to the gaps. We note that the band-gap scaling (3.18) is inspired by the spectrum of the periodic Lax operator (2.2) in the semiclassical limit [71, 103].

We shall call the band-gap scaling (3.18) the exponential *thermodynamic spectral scaling* and denote the limit as $N \to \infty$ of a function $F(\boldsymbol{\lambda})$ considered on the set $\{\lambda_j\}$ obeying this scaling as $\mathfrak{T}\text{-}\lim F(\boldsymbol{\lambda})$. For the thermodynamic scaling (3.18), we have $r_j = |\gamma_j|/|c_j| \to 0 \ \forall \ j$, essentially yielding an infinite-soliton limit, in full agreement with our intention to describe soliton gas. Other meaningful scalings (sub-exponential, super-exponential) compatible with (3.17) and leading to special cases of soliton gases are possible and will be discussed later.

We will show that the application of the thermodynamic limit to the kinematic modulation system (3.15) results in the kinetic equation for soliton gas

$$f_{\tilde{T}} + (sf)_{\tilde{X}} = 0, \qquad s(\lambda) = \mathcal{S}[f(\lambda)], \tag{3.19}$$

where $\mathcal{S}[\cdots]$ is a functional and

$$f(\lambda) = \frac{\mathrm{d}}{\mathrm{d}\lambda}\left\{\mathfrak{T}\text{-}\lim \sum_{j=1}^{M\leqslant N} k_j\right\}, \qquad s(\lambda) = \mathfrak{T}\text{-}\lim \frac{\omega_j}{k_j} \tag{3.20}$$

J. Stat. Mech. (2021) 114001

are the DOS and the transport velocity, respectively, both depending on the continuous parameter $\lambda \in \Gamma$ and on the 'superslow' spacetime variables $\tilde{X} = \delta x$, $\tilde{T} = \delta t$, where $\delta \ll \varepsilon \ll 1$ is a small parameter that scales the typical spatiotemporal modulations of soliton gas, which are much slower than those associated with the typical Whitham modulations of finite-gap potentials. In practice, we will not be introducing the small parameters ε and δ explicitly, assuming that the typical x, t-variations of u and $f(\lambda)$ occur on disparate micro- and macroscopic scales, respectively.

The outlined construction was concerned with the spectral characterisation of soliton gas defined as a thermodynamic limit of finite-gap potentials and can be symbolically represented as $\mathscr{S}_N \to f(\lambda)$. However, this description is incomplete as the Lax spectrum $\mathscr{S}_N$ determines the finite-gap potential (3.5) only up to N initial phases, $\boldsymbol{\theta}^0 \in \mathbb{T}^N$. For a general finite-gap potential, the respective incommensurability of the components of the wavenumber and frequency vectors in (3.5) implies dense winding on the phase torus. Then, the natural assumption for the construction of soliton gas would be to let the components of $\boldsymbol{\theta}^0$ be independent random values, each distributed uniformly on $[0, 2\pi)$. This is the so-called random phase approximation, the standard assumption in the wave turbulence theory [1], which has also been used for the construction of random finite-gap solutions of the KdV equation in [104] and of the focusing NLS equation in [105, 106]. Following the classical construction of the configuration space of the ideal one-dimensional gas of non-interacting particles (see e.g. [107]), it can be shown that, upon the thermodynamic limit the uniform distribution of the initial phase vector $\boldsymbol{\theta}^0$ over the invariant torus $\mathbb{T}^N$ transforms into the Poisson distribution on $\mathbb{R}$ with the density $\beta = \int_0^1 f(\lambda)\mathrm{d}\lambda$ for the position phases $x_j = \theta_j^0/k_j$ [34], which is consistent with the distribution of the soliton centres in the phenomenologically introduced rarefied soliton gas (2.8). The derivation of the Poisson distribution for the position phases in the KdV soliton gas will be presented in section 3.2.3.

3.2. Soliton gas for the KdV equation

3.2.1. Thermodynamic limit and nonlinear dispersion relations for soliton gas. We now realise the thermodynamic spectral limit construction of soliton gas for the KdV equation (2.1) following [32, 34]. The Lax spectrum (3.7) of the N-phase KdV solution (3.5) lies in the union of bands,

$$\lambda \in [\lambda_1, \lambda_2] \cup [\lambda_3, \lambda_4] \cup \cdots \cup [\lambda_{2N+1}, \infty). \tag{3.21}$$

The state vector $\boldsymbol{\lambda} = (\lambda_1, \lambda_2, \cdots, \lambda_{2N+1})$ parameterises the N-gap KdV solution up to N initial phases θ_j^0, which we assume to be independent random values, each uniformly distributed on $[0, 2\pi)$. In what follows, we take advantage of some known results from the KdV finite-gap theory [4, 5, 35] and apply them to the description of the KdV soliton gas.

(a) *Nonlinear dispersion relations for finite-gap potentials*

To formulate the nonlinear dispersion relations (3.8) for the multiphase KdV solutions, we need to introduce several fundamental objects underlying the algebraic structure of finite-gap potentials expressible in terms of multidimensional Riemann theta-functions [108]. In the finite-gap theory, the vector $\boldsymbol{\lambda} =$

J. Stat. Mech. (2021) 114001

$(\lambda_1, \lambda_2, \cdots, \lambda_{2N+1})$ of the endpoints of the spectral bands defines the two-sheeted hyperelliptic Riemann surface $\mathcal{R}$ of genus N via

$$R(z) = \prod_{j=1}^{2N+1} (z - \lambda_j)^{1/2}, \quad z \in \mathbb{C}, \tag{3.22}$$

with $R \sim z^{N+1/2}$ as $z \to \infty$. We make the branch cuts of $R(z)$ along the spectral bands $[\lambda_1, \lambda_2]$, $\cdots$, $[\lambda_{2j-1}, \lambda_{2j}]$, $\cdots$, $[\lambda_{2N+1}, \infty)$ and introduce a canonical homology basis on $\mathcal{R}$ as follows (see figure 7): the α_j-cycle surrounds the jth band clockwise on the upper sheet, and the β_j-cycle is canonically conjugated to α_j, such that the closed contour β_j starts at λ_{2j}, goes to $+\infty$ on the upper sheet and returns to λ_{2j} on the lower sheet.

We introduce a basis of holomorphic differentials on $\mathcal{R}$:

$$w_j = \sum_{k=0}^{N-1} \kappa_{jk} \frac{z^k}{R(z)} \, \mathrm{d}z, \quad j = 1, \cdots, N, \tag{3.23}$$

where the coefficients $\kappa_{jk}(\boldsymbol{\lambda})$ are determined by the normalisation over the α-cycles

$$\oint_{\alpha_k} w_j = \delta_{jk}, \tag{3.24}$$

while the integrals over the β-cycles give the entries of the symmetric $N \times N$ Riemann period matrix B,

$$B_{ij} = \oint_{\beta_j} w_i \tag{3.25}$$

with positive definite imaginary part.

The components k_j, ω_j of the wavenumber and frequency vectors are expressed in terms of the branch points λ_j of the spectral Riemann surface (3.22) by the relations [35]

$$\begin{aligned} \boldsymbol{k} &= -4\pi i B^{-1} \boldsymbol{\kappa}^{(N-1)}, \\ \boldsymbol{\omega} &= 8\pi i B^{-1} \left(\boldsymbol{\kappa}^{(N-1)} \sum_{j=1}^{2N+1} \lambda_j + 2\boldsymbol{\kappa}^{(N-2)} \right), \end{aligned} \tag{3.26}$$

where $[\boldsymbol{\kappa}^{(M)}]_i \equiv \kappa_{iM}$. These are the nonlinear dispersion relations (3.8) for finite-gap KdV solutions.

(b) *Thermodynamic spectral scaling*

We now introduce the exponential thermodynamic scaling (3.18) for the spectrum (3.21) of the KdV finite-gap solutions. We fix $\lambda_1 = -1$, $\lambda_{2N+1} = 0$ and, following [71], consider the lattice of points $0 < \eta_N < \eta_{N-1} < \cdots < \eta_1 < 1$, where

$$-\eta_j^2 = \frac{1}{2} (\lambda_{2j-1} + \lambda_{2j}) \tag{3.27}$$

J. Stat. Mech. (2021) 114001

are the centres of the spectral bands. Let $|\delta_j| = \lambda_{2j} - \lambda_{2j-1}$ and $|c_j| = \lambda_{2j+1} - \lambda_{2j}$ be the j-th band and j-th gap widths, respectively. We then define two positive smooth functions on $[0, 1]$:

(i) The normalised density $\varphi(\eta) > 0$ of the band centre points η_j, introduced such that

$$\eta_j - \eta_{j+1} \sim \frac{1}{N\varphi(\eta_j)},\ j = 1, \cdots, N,\ N \gg 1, \qquad \int_0^1 \varphi(\eta)\mathrm{d}\eta = 1, \tag{3.28}$$

i.e. $\varphi(\eta)\mathrm{d}\eta$ is the probability measure on $[0, 1]$.

(ii) The normalised logarithmic band width distribution $\tau(\eta) > 0$ defined by

$$\tau(\eta_j) \sim -\frac{1}{N} \ln\left(\lambda_{2j} - \lambda_{2j-1}\right),\ j = 1, \cdots, N,\ N \gg 1. \tag{3.29}$$

The functions $\varphi(\eta)$ and $\tau(\eta)$ asymptotically define the Riemann surface $\mathcal{R}$ (3.22) for $N \gg 1$. The asymptotics (3.28) and (3.29) imply the exponential spectral scaling (cf (3.18))

$$|c_j| \sim \frac{1}{\varphi(\eta_j)N}, \qquad |\gamma_j| \sim \exp\{-N\tau(\eta_j)\}, \quad j = 1, \cdots, N,\ N \gg 1. \tag{3.30}$$

Other spectral scalings of interest are the sub-exponential scaling: $\mathrm{e}^{-aN} \ll |\gamma_j| \ll \frac{1}{N},\ j = 1, \cdots, N$ for any $a > 0$, and super-exponential scaling: $\mathrm{e}^{-aN} \gg |\gamma_j|, j = 1, \cdots, N$ for any $a > 0$. The latter corresponds to the case of an 'ideal' soliton gas consisting of noninteracting solitons, and the former to the special kind of soliton gas termed *soliton condensate*. These scalings were introduced in [38] in the context of the focusing NLS soliton gas and will be considered in section 3.3.

(c) *Nonlinear dispersion relations for soliton gas*

We rewrite the nonlinear dispersion relations (3.26) as

$$B\boldsymbol{k} = -4\pi i\boldsymbol{\kappa}^{(N-1)}, \qquad B\boldsymbol{\omega} = 8\pi i\left(\boldsymbol{\kappa}^{(N-1)}\sum_{j=1}^{2N+1}\lambda_j + 2\boldsymbol{\kappa}^{(N-2)}\right) \tag{3.31}$$

and apply the thermodynamic spectral scaling (3.30). For that, we introduce the lattice (3.27) and the large N expansions (3.28), (3.29) in (3.23)–(3.25), which gives at leading order [71] (cf (3.13)):

$$B_{jj} \sim \frac{i}{\pi}N\tau(\eta_j), \qquad B_{kj} \sim \frac{i}{\pi}\ln\left|\frac{\eta_k + \eta_j}{\eta_k - \eta_j}\right| \quad \text{when } k \neq j, \tag{3.32}$$

$$\kappa_{j,N-1} \sim -\frac{\eta_j}{2\pi}, \qquad \kappa_{j,N-1}\sum_{j=1}^{2N+1}\lambda_j + 2\kappa_{j,N-2} \sim \frac{\eta_j^3}{\pi}. \tag{3.33}$$

J. Stat. Mech. (2021) 114001

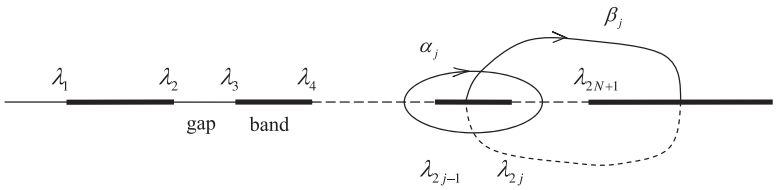

Figure 7. Spectrum of N-gap solution of the KdV equation and the canonical homology basis on the Riemann surface $\mathcal{R}$ (3.22).

In view of (3.32) and (3.33), the balance of terms in the dispersion relations (3.31) necessitates the following scaling for the components of the wavenumber and frequency N-vectors (cf (3.17)):

$$k_j \sim \frac{\varkappa(\eta_j)}{N}, \qquad \omega_j \sim \frac{\nu(\eta_j)}{N}, \quad N \gg 1, \tag{3.34}$$

where $\varkappa(\eta) \geqslant 0$ and $\nu(\eta)$ are smooth functions on $[0,1]$.

Substituting (3.32)–(3.34), in (3.31), we arrive at two algebraic systems for $\varkappa(\eta_k)$, $\nu(\eta_k)$, $k = 1, \cdots, N$:

$$\sum_{j=1}^{N} \frac{1}{N} \ln\left|\frac{\eta_k+\eta_j}{\eta_k-\eta_j}\right| \varkappa(\eta_j) + \tau(\eta_k)\varkappa(\eta_k) = 2\pi\eta_k, \tag{3.35}$$

$$\sum_{j=1}^{N} \frac{1}{N} \ln\left|\frac{\eta_k+\eta_j}{\eta_k-\eta_j}\right| \nu(\eta_j) + \tau(\eta_k)\nu(\eta_k) = 8\pi\eta_k^3. \tag{3.36}$$

Passing to the continuum limit as $N \to \infty$, we obtain the nonlinear dispersion relations for soliton gas:

$$\int_0^1 \ln\left|\frac{\eta+\mu}{\eta-\mu}\right| f(\mu)\mathrm{d}\mu + \sigma(\eta)f(\eta) = \eta, \tag{3.37}$$

$$\int_0^1 \ln\left|\frac{\eta+\mu}{\eta-\mu}\right| v(\mu)\mathrm{d}\mu + \sigma(\eta)v(\mu) = 4\eta^3, \tag{3.38}$$

where

$$f(\eta) = \frac{1}{2\pi}\varphi(\eta)\varkappa(\eta)\,; \qquad v(\eta) = \frac{1}{2\pi}\varphi(\eta)\nu(\eta), \qquad \sigma(\eta) = \frac{\tau(\eta)}{\varphi(\eta)} > 0. \tag{3.39}$$

For a given function $\sigma(\eta)$, which encodes the Lax spectrum in the thermodynamic limit, the integral equations (3.37) and (3.38) specify two functions $f(\eta)$ and $v(\eta)$, which we identify below as the DOS and the spectral flux density of the soliton gas, respectively.

Consider a partial sum $K_M = \frac{1}{2\pi}\sum_{j=1}^{M} k_j$ over the spectral lattice $\{\eta_1, \eta_2, \cdots, \eta_N\}$, where $1 \leqslant M \leqslant N$. Given that $2\pi k_j$ is the spatial density of waves (which we treat as quasiparticles) associated with the jth spectral band, the quantity K_M has the meaning

J. Stat. Mech. (2021) 114001

of the integrated DOS [99, 109]. Invoking the scaling (3.34) and passing to the continuum limit $N \to \infty$, $\eta_M \to \eta$, we obtain

$$K_M = \frac{1}{2\pi}\sum_{j=1}^{M} \frac{\varkappa(\eta_j)}{N} \to \frac{1}{2\pi}\int_0^{\eta} \varkappa(\mu)\varphi(\mu)\mathrm{d}\mu \equiv \mathcal{K}(\eta). \tag{3.40}$$

Then, the DOS is given by

$$\mathcal{K}'(\eta) = \frac{1}{2\pi}\varkappa(\eta)\varphi(\eta) = f(\eta). \tag{3.41}$$

Similarly, for the temporal counterpart of the integrated DOS—the spectral flux—we have

$$\Omega_M = \frac{1}{2\pi}\sum_{j=1}^{M} \omega_j = \frac{1}{2\pi}\sum_{j=1}^{M} \frac{\nu(\eta_j)}{N} \to \frac{1}{2\pi}\int_0^{\eta} \nu(\mu)\varphi(\mu)\mathrm{d}\mu \equiv \mathcal{V}(\eta), \tag{3.42}$$

so that the spectral flux density in a soliton gas is given by

$$\mathcal{V}'(\eta) = \frac{1}{2\pi}\nu(\eta)\varphi(\eta) = v(\eta). \tag{3.43}$$

3.2.2. Equation of state and spectral kinetic equation. Eliminating σ from the nonlinear dispersion relations (3.37) and (3.38), we obtain for $s(\eta) = v(\eta)/f(\eta)$

$$s(\eta) = 4\eta^2 + \frac{1}{\eta}\int_0^1 \ln\left|\frac{\eta+\mu}{\eta-\mu}\right| f(\mu)[s(\eta) - s(\mu)]\mathrm{d}\mu, \tag{3.44}$$

which is exactly the equation of state (2.11) obtained in section 2 under the collision rate assumption (2.12). Hence, this assumption is now justified.

As suggested by the phenomenological derivation in section 2, the function $s(\eta)$ in (3.44) has the meaning of the effective soliton velocity (i.e. the transport velocity) in a soliton gas. We will now show how this interpretation is justified within the thermodynamic limit framework. To this end, we consider non-equilibrium soliton gas with $f(\eta) \equiv f(\eta, x, t)$, $s(\eta) \equiv s(\eta, x, t)$ and derive the evolution equation for the DOS. We go back to the original, discrete wavenumber and frequency components $k_j(\boldsymbol{\lambda})$, $\omega_j(\boldsymbol{\lambda})$ of the finite-gap potential, defined in terms of the fixed branch points $\boldsymbol{\lambda}$ of the Riemann surface $\mathcal{R}$ of (3.22). Let us now consider a slowly modulated finite-gap potential with $\boldsymbol{\lambda} = \boldsymbol{\lambda}(x, t)$. The modulation system describing the evolution of $2N + 1$ parameters $\lambda_1(x, t), \lambda_2(x, t), \cdots, \lambda_{2N+1}(x, t)$ has been derived in [35]. This system admits an infinite number of hyperbolic conservation laws that include a finite subset of N wave conservation laws (3.15), which can be manipulated into the equivalent system

$$\partial_t K_M + \partial_x \Omega_M = 0, \quad M = 1, \cdots, N, \tag{3.45}$$

where $K_M = \frac{1}{2\pi}\sum_{j=1}^{M} k_j$ and $\Omega_M = \frac{1}{2\pi}\sum_{j=1}^{M} \omega_j$ as defined in the previous section. Applying the thermodynamic limit (3.40)–(3.43) to (3.45) yields the transport equation for DOS

$$f_t + (fs)_x = 0, \tag{3.46}$$

J. Stat. Mech. (2021) 114001

where $s = v/f$ is identified as the transport velocity of soliton gas, as expected. Thus, we have derived the kinetic equation for the KdV soliton gas as the thermodynamic limit of the multiphase Whitham modulation system.

Integrating equation (3.46) over the spectral interval $[0, 1]$, we obtain the conservation equation

$$\beta_t + \zeta_x = 0 \tag{3.47}$$

for the total integrated density of solitons in the gas $\beta(x,t) = \int_0^1 f(\eta, x, t)\mathrm{d}\eta$. The function $\zeta(x,t) = \int_0^1 v(\eta, x, t)\mathrm{d}\eta$ has the meaning of the soliton gas frequency. Generally, multiplying (3.46) by an arbitrary nonsingular function $p(\eta)$ and integrating over spectrum, we obtain the conservation law for $M(x,t) = \int_0^1 p(\eta) f(\eta, x, t)\mathrm{d}\eta$. In particular, choosing $p(\eta) = C_n \eta^{2n-1}$, $n \in \mathbb{N}$ with $C_n = \frac{2^{2n}}{2n-1}$, we obtain the series of averaged conservation laws for the KdV equation—the Whitham equations for soliton gas (2.45), where the ensemble averages of the polynomial conserved densities (the Kruskal integrals, see section 2.3) are expressed in terms of the DOS as [32, 91]

$$\langle P_n[u] \rangle = \frac{2^{2n}}{2n-1} \int_0^1 \eta^{2n-1} f(\eta)\mathrm{d}\eta. \tag{3.48}$$

In particular, for $n = 1, 2$ the Kruskal integrals coincide with the respective statistical moments of u—the observables of the KdV soliton gas field—and have the form

$$\langle u \rangle(x,t) = 4 \int_0^1 \eta f(\eta, x, t)\mathrm{d}\eta, \qquad \langle u^2 \rangle(x,t) = \frac{16}{3} \int_0^1 \eta^3 f(\eta, x, t)\mathrm{d}\eta, \tag{3.49}$$

in full agreement with the result (2.41) obtained by the heuristic 'windowing' procedure in section 2.3.

Concluding this section, we note that in the presented construction of soliton gas it was assumed that solitons propagate on a fixed (zero) background, which was achieved by fixing the endpoint $\lambda_{2N+1} = 0$ of the spectrum (3.21). A generalisation to a slowly varying background is possible following the modulation construction of solitonic dispersive hydrodynamics in [17, 110]. Such a generalisation could provide interesting insights into new soliton gas phenomena.

3.2.3. Poisson distribution for position phases. Having defined the thermodynamic limit for the spectrum of finite-gap potentials $F_N(\boldsymbol{\theta})$, $\boldsymbol{\theta} \in \mathbb{T}^N$, we now need to determine what happens with the phases $\theta_j = k_j x - \omega_j t + \theta_j^{(0)}$, $j = 1, \cdots, N$ in this limit.

As discussed in section 3.1.2 we adopt the random phase approximation in which the initial phases $\theta_j^{(0)}$ are assumed to be N independent random values uniformly distributed on $[0, 2\pi)$. Under the random phase approximation, the finite-gap potential $u(x,t)$ transforms into an ergodic random process [99], both as functions of x and t. We now fix $t = t^*$ and represent the cyclic phases $\theta_j (\mathrm{mod}\, 2\pi)$ in the form $\theta_j = k_j(x - x_j)$, where the position phases $x_j = x_j^0 + c_j t^*$ with $c_j = \omega_j / k_j$ being the phase velocities. The initial position phases $x_j^0 = -\theta_j^{(0)}/k_j$ are independent random values, each distributed uniformly on the respective period interval $[0, 2\pi/k_j)$ or, equivalently, $[-\pi/k_j, \pi/k_j)$.

J. Stat. Mech. (2021) 114001

The deterministic shifts $c_j t^*$ can be absorbed into the random initial positions so that we shall replace $x_j^{(0)} \to x_j$.

The thermodynamic spectral scaling (3.30) implies that in the limit $N \to \infty$ all wavenumbers vanish, $k_j \to 0$, i.e. all spatial periods of the finite-gap solution become infinite. We now demonstrate that, upon the thermodynamic limit (3.16) the uniform distribution of $\boldsymbol{\theta}^{(0)}$ on $\mathbb{T}^N$ transforms into the Poisson distribution for the position phases $x_j \in \mathbb{R}$.

Let Δ be an arbitrary finite interval on the line. We assume that for sufficiently small k_j's we have $\Delta \subset [-\pi/k_j, \pi/k_j)\, \forall j = 1, 2, \cdots, N$. We introduce a random value $\xi_j = \chi_\Delta(x_j)$, where

$$\xi_j = \begin{cases} 1 & \text{if } x_j \in \Delta \\ 0 & \text{if } x_j \notin \Delta, \end{cases} \tag{3.50}$$

with the probabilities $p(\xi_j = 1) = (k_j/2\pi)\Delta$, $p(\xi_j = 0) = 1 - (k_j/2\pi)\Delta$. The probability-generating function $\Phi_j(z)$ for ξ_j is

$$\Phi_j(z) = (1 - p_j) + z p_j. \tag{3.51}$$

Now let $\xi^{(N)} \equiv \sum_{j=1}^N \xi_j$, which is the number of points x_j that have fallen into the interval Δ. Since ξ_j are independent random variables, the probability-generating function for $\xi^{(N)}$ is

$$\Phi^{(N)}(z) = \prod_{j=1}^N \Phi_j(z) = \prod_{j=1}^N (1 + (z-1)p_j) = \prod_{j=1}^N \left(1 + \frac{(z-1)k_j|\Delta|}{2\pi}\right). \tag{3.52}$$

For $N \gg 1$ the thermodynamic scaling implies $k_j \sim N^{-1} \ll 1$ and we have

$$\ln \Phi^{(N)} = (z-1)\frac{|\Delta|}{2\pi}\sum_{j=1}^N k_j + \mathcal{O}(N^{-1}). \tag{3.53}$$

Taking the thermodynamic limit we obtain:

$$\mathfrak{T}\text{-}\lim\, \Phi^{(N)}(z) = \exp[(z-1)\beta|\Delta|] = \mathrm{e}^{-\beta|\Delta|}\,\mathrm{e}^{\beta|\Delta|z} = \sum_{n=0}^\infty z^n \left(\mathrm{e}^{-\beta|\Delta|}\frac{(\beta|\Delta|)^n}{n!}\right), \tag{3.54}$$

where

$$\beta = \mathfrak{T}\text{-}\lim\left\{\frac{1}{2\pi}\sum_{j=1}^N k_j\right\} = \int_0^1 f(\eta)\mathrm{d}\eta.$$

Hence, the probability of having n points x_i in the interval Δ is given by the Poisson distribution

$$P_\Delta(n, \beta) = \mathrm{e}^{-\beta|\Delta|}\frac{(\beta|\Delta|)^n}{n!} \tag{3.55}$$

J. Stat. Mech. (2021) 114001

with parameter β, the total integrated DOS in the soliton gas. The position phases $x_j \in \mathbb{R}$ coincide with the soliton centres in the stochastic soliton lattice model (2.8) of a rarefied gas. The random process (2.8) can then be associated with a compound Poisson process [111], a stochastic process with jumps. The jumps, associated with solitons, are distributed on the line randomly according to a Poisson distribution with probability (3.55) and the size of the jumps (the soliton amplitudes $a_i = 2\eta_i^2$) is also random, where the spectral parameter η has the probability distribution $\varphi(\eta) = \beta^{-1} f(\eta)$.

3.3. Focusing NLS equation: soliton and breather gas

The spectral theory of soliton gas for the KdV equation was generalised in [38] to the case of the focusing NLS equation (2.30). As was mentioned in section 2.2.2, the essential difference between the KdV and focusing NLS equations at the level of the IST is that the Lax (Zakharov–Shabat) operator (2.31) for the focusing NLS has a complex-valued spectrum satisfying the Schwartz symmetry property. This results in the availability of the qualitatively new, compared to KdV, families of localised wave solutions and, consequently, to new types of soliton gases. Along with the individual fundamental solitons propagating on zero background, the focusing NLS equation supports a family of the so-called bound state N-soliton solutions, the complexes of strongly interacting, co-propagating (i.e. having the same, possibly zero, velocity) solitons. Another important family of localised solitonic structures supported by the focusing NLS equation are breathers, which can be viewed as solitons on finite background. All of these localised solutions can serve as quasiparticles in the respective soliton or breather gases, which we consider in this section.

3.3.1. Solitons, breathers and finite-gap spectral solutions.

3.3.1.1. Solitons and breathers. The fundamental soliton solution of the focusing NLS equation is given by formula (2.32) (see figure 8(a) for the profile of $|\psi(x)|$ in such soliton). The inherent feature of the fundamental solution is that it can only exist on the zero background, which makes it very different from KdV solitons and solitons in the defocusing NLS/resonant NLS dispersive hydrodynamics. The IST spectral portrait of the fundamental soliton consists of two complex conjugate points $\lambda \in \{\lambda_1, \bar{\lambda}_1\}$ (see the inset in figure 8(a)). Apart from the fundamental solitons (2.32), the focusing NLS equation supports a more general family of localised solutions, called breathers, which can be viewed as solitons on finite background. The Lax spectrum of a breather consists of a vertical band $\gamma_0 = [-iq, iq]$, $q > 0$ complemented by two complex conjugate solitonic discrete points $\lambda_1, \bar{\lambda}_1$. In physical space, such a breather, sometimes called the Tajiri–Watanabe (TW) breather, represents a localised nonlinear wavepacket propagating on a uniform nonzero background described at $x \to \pm\infty$ by the plane wave solution $\psi = q\, \mathrm{e}^{\mathrm{i}2q^2 t}$ (see figure 8(b) for the typical behaviour of $|\psi|$ in the TW breather along with the spectral portrait in the inset). The analytical expression for the TW breather solution is available elsewhere (see e.g. [112–114]), here we only present its group (envelope) and phase (carrier wave) velocities:

$$c_{\mathrm{g}} = -2\,\frac{\mathrm{Im}[\lambda_1 R_0(\lambda_1)]}{\mathrm{Im}[R_0(\lambda_1)]}, \qquad c_{\mathrm{p}} = -\frac{2\,\mathrm{Re}[\lambda_1 R_0(\lambda_1)]}{\mathrm{Re}[R_0(\lambda_1)]}, \tag{3.56}$$

J. Stat. Mech. (2021) 114001

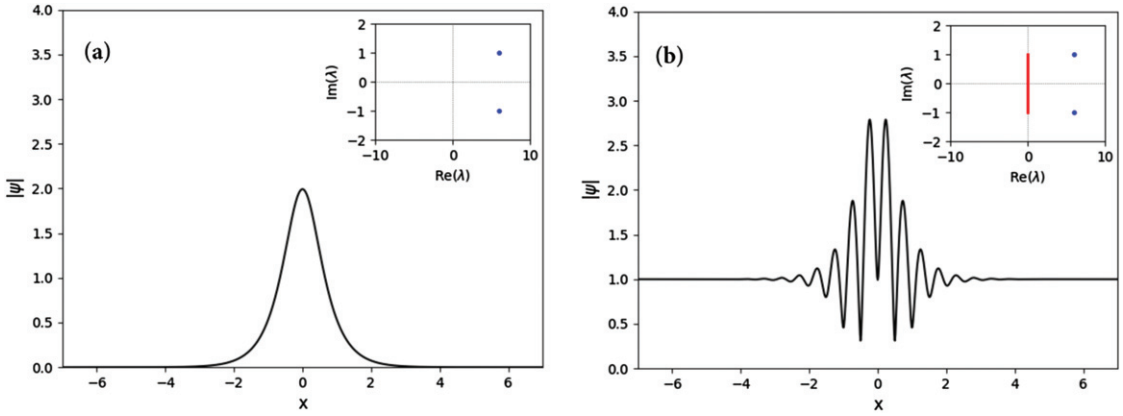

Figure 8. Fundamental soliton (a) and Tajiri–Watanabe (TW) breather (b) solutions of the focusing NLS equation. Shown are $|\psi(x,0)|$ and the Lax spectrum (IST spectral portrait) (inset).

where λ_1 is the IST solitonic spectral point characterising the TW breather and $R_0(\lambda) = \sqrt{\lambda^2+q^2}$. The transition from the TW breather solution to the fundamental soliton (2.32) is achieved by vanishing the background, $q \to 0$.

The TW breather has three special reductions, spectrally realised by placing the soliton discrete eigenvalues $\lambda_1, \bar{\lambda}_1$ on the imaginary axis. These reductions are the Akhmediev breather (AB), the Kuznetsov-Ma (KM) breather and the Peregrine soliton (PS) and they, particularly the PS, are often considered as 'analytical prototypes' for rogue, or anomalous waves (see e.g. [116–119] and references therein). All three of these special families of breathers possess specific localisation properties: the AB is localised in time and is periodic in space, the KM breather is localised in space and is periodic in time, and, finally, the PS exhibits both temporal and spatial localisation. Their IST spectral characterisation is as follows (see e.g. [115]).

Let the spectral band corresponding to the plane wave background of the breather be $\gamma_0 = [-iq, iq]$ for some $q > 0$, and the solitonic discrete spectrum points $\lambda_1 = ip$, $\bar{\lambda}_1 = -ip$, $p > 0$. Then, $p < q$ corresponds to AB, $p > q$ to KM breather and $p = q$ to PS. The behaviours of $|\psi(x,t)|$ in the AB, KM and PS breathers, along with their spectral portraits, are displayed in figure 9.

3.3.1.2. Finite-gap solutions. Similar to the KdV equation, the focusing NLS equation (2.30) supports finite-gap solutions, which transform into the solitonic solutions when the spectral bands collapse. An n-gap solution $\psi = \psi_n(x,t)$ of the focusing NLS equation (2.30) is defined by a fixed set of $2n+2$ endpoints $\{\lambda_j, \bar{\lambda}_j,\ j = 0,1,2,\cdots,n\}$ of spectral bands γ_j, $j = 0,1,\cdots,n+1$, and depends on n real phases $\boldsymbol{\theta}(x,t) = \boldsymbol{k}x - \boldsymbol{\omega}t + \boldsymbol{\theta}^0$ with the initial phase vector $\boldsymbol{\theta}^0 \in \mathbb{T}^n$, so that $|\psi_n(x,t)| = F_n(\boldsymbol{\theta}(x,t))$, where F_n is a multi-phase (quasiperiodic) function in both x and t, which can be expressed in terms of the Riemann theta-functions [120]. The n-component wavenumber $\boldsymbol{k}$ and the frequency $\boldsymbol{\omega}$ vectors depend on the endpoints $\{\lambda_j, j = 0,1,2,\cdots,n\}$ of the spectral bands, which define a hyperelliptic Riemann surface $\mathcal{R}$ of genus n given by (cf equation (3.22) for the

J. Stat. Mech. (2021) 114001

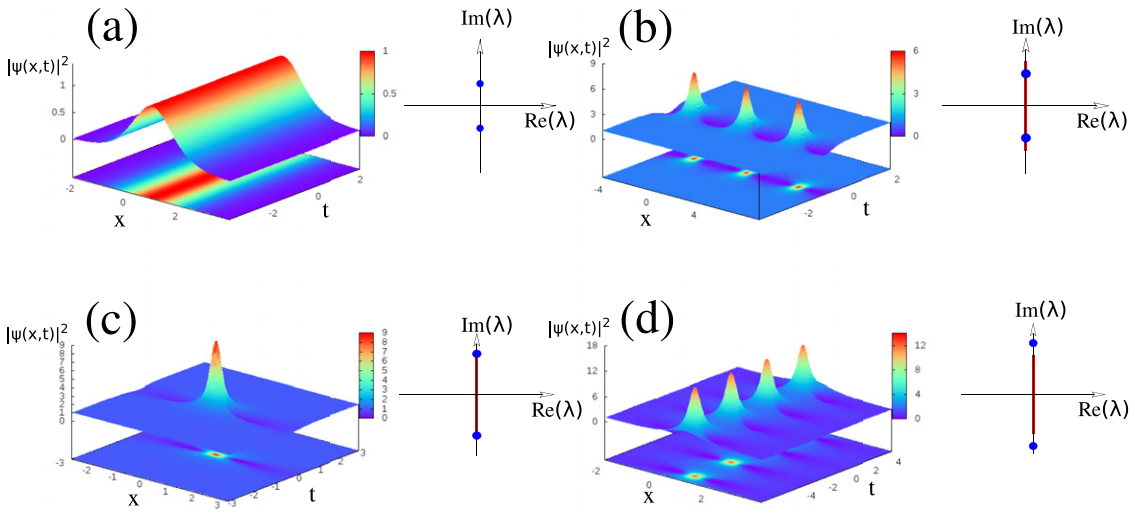

Figure 9. Solitonic solutions of the FNLS equation along with their IST spectral portraits: (a) fundamental soliton; (b) Akhmediev breather (AB); (c) Peregrine soliton (PS); (d) Kuznetsov-Ma (KM) soliton. Reproduced from [115]. CC BY 4.0.

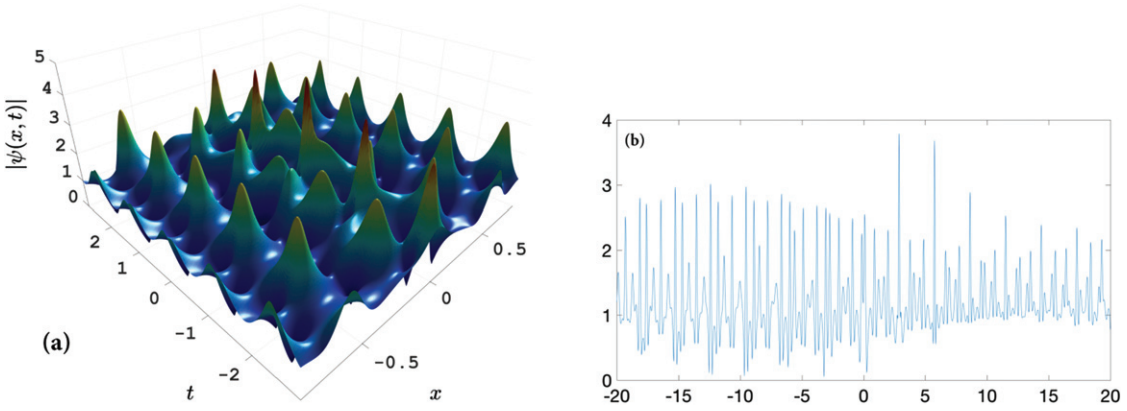

Figure 10. Genus 4 multiphase focusing NLS solution with the endpoints of the spectral bands $\boldsymbol{\lambda} = (-0.392\,71 + i, -0.213\,36 + i, 0.010\,556 + i, 0.205\,25 + i, 0.390\,27 + i)$; (a) plot of $|\psi_4(x,t)|$; (b) plot $|\psi_4(x)|$ for a fixed t. Reproduced with permission from [105]. © 2016 The Authors.

KdV equation):

$$R(z) = \prod_{j=0}^{n} (z-\lambda_j)^{\frac{1}{2}}(z-\bar{\lambda}_j)^{\frac{1}{2}}, \qquad \lambda_j = a_j + ib_j, \quad b_j > 0. \tag{3.57}$$

$z \in \mathbb{C}$ is a complex spectral parameter in the Zakharov-Shabat scattering problem; $R_n(z) \sim z^{n+1}$ as $z \to \infty$. The branch cuts of $R(z)$ are made along spectral bands, which will be specified below. An example of the behavior of $|\psi(x,t)|$ in a genus 4 solution is shown in figure 10.

J. Stat. Mech. (2021) 114001

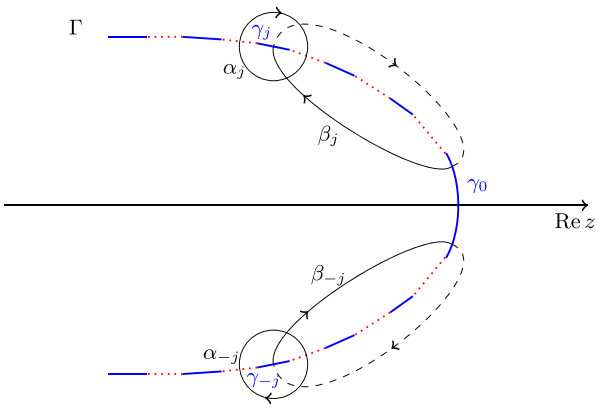

Figure 11. The spectral geometry of the finite-gap solution of the focusing NLS equation and the canonical homology basis used in the construction of breather and soliton gases. The branch cuts (bands) $\gamma_{\pm j}$ of the hyperelliptic Riemann surface $\mathcal{R}$ and the gaps $c_{\pm j}$ (shown by red dotted lines) are located on the 1D Schwarz symmetric curve Γ.

There are two qualitatively different types of spectral bands characterising finite-gap NLS solutions: (i) the bands that cross the real axis in the complex spectral plane $z \in \mathbb{C}$ and connect the complex conjugate spectral points λ_j and $\bar{\lambda}_j$ (these are often called the Stokes bands, see e.g. [6]); (ii) the Schwartz symmetric bands that do not cross the real axis (we shall call them the solitonic bands). By manipulating the spectral bands, one can achieve various wave configurations for the field $\psi_n(x,t)$, e.g. collapsing a pair of solitonic bands into two complex conjugate double points of the spectrum gives rise to a localised mode in the solution, a soliton on the finite-gap background, a generalised breather (see e.g. [121]). Collapsing a Stokes band into a double point on the real axis implies vanishing of one of the background plane wave modes. By collapsing all Stokes and solitonic bands into double points of the spectrum, a finite-gap solution is transformed into a multi-soliton solution. Keeping one of the Stokes bands finite, but collapsing all other bands, implies a multi-breather solution.

The finite-gap analogues of the TW breather solutions and their reductions (AB, KM and PS) have genus $n = 2$ and contain one Stokes band in their Lax spectrum. We shall consider a generalisation of these solutions for an arbitrary genus and, keeping in mind the construction of soliton and breather gas, make two simplifying assumptions:

(a) *Assume an even genus $n = 2N$ of the spectral Riemann surface;*

(b) *Assume that the Lax spectrum of the finite-gap potential is located on a Schwarz symmetric, simply connected 1D curve* $\Gamma \subset \mathbb{C}$, see figure 11.

Thus, we have one Stokes band γ_0 between λ_0 and $\overline{\lambda}_0$ and $2N$ solitonic bands: γ_j, $j = 1, \cdots, N$ between λ_{2j-1} and λ_{2j}, and their Schwarz symmetric counterparts γ_{-j}, $j = 1, \cdots, N$ between $\overline{\lambda}_{2j-1}$ and $\overline{\lambda}_{2j}$ in the lower half-plane. We note that the described spectral geometry also covers the case of an odd genus (achieved by collapsing the Stokes band) and a 'bound state' configuration, when Γ lies on a vertical line so that all the solitons or breathers corresponding to the collapsed bands have the same velocity. Due

J. Stat. Mech. (2021) 114001

to the symmetry of the curve Γ, it is sufficient to consider only the upper complex half-plane ($\mathbb{C}^+$) part of it, which we denote Γ^+ (so that $\Gamma^+ = \Gamma \cap \mathbb{C}^+$).

While appearing quite restrictive, the described 1D spectral geometry provides a major insight into the properties of breather and soliton gases and admits a straightforward generalisation in the more physically realistic case, where the spectral bands γ_j are located in some (Schwarz symmetric) 2D regions $\Lambda \subset \mathbb{C}$. It also admits generalisation to the case of more than one Stokes bands.

3.3.1.3. Wavenumbers and frequencies. The wavenumber and frequency vectors, $\boldsymbol{k}$ and $\boldsymbol{\omega}$, respectively, associated with a given finite-gap solution $\psi_{2N}(x,t)$ of the focusing NLS equation, are not uniquely defined since any linear combination of the wavenumber (frequency) vector components with integer coefficients is also a wavenumber (frequency). The construction of the thermodynamic limit outlined in section 3.1.2 and realised in section 3.2 for the KdV equation relies on the availability of the wavenumbers and frequencies that vanish in the limit when the relevant bands collapse into double points. Such wavenumbers and frequencies automatically appear in the finite-gap KdV theory [35]. The situation for the focusing NLS equation is different since the sets of the wavenumbers and frequencies that arise 'naturally' in the focusing NLS finite-gap theory (see e.g. [122–124]) do not necessarily possess the requisite property.

The special, *fundamental* wavenumber and frequency vectors

$$\boldsymbol{k} = (k_1, \cdots, k_N, \tilde{k}_1, \cdots, \tilde{k}_N) \quad \text{and} \quad \boldsymbol{\omega} = (\omega_1, \cdots, \omega_N, \tilde{\omega}_1, \cdots, \tilde{\omega}_N), \tag{3.58}$$

which possess the properties necessary for the application of the thermodynamic limit have been identified in [38]. The definitions of the fundamental vectors $\boldsymbol{k}$ and $\boldsymbol{\omega}$ can be found in appendix A (see (A.1) and (A.2)). Here, we only highlight their main properties and the principal differences between the components $\{k_1, \cdots, k_N\}, \{\omega_1, \cdots, \omega_N\}$ and $\{\tilde{k}_1, \cdots, \tilde{k}_N\}, \{\tilde{\omega}_1, \cdots, \tilde{\omega}_N\}$.

Following the KdV construction in section 3.2, we introduce two new quantities characterising the finite-gap potentials instead of the endpoints of spectral bands (we consider only the upper half-plane with positive indices of spectral bands γ_j and gaps c_j for convenience):

$$\eta_j = \frac{1}{2}(\lambda_{2j-1} + \lambda_{2j}), \qquad \delta_j = \frac{1}{2}(\lambda_{2j} - \lambda_{2j-1}), \tag{3.59}$$

where $j = 1, \cdots, N$. We shall call the point η_j the centre of the jth band γ_j and $2|\delta_j|$ the jth band width. Also, for the Stokes band we have $\delta_0 = i \operatorname{Im} \lambda_0$. Note that the notations and the band numeration we are using here are slightly different from those used in [38].

It then follows that the fundamental wavenumbers and frequencies defined by (A.1) and (A.2) have drastically different asymptotic properties in the soliton/breather limit, when one of the solitonic spectral bands collapses into a double point, $\lambda_{2i-1}, \lambda_{2j} \to \eta_j$. Namely,

$$\begin{aligned} &\delta_j \to 0 \implies k_j, \omega_j \to 0, \qquad \tilde{k}_j, \tilde{\omega}_j = \mathcal{O}(1), \\ &j = 1, \cdots, N. \end{aligned} \tag{3.60}$$

J. Stat. Mech. (2021) 114001

In particular, for $N = 1$ (genus 2), the limit (3.60) ($k_1 \to 0$, $\omega_1 \to 0$) with non-zero Stokes band γ_0 (i.e. $\delta_0 \neq 0$) corresponds to the TW breather limit of the two-phase nonlinear wave solution. The remaining wavenumber and frequency $\tilde{k}_1 = \mathcal{O}(1)$, $\tilde{\omega}_1 = \mathcal{O}(1)$ correspond to the 'carrier' wave of the TW breather (see figure 8). If we further tend $\delta_0 \to 0$, then $\tilde{k}_1 \to 0$, $\tilde{\omega} \to 0$ and the TW breather transforms into a fundamental soliton. Motivated by these properties for $N = 1$, we shall call the components k_j, ω_j of the wavenumber and the frequency vectors $\boldsymbol{k}$ and $\boldsymbol{\omega}$ the *solitonic components* and the components $\tilde{k}_j$, $\tilde{\omega}_j$—the *carrier components*. The solitonic components k_j, ω_j are the focusing NLS counterparts of the conventional KdV wavenumbers and frequencies specified by (3.26), while the carrier components $\tilde{k}_j$, $\tilde{\omega}_j$ do not have analogues in the KdV theory.

Generally the limit (3.60) for finite N corresponds to N-breather solution if $\delta_0 \neq 0$ and to N-soliton solution if $\delta_0 = 0$.

3.3.1.4. Nonlinear dispersion relations. It was shown in [38] that the solitonic components k_m, ω_m satisfy the following nonlinear dispersion relations (again, considering only the upper half plane):

$$\sum_{m=1}^{N} k_m \operatorname{Im} \oint_{\beta_m} \frac{P_j(\zeta)\mathrm{d}\zeta}{R(\zeta)} = \pi \operatorname{Re} \kappa_{j,1},$$

$$\sum_{m=1}^{N} \omega_m \operatorname{Im} \oint_{\beta_m} \frac{P_j(\zeta)\mathrm{d}\zeta}{R(\zeta)} = 2\pi \operatorname{Re} \left(\kappa_{j,1} \sum_{k=0}^{2N} \operatorname{Re} \lambda_k + \kappa_{j,2} \right),$$

$$j = 1, \cdots, N, \tag{3.61}$$

where

$$P_j(z) = \kappa_{j,1} z^{2N-1} + \kappa_{j,2} z^{2N-2} + \cdots + \kappa_{j,2N}, \tag{3.62}$$

and $\kappa_{i,j}$ are the coefficients of the normalized holomorphic differentials w_j defined by:

$$w_j = [P_j(z)/R(z)]\mathrm{d}z, \qquad \oint_{\alpha_i} w_j = \delta_{ij}, \quad i, j = 1, \cdots, N. \tag{3.63}$$

The contours α_j, β_j on the Riemann surface $\mathcal{R}$ are defined as follows (see figure 11): the α_j-contours surround the bands γ_j clockwise, and the β_j-contours start at the Stokes band γ_0, go to the band γ_j on the upper sheet clockwise and return to the band γ_0 on the lower sheet of the Riemann surface. The derivation of (3.61) is outlined in appendix A.

Relations (3.61) are the analogs of the nonlinear dispersion relations (3.26) for the finite-gap potentials of the KdV equation. Similar relations are available for the carrier components [38], but we do not present them here as they play a secondary role in thermodynamic limit construction.

3.3.2. Thermodynamic spectral scalings. We now fix the endpoints of the band spectrum, $\lambda_1 = a$, $\lambda_{2N} = b$, and assume that for $N \gg 1$ the centres η_j of the bands γ_j, $j = 1, \cdots, N$, are distributed along $\operatorname{arc}(a, b) \subset \Gamma^+$ with some limiting density $\varphi(\lambda) > 0$,

J. Stat. Mech. (2021) 114001

$\lambda \in \Gamma^+$, which is smooth on Γ^+, so that $\int_a^b \varphi(\mu)|\mathrm{d}\mu| = 1$. It then follows that $|\eta_j - \eta_{j+1}| \sim 1/N$.

As for the scaling of the band widths, we consider the following options for $N \gg 1$ (cf equation (3.30) for KdV):

(a) *Exponential spectral scaling*: the band widths $|\delta_j|$ are exponentially small in N:

$$|\delta_j| \sim \mathrm{e}^{-N\tau(\eta_j)}, \quad j = 1, \cdots, N, \tag{3.64}$$

where $\tau(\lambda)$ is a smooth positive function on Γ^+ having the meaning of the normalised logarithmic band width ($\tau(\eta_j) \sim -\ln|\delta_j|/N$).

(b) *Sub-exponential spectral scaling*: for any $a > 0$

$$\mathrm{e}^{-aN} \ll |\delta_j| \ll \frac{1}{N}, \quad j = 1, \cdots, N, \tag{3.65}$$

It is clear that in this limit $\tau(\lambda) \to 0$.

(c) *Super-exponential spectral scaling*: for any $a > 0$

$$\mathrm{e}^{-aN} \gg |\delta_j|, \quad j = 1, \cdots, N. \tag{3.66}$$

In this limit $\tau(\lambda) \to \infty$.

Note that in all three scalings $|\delta_j| \ll |\eta_j - \eta_{j+1}|$, hence the gap width $|c_j| \sim N^{-1}$, $j = 1, 2, \cdots, N$ and so $|\delta_j|/|c_j| \to 0$ as $N \to \infty$. We then say that in the limit each collapsed band $\gamma_j \to \eta_j$ corresponds to a soliton (breather) state within a soliton (breather) gas. We remind that for breather gas $\delta_0 \neq 0$ and for soliton gas $\delta_0 = 0$.

We also note that the exponential and sub-exponential spectral scalings have the 'thermodynamic' property in the sense that they preserve the finiteness of the total density of waves $K_N = \sum_{j=1}^N k_j$ in the limit $N \to \infty$ so that $\lim_{N\to\infty} K_N = \beta$, where $0 < \beta < \infty$. Note that for the super-exponential scaling $\beta \to 0$.

3.3.3. Nonlinear dispersion relations and kinetic equation. We first present the results for the general case of breather gas by evaluating the thermodynamic limit of the nonlinear dispersion relations (3.61) for the exponential spectral scaling (3.64). Without much loss of generality, we assume that the Stokes band lies on the imaginary axis, $\gamma_0 = [-iq, iq]$, $q > 0$ (so that $\delta_0 = iq$) and that $\eta_i \in \mathrm{arc}(a, b) \subset \Gamma^+$, and introduce the simultaneous scaling for the solitonic wavenumbers and frequencies (cf (3.34))

$$k_j = \frac{\kappa(\eta_j)}{N}, \qquad \omega_j = \frac{\nu(\eta_j)}{N}, \quad N \gg 1, \tag{3.67}$$

where $\varkappa(\lambda) \geqslant 0$ and $\nu(\lambda)$ are smooth functions. Similar to the KdV case, the scaling (3.67) provides a balance of terms in relations (3.61) for $N \gg 1$.

The resulting nonlinear dispersion relations for breather gas have the form (we refer the reader to [38] for details of the derivation):

$$\int_{\Gamma^+} D(\lambda, \mu) f(\mu)|\mathrm{d}\mu| + \sigma(\lambda) f(\lambda) = \mathrm{Im}[R_0(\lambda)], \tag{3.68}$$

J. Stat. Mech. (2021) 114001

$$\int_{\Gamma^+} D(\lambda,\mu)v(\mu)|\mathrm{d}\mu| + \sigma(\lambda)v(\lambda) = -2\,\mathrm{Im}[\lambda R_0(\lambda)], \tag{3.69}$$

where $R_0(z) = \sqrt{z^2+q^2}$ (with the branch cut $[-iq, iq]$, and the branch of the radical defined by $R_0(z) \to z$ as $z \to \infty$), and with a slight abuse of notation, we denoted $\int_a^b \cdots |\mathrm{d}\mu| \equiv \int_{\Gamma^+} \cdots |\mathrm{d}\mu|$. Further,

$$D(\lambda,\mu) = \left[\ln\left|\frac{\mu-\bar\lambda}{\mu-\lambda}\right| + \ln\left|\frac{R_0(\lambda)R_0(\mu)+\lambda\mu+q^2}{R_0(\bar\lambda)R_0(\mu)+\bar\lambda\mu+q^2}\right|\right], \tag{3.70}$$

$$f(\lambda) = \frac{1}{2\pi}\varkappa(\lambda)\varphi(\lambda), \qquad v(\lambda) = \frac{1}{2\pi}\nu(\lambda)\varphi(\lambda), \qquad \sigma(\lambda) = \frac{2\tau(\lambda)}{\varphi(\lambda)}. \tag{3.71}$$

Equations (3.68) and (3.69) are the focusing NLS counterparts of the nonlinear dispersion relations (3.37) and (3.38) for the KdV soliton gas with $f(\lambda)$ and $v(\lambda)$ having the meanings of the DOS and the spectral flux density, respectively, and the function $\sigma(\lambda)$ encoding the Zakharov–Shabat spectrum of the finite-gap potentials in the thermodynamic limit.

The soliton gas limit in (3.68) and (3.69) is achieved by collapsing the Stokes band, $q \to 0$, resulting in

$$\int_{\Gamma^+} \ln\left|\frac{\mu-\bar\lambda}{\mu-\lambda}\right| f(\mu)|\mathrm{d}\mu| + \sigma(\lambda)f(\lambda) = \mathrm{Im}\,\lambda, \tag{3.72}$$

$$\int_{\Gamma^+} \ln\left|\frac{\mu-\bar\lambda}{\mu-\lambda}\right| v(\mu)|\mathrm{d}\mu| + \sigma(\lambda)v(\lambda) = -4\,\mathrm{Im}\,\lambda\,\mathrm{Re}\,\lambda. \tag{3.73}$$

Eliminating the function $\sigma(\lambda)$ from the nonlinear dispersion relations (3.68), (3.69), (3.72), (3.73), we obtain the equation of state

$$s(\lambda) = s_0(\lambda) + \int_{\Gamma^+} G(\lambda,\mu)[s(\lambda)-s(\mu)]f(\mu)|\mathrm{d}\mu|, \tag{3.74}$$

where $s(\lambda) = v(\lambda)/f(\lambda)$ is the effective velocity of the tracer soliton (breather) in the gas, and $s_0(\lambda)$, $G(\lambda,\ \mu)$ are defined as follows.

For breather gas:

$$s_0(\lambda) = -2\,\frac{\mathrm{Im}[\lambda R_0(\lambda)]}{\mathrm{Im}[R_0(\lambda)]}, \qquad G(\lambda,\mu) = \frac{1}{\mathrm{Im}[R_0(\lambda)]}D(\lambda,\mu), \tag{3.75}$$

and for soliton gas:

$$s_0(\lambda) = -4\,\mathrm{Re}\,\lambda, \qquad G(\lambda,\mu) = \frac{1}{\mathrm{Im}\,\lambda}\ln\left|\frac{\mu-\bar\lambda}{\mu-\lambda}\right|. \tag{3.76}$$

One can see that $s_0(\lambda)$ in (3.75) coincides with the group velocity $c_g(\lambda)$ of an isolated TW breather (3.56) and $s_0(\lambda)$ in (3.76) coincides with the group velocity of the fundamental soliton of the focusing NLS equation. Furthermore, the integral kernel $G(\lambda,\ \mu)$ in (3.76) coincides with the absolute value of the position shift (2.33) in the two-soliton collision for the focusing NLS equation. As one may expect, the expression for $G(\lambda,\ \mu)$

J. Stat. Mech. (2021) 114001

in equation (3.75) is identified with the position shift in two-breather collisions [114, 125] (see the proof in [40]). Thus, the outlined derivation provides the justification of the collision rate assumption (2.12) for dense soliton and breather gases of the focusing NLS equation.

The integral equations (3.72) and (3.73) have recently been studied in a rather general spectral geometry [44]. The existence and uniqueness of their solutions were investigated and the non-negativity of the solutions for the DOS $f(\lambda)$ was proved.

3.3.3.1. Spectral kinetic equation for nonequilibrium gas. The derivation of the transport equation for non-equilibrium soliton and breather gases for the focusing NLS equation follows the general modulation construction outlined in section 3.1 and realised for the KdV equation in section 3.2.2, albeit with some important differences.

The multiphase Whitham modulation theory for n-gap solutions of the focusing NLS equation [122, 124] includes the system of $n = 2N$ conservation laws $\boldsymbol{k}_t + \boldsymbol{\omega}_x = 0$, which is split into two distinct subsystems

$$\partial_t k_j(\boldsymbol{\lambda}) + \partial_x \omega_j(\boldsymbol{\lambda}) = 0, \quad j = 1, \cdots, N, \tag{3.77}$$

$$\partial_t \tilde{k}_j(\boldsymbol{\lambda}) + \partial_x \tilde{\omega}_j(\boldsymbol{\lambda}) = 0, \quad j = 1, \cdots, N \tag{3.78}$$

for the solitonic and carrier components of the fundamental wavenumber and frequency vectors (see section 3.3.1). These subsystems are complemented by the respective nonlinear dispersion relations

$$k_j = K_j(\boldsymbol{\lambda}), \qquad \omega_j = \Omega_j(\boldsymbol{\lambda}), \quad j = 1, \cdots, N, \tag{3.79}$$

$$\tilde{k}_j = \tilde{K}_j(\boldsymbol{\lambda}), \qquad \tilde{\omega}_j = \tilde{\Omega}_j(\boldsymbol{\lambda}), \quad j = 1, \cdots, N, \tag{3.80}$$

obtained by taking the imaginary and the real part of the basic system (A.4) (see appendix A). In particular, the dispersion relations for the solitonic components are explicitly given by the system (3.61).

Application of the thermodynamic limit to the modulation system (3.77) and (3.79) for the solitonic wavenumbers (see section 3.2.2 for the similar derivation in the KdV context) yields the spectral transport equation

$$f_t + (fs)_x = 0 \tag{3.81}$$

for the DOS $f(\lambda, x, t)$. The transport equation (3.81) is complemented by the equation of state (3.74) and (3.75) for breather gas (or (3.74) and (3.76) for soliton gas). One can see that the kinetic equation for soliton gas agrees with equation (2.34) derived via the phenomenological approach based on the collision rate assumption (2.12).

The carrier wave modulation system (3.78) and (3.80) in the thermodynamic limit becomes (see [38] for details)

$$\tilde{f}_t + (\tilde{f}\tilde{s})_x = 0, \qquad \tilde{f}(\lambda) = \tilde{\mathcal{F}}[f(\lambda)], \qquad \tilde{s}(\lambda) = \tilde{\mathcal{S}}[f(\lambda)], \tag{3.82}$$

where $\tilde{f}(\lambda, x, t)$ and $\tilde{f}\tilde{s} = \tilde{v}(\lambda, x, t)$ are some smooth functions on Γ^+ interpolating $\tilde{k}_j, \tilde{\omega}_j$, that is, $\tilde{f}(\eta_j) = \tilde{k}_j$, $\tilde{v}(\eta_j) = \tilde{\omega}_j$, $j = 1, \cdots, N$, where η_j are the centres of the bands (3.59). The dependencies of $\tilde{f}(\lambda)$ and $\tilde{s}(\lambda)$ on the DOS $f(\lambda)$ in (3.82) are given by

J. Stat. Mech. (2021) 114001

somewhat lengthy expressions, which we do not present here. We only mention that in the limit of zero density, $f(\lambda) \to 0$, the quantity $\tilde{s}$ transforms into the phase velocity $s_{\rm p}(\lambda) = -2\,{\rm Re}[\lambda^2]/{\rm Re}\,\lambda$ of the fundamental soliton (2.32) if $q = 0$ or the phase velocity $c_{\rm p}(\lambda) = -2\,{\rm Re}[\lambda R_0(\lambda)]/{\rm Re}[R_0(\lambda)]$ (3.56) of the TW breather ($q \neq 0$).

3.3.3.2. Generalisation to 2D case. The above derivation of the spectral kinetic equation for the focusing NLS soliton and breather gases involves the basic assumption that the DOS $f(\lambda)$ is supported on a 1D symmetric curve Γ in the complex plane. This restriction can be readily removed as we show below.

In the case when the shrinking bands γ_j, $j > 0$ fill a compact 2D region Λ^+ of the upper complex half-plane, the counterpart of the exponential scaling (3.64) is

$$|\delta_j| \sim {\rm e}^{-N^2\tau(\eta_j)}, \tag{3.83}$$

where $\tau(\lambda)$ is a positive smooth function on Λ^+. The scaling of the gaps remains $\mathcal{O}(1/N)$, where by the gap width we understand the closest distance between the bands. In this case, $\varphi(\lambda) > 0$ is the 2D density of bands (and we also distinguish the cases of the exponential, sub-exponential and super-exponential scalings of bands, similarly to the 1D case).

We now assume one of the 2D spectral thermodynamic spectral scalings (exponential, sub-exponential, and super-exponential) when the shrinking bands γ_j fill a 2D region Λ of the complex plane, see section 3.2. For the wave numbers and frequencies instead of (3.67), we introduce

$$k_j = \frac{\kappa(\eta_j)}{N^2}, \qquad \omega_j = \frac{\nu(\eta_j)}{N^2}, \quad N \gg 1, \tag{3.84}$$

where the functions $\varkappa(\lambda) \geqslant 0$, $\nu(\lambda)$ are assumed to be smooth on Λ^+.

Then the 2D thermodynamic limit of the nonlinear dispersion relations (3.61) leads to the same integral equations (3.68)–(3.74) but with the line integration along Γ^+ replaced by the integration over a 2D compact domain Λ^+:

$$\int_{\Gamma^+} \cdots |{\rm d}\mu| \to \iint_{\Lambda^+} \cdots {\rm d}\xi\,{\rm d}\zeta, \tag{3.85}$$

where $\mu = \xi + i\zeta$.

For convenience of exposition we shall be using the notation $\int_{\Gamma^+} \cdots |{\rm d}\mu|$ in both the 1D and 2D cases, keeping in mind that in the 2D case the meaning of the integral is given by equation (3.85).

3.3.4. Rarefied soliton gas and soliton condensate. The dispersion relations and the equations of state for soliton and breather gases were derived under the assumption of the exponential spectral scaling (3.64) (or (3.83) in 2D case). We now consider the two other scalings of interest: the superexponential scaling (3.66) and subexponential scaling (3.65). We will restrict our exposition to soliton gas but will indicate when the results can be extended to breather gas.

J. Stat. Mech. (2021) 114001

It is convenient to characterise the spectral scalings and the corresponding soliton gases in terms of the function $\sigma(\lambda)$ parametrising the nonlinear dispersion relations (3.68) and (3.72). From equation (3.68), we have:

$$\sigma(\lambda) = \frac{\operatorname{Im}\lambda - \int_{\Gamma^+} \ln\left|\frac{\mu-\bar{\lambda}}{\mu-\lambda}\right| f(\mu)|\mathrm{d}\mu|}{f(\lambda)} \geqslant 0, \tag{3.86}$$

(there is a similar expression for breather gas, which we do not present here). For the exponential scaling $\sigma(\eta) = \mathcal{O}(1)$, while the limiting cases $\sigma \to \infty$ and $\sigma \to 0$ correspond to the super- and sub-exponential spectral scalings, respectively.

3.3.4.1. Rarefied soliton gas. Rarefied soliton gas represents an infinite random ensemble of weakly interacting solitons characterized by a small DOS, $f \ll 1$, and therefore, $\sigma \gg 1$ by (3.86). We shall refer to the limit $f \to 0$, $\sigma \to \infty$, $f\sigma = \mathcal{O}(1)$ as the *ideal gas limit* as it corresponds to the gas of non-interacting breathers (solitons). Spectrally, this limit corresponds to the super-exponential spectral scaling (3.66).

For a rarefied gas the interaction (integral) term in the equation of state (3.74) is sub-dominant so the leading order term $s(\lambda) = s_0(\lambda)$ describes the group velocity distribution in an ideal breather (soliton) gas. Then the first correction to the ideal gas velocity $s_0(\lambda)$ is readily computed to give:

$$s(\lambda) \approx s_0(\lambda) + \int_{\Gamma^+} G(\lambda,\mu)[s_0(\lambda) - s_0(\mu)] f(\mu)|\mathrm{d}\mu|. \tag{3.87}$$

Equation (3.87) represents the focusing NLS counterpart of equation (2.9) for the effective soliton velocity in a rarefied KdV soliton gas introduced by Zakharov [28].

All of the above results apply to breather gas as well.

3.3.4.2. Soliton condensate. The inequality $\sigma(\lambda) \geqslant 0$ in (3.86) imposes a fundamental constraint on the DOS $f(\lambda)$. As follows from the discussion in section 3.3.2, the critical value $\sigma(\eta) = 0$ corresponds to the sub-exponential spectral scaling (3.65). One can see from the nonlinear dispersion relations (3.72) and (3.73) that in this case the gas properties are fully determined by the interaction (integral) terms, while the information about the individual quasi-particles (described by the non-integral, secular, terms) is completely lost. By analogy with Bose–Einstein condensation, we shall call the soliton gas at $\sigma = 0$ the *soliton condensate*. From (3.72) and (3.73) we obtain the dispersion relations for the focusing NLS soliton condensate

$$\int_{\Gamma^+} \ln\left|\frac{\mu-\bar{\lambda}}{\mu-\lambda}\right| f(\mu)|\mathrm{d}\mu| = \operatorname{Im}\lambda, \qquad \int_{\Gamma^+} \ln\left|\frac{\mu-\bar{\lambda}}{\mu-\lambda}\right| v(\mu)|\mathrm{d}\mu| = -4\operatorname{Im}\lambda \operatorname{Re}\lambda. \tag{3.88}$$

Equations (3.88) represent integral equations (the Fredholm equations of the first kind) for the critical DOS $f = f_{\mathrm{c}}(\lambda)$ and the corresponding spectral flux density $v = v_{\mathrm{c}}(\lambda)$. The existence and uniqueness of their solutions depend on the geometry of the spectral locus Γ^+ (generally 2D). Below, we present a particular case where an explicit solution is available.

If the spectral support Γ of the DOS belongs to a vertical line, $\Gamma^+ \subset i\mathbb{R}^+$, the second equation (3.88) implies $v(\lambda) = 0$ and, hence, $s(\lambda) = 0$. We shall generally call such a

J. Stat. Mech. (2021) 114001

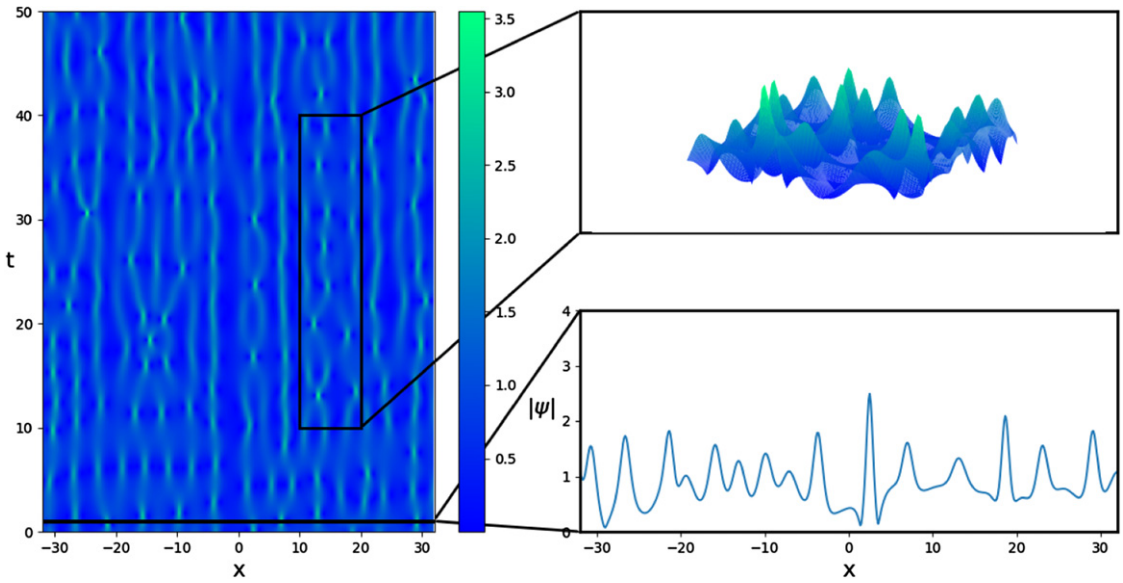

Figure 12. Numerical realisation of the bound state soliton condensate for the focusing NLS equation. Shown is the central portion of a random 100-soliton ensemble.

non-propagating gas a *bound state soliton gas*, and it will be the bound state soliton condensate in the present context. Let $\Gamma = [-iq, iq]$ for some $q > 0$ and assume that $f(\bar{\mu}) = -f(\mu)$ for all $\mu \in [0, iq]$ (an odd extension of $f(\mu)$ onto $[-iq, 0]$). Then, as was shown in [38] the first equation (3.88) for the DOS reduces to

$$\pi H[\hat{f}](\xi) := \int_{-q}^{q} \frac{\hat{f}(y)\mathrm{d}y}{y - \xi} = 1, \tag{3.89}$$

where $\hat{f}(y) = f(iy)$, $\xi = \operatorname{Im}\lambda$, and $H[\hat{f}]$ denotes the finite Hilbert transform (FHT) of $\hat{f}$ over $[-q, q]$ [126, 127]. Inverting the FHT H subject to the additional constraint $H[\hat{f}](0) = 0$, we obtain the DOS $f = f_{\mathrm{c}}(\lambda)$ for the bound state soliton condensate

$$f_{\mathrm{c}}(\lambda) = \frac{-i\lambda}{\pi\sqrt{\lambda^2 + q^2}}, \quad \lambda \in (-iq, iq). \tag{3.90}$$

One can observe that the DOS (3.90) coincides with the appropriately normalised semi-classical distribution of discrete Zakharov–Shabat spectrum for the potential $\psi \in \mathbb{R}$ in the form of a broad rectangular barrier. Equation (3.90) (up to a norming factor) is obtained as a derivative of the corresponding Weyl's law following from the Bohr–Sommerfeld quantisation rule for the Zakharov–Shabat operator [84]. A numerical realisation of the bound state soliton condensate is shown in figure 12. It is achieved by building a dense (as dense as possible) ensemble of 100 strongly interacting solitons with the discrete spectrum eigenvalues distributed according to the Bohr–Sommerfeld rule and random phases of the norming constants (see [26] for the details of the effective numerical implementation of dense N-soliton ensembles with N large).

J. Stat. Mech. (2021) 114001

It was shown in [25] that the bound state soliton condensate dynamics reproduces with remarkable accuracy the statistical characteristics of stationary integrable turbulence generated at the nonlinear stage of the development of the noise-induced modulational instability [8, 10], a fundamental and ubiquitous physical phenomenon in focusing nonlinear media [6, 128, 129]. Furthermore, it was demonstrated in [27] that the nonlinear wave field in the bound state soliton condensate exhibits a spontaneous emergence of rogue waves, offering a new perspective on the dynamical and statistical mechanisms underlying this phenomenon observed in water waves, nonlinear optics and matter waves (see [118] and references therein).

The bound state soliton condensate DOS (3.90) is a particular solution of the dispersion relations (3.88). Another explicit solution of the soliton condensate dispersion relations (3.88) is available in the special case when the spectral support Γ of the DOS represents a circle or a circular arc in the complex plane. This solution with nonzero spectral flux density $v(\lambda)$ obtained in [38] corresponds to a dynamic (non-bound state) soliton condensate.

In conclusion, we note that the soliton condensate regime is also available for the KdV soliton gas. Indeed, substitution of $\sigma = 0$ in the KdV soliton gas dispersion relations (3.37) and (3.38) yields

$$\int_0^1 \ln\left|\frac{\eta+\mu}{\eta-\mu}\right| f(\mu)\mathrm{d}\mu = \eta, \qquad \int_0^1 \ln\left|\frac{\eta+\mu}{\eta-\mu}\right| v(\mu)\mathrm{d}\mu = 4\eta^3. \tag{3.91}$$

One can see that the soliton condensate dispersion relations (3.88) and (3.91) represent particular cases of the general conditions (2.15) for singular solutions of the soliton gas' equation of state (2.13).

3.3.5. Special breather gases. In section 3.3.1, we presented some properties of breather solutions to the focusing NLS equation and indicated three special cases: the AB, the KM breather and the PS, which are often considered as mathematical models for rogue waves in fluids and nonlinear optical media. These breathers can be viewed as quasiparticles of the special, 'rogue wave breather gases'.

Assuming the Stokes band $\gamma_0 = [-iq, iq]$, $q > 0$ the AB and KM breather gases are characterised by the DOS $f(\lambda)$ that is supported on the appropriate intervals of the imaginary axis, $\lambda \in \Gamma^+$: $\Gamma^+ = [0, ip]$, $p < q$ for AB gas and $\Gamma^+ = [ip, ib]$, $b > p > q$ for KM gas. For PS gas the DOS is given by $f(\lambda) = w\delta(\lambda - iq)$, where $w > 0$ is the PS gas density. The three types of the rogue wave breather gases were realised numerically in [40] by building a random ensemble of $N \sim 50$ breathers via the Darboux transform recursive scheme in high precision arithmetic, see figure 13. The interaction properties of the constructed breather gases were investigated by propagating through them a trial generic breather (TW) and comparing the effective (mean) propagation velocity with the predictions following from the equation of state (3.74). One of these predictions is that the propagation through the PS breather gas is ballistic, i.e. the PS breather gas does not alter the velocity $s_0(\lambda)$ (3.75) of the trial breather due to vanishing of the logarithmic interaction kernel $G(\lambda, \mu)$ (3.75) evaluated at $\mu = iq$ [38]. Other predictions, confirmed by detailed quantitative comparisons with numerical simulations in [40], are

J. Stat. Mech. (2021) 114001

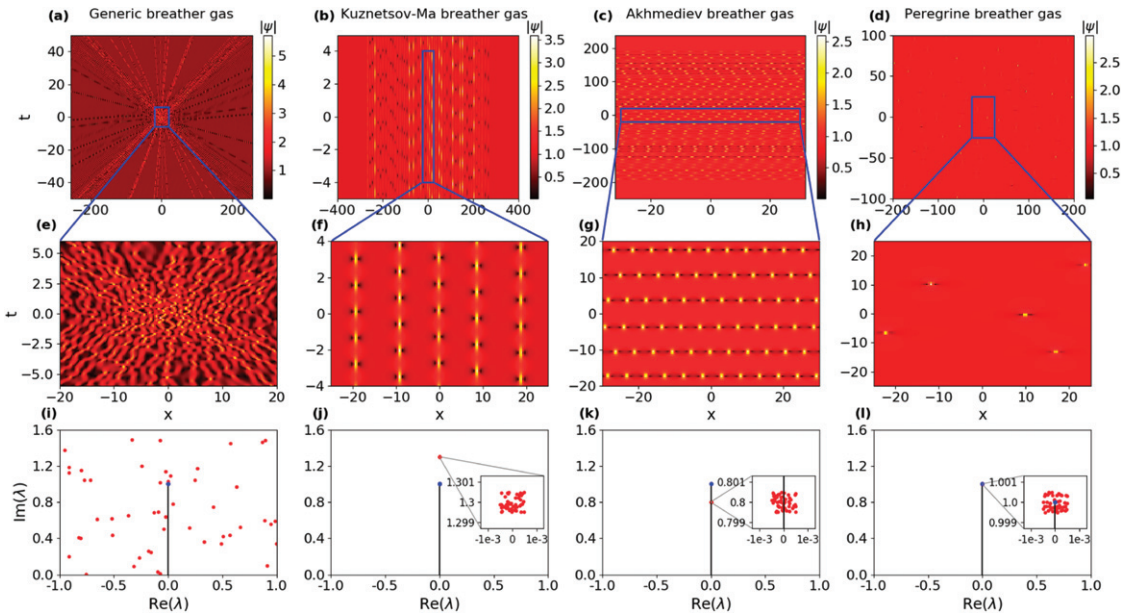

Figure 13. Numerical synthesis of a generic breather gas (left column (a), (e), (i)) and of three single-component breather gases: KM gas (second column (b), (f), (j)), AB gas (third column (c), (g), (k)) and PS gas (fourth column (d), (h), (i)). The four breather gases are parametrised by $N = 50$ complex eigenvalues λ_n, see bottom row. The first row (a)–(d) represents the space-time evolution of the breather gases, with the second row (e)–(h) being an enlarged view of some restricted region of the $(x - t)$ plane. The third row (i)–(l) represents the spectral portraits of each breather gas with the vertical line between 0 and $+i$ being the branch cut (Stokes band) associated with the plane wave background. Each point in the upper complex plane in (i)–(l) represents a discrete eigenvalue in the IST problem with non-zero boundary conditions. The eigenvalues parametrising the single-component breather gases are densely placed in a small square region that is centred around a point λ_0 of the imaginary vertical axis and is strongly enlarged in the insets shown in (j)–(l). The individual breather 'positions' x_j are uniformly distributed in the range $[-1, 1]$ for the generic breather gas (a) and for the PS gas (d), while they are uniformly distributed in the range $[-32, 32]$ for the KM gas (b) and the AB gas (c), see [40] for details. Reprinted figure with permission from [40], Copyright (2021) by the American Physical Society.

that the effective velocity of propagation $s(\lambda)$ of a trial TW breather through a rogue wave gas is greater than s_0 for the KM gas and less than s_0 for the AB gas.

4. Hydrodynamic reductions and integrability

In this section, we review some general mathematical properties of the kinetic equation for soliton gas studied in [41, 42]. For convenience we reproduce here the generalised kinetic equations (2.10) and (2.13) for unidirectional/bidirectional isotropic

J. Stat. Mech. (2021) 114001

soliton gas:

$$f_t + (fs)_x = 0, \qquad s(\lambda, x, t) = s_0(\lambda) + \int_\Gamma G(\lambda, \mu) f(\mu, x, t)[s(\lambda, x, t) - s(\mu, x, t)]\mathrm{d}\mu, \tag{4.1}$$

where $f(\lambda, x, t)$, $s(\lambda, x, t)$, $s_0(\lambda)$ and $G(\lambda,\ \mu)$ are real functions and the parameters $\lambda,\ \mu$ can be real or complex. For unidirectional gas the spectral support Γ of the DOS $f(\lambda, x, t)$ is an interval in $\mathbb{R}$. For bidirectional isotropic gas Γ is either a symmetric interval $[-a, a] \subset \mathbb{R}$ (cf (2.26)) or a Schwarz symmetric compact domain in $\mathbb{C}$ (1D or 2D, see (3.85) for the formal correspondence between the two cases).

Consider a soliton gas composed of a finite ($M \in \mathbb{N}$) number of distinct components, termed monochromatic, or cold, components modelled by the DOS in the form of a linear combination of the Dirac delta-functions centred at distinct spectral points $\zeta_j \in \Gamma$,

$$f(\lambda, x, t) = \sum_{j=1}^{M} w_j(x, t)\delta(\lambda - \zeta_j), \tag{4.2}$$

where $w_j(x, t) > 0$ are the components' weights, and $\{\zeta_j\}_{j=1}^M \subset \Gamma$, $(\zeta_j \neq \zeta_k \Leftrightarrow j \neq k)$. Substitution of (4.2) into the kinetic equation (4.1) reduces it to a system of hydrodynamic conservation laws

$$(w_i)_t + (w_i s_i)_x = 0, \quad i = 1, \cdots, M, \tag{4.3}$$

where the component densities $w_i(x, t)$ and the transport velocities $s_j(x, t) \equiv s(\zeta_j, x, t)$ are related algebraically:

$$s_j = s_{0j} + \sum_{m=1, m\neq j}^{M} G_{jm} w_m (s_j - s_m), \quad j = 1, 2, \cdots M. \tag{4.4}$$

Here, we used the notation

$$s_{0j} \equiv s_0(\zeta_j), \qquad G_{jm} \equiv G(\zeta_j, \zeta_m), \quad j \neq m. \tag{4.5}$$

We note that, although we derived the hydrodynamic reduction (4.3) and (4.4) in the context of unidirectional/isotropic soliton gas, it can be readily generalised to the bidirectional anisotropic case, see [37]. In the latter case, the ansatz (4.2) is introduced separately for the slow and fast soliton branches so that the pair of distributions

$$f_-(\lambda, x, t) = \sum_{i=1}^{M_-} w_i(x, t)\delta(\lambda - \zeta_i), \qquad f_+(\lambda, x, t) = \sum_{i=M_-+1}^{M_-+M_+} w_i(x, t)\delta(\lambda - \zeta_i), \tag{4.6}$$

is transformed into a M-dimensional vector $\boldsymbol{w} = (w_1, \cdots, w_M)$, where $M = (M_- + M_+)$.

For $M = 2$ system (4.4) can be solved to give explicit expressions for $s_{1,2}(w_1, w_2)$:

$$s_1 = s_{01} + \frac{G_{12} w_2 (s_{01} - s_{02})}{1 - (G_{12} w_2 + G_{21} w_1)}, \qquad s_2 = s_{02} - \frac{G_{21} w_1 (s_{01} - s_{02})}{1 - (G_{12} w_2 + G_{21} w_1)}. \tag{4.7}$$

J. Stat. Mech. (2021) 114001

An important remark is in order on the meaning of the delta-function ansatz (4.2) for the DOS $f(\lambda)$. As a matter of fact, the representation (4.2) is a mathematical idealisation, which has a formal sense in the context of the integral equation of state (4.1), but cannot be applied to the original dispersion relations where it appears in both the integral and the secular terms (cf (3.37) and (3.38) for the KdV equation). In a physically realistic description, the delta-functions in (4.2) should be replaced by some narrow distributions around the spectral points ζ_j, i.e. we first take the thermodynamic limit $N \to \infty$ and then allow the distributions to become sharply peaked. As a result, the non-condensate condition $\sigma > 0$ in the dispersion relation for the DOS (equation (3.37) for KdV or equation (3.68) for focusing NLS) would impose a constraint $\int_\Gamma G(\lambda,\ \mu) f(\lambda) \mathrm{d}\mu < 1$ on $f(\lambda)$, which, among other things, implies that the denominators in (4.7) must be positive. It is interesting to note that a variant of hydrodynamic system (4.3) and (4.7) has been recently derived in [130] in the context of $T\bar{T}$-deformed conformal field theories out of equilibrium.

We now assume that the integral kernel $G(\lambda,\ \mu)$ in the equation of state (4.1) can be represented as

$$G(\lambda,\mu) = a(\mu)\epsilon(\lambda,\mu), \quad \text{where } \epsilon(\lambda,\mu) = \epsilon(\mu,\lambda) > 0,\ \lambda \neq \mu \tag{4.8}$$

for some non-singular real functions $a(\mu) \neq 0$. This structure of the soliton interaction kernel is typical for integrable dispersive hydrodynamics and is indeed shared by the equations of state of the KdV, defocusing and focusing NLS unidirectional/isotropic soliton gases (see (3.44), (2.26) and (2.34)). For example, for KdV we have $a(\mu) = \ \mu$, $\epsilon(\lambda,\mu) = \frac{1}{\lambda\mu} \ln\left|\frac{\lambda+\mu}{\lambda-\mu}\right|$, see (2.11).

We then have

$$G_{jk} = a_k \epsilon_{jk}, \qquad \epsilon_{jk} = \epsilon_{kj}, \quad j \neq k, \tag{4.9}$$

where $a_k = a(\zeta_k)$, $\epsilon_{jk} = \epsilon(\zeta_j, \zeta_k)$. Solving equation (4.7) for $w_{1,2}$ gives

$$a_1 w_1 = \frac{1}{\epsilon_{12}} \frac{s_2 - s_{02}}{s_2 - s_1}, \qquad a_2 w_2 = \frac{1}{\epsilon_{12}} \frac{s_1 - s_{01}}{s_1 - s_2}. \tag{4.10}$$

Substituting (4.10) in (4.3) for $M = 2$ we obtain a diagonal system [36]:

$$\frac{\partial s_1}{\partial t} + s_2 \frac{\partial s_1}{\partial x} = 0, \qquad \frac{\partial s_2}{\partial t} + s_1 \frac{\partial s_2}{\partial x} = 0 \tag{4.11}$$

with $s_{1,2}$ being the Riemann invariants. One can see that system (4.11) is *linearly degenerate* because its characteristic velocities do not depend on the corresponding Riemann invariants. System (4.11) represents the diagonal form of the so-called Chaplygin gas equations, the system of isentropic gas dynamics with the equation of state $p = -A/\rho$, where p is the pressure, ρ is the gas density and $A > 0$ is a constant. The Chaplygin gas equations occur in certain theories of cosmology (see e.g. [131]) and is also equivalent to the 1D Born–Infeld equation [33, 132] arising in nonlinear electromagnetic field theory.

As any two-component quasilinear hyperbolic system, system (4.11) is integrable (linearisable) via the classical hodograph transform. However, for any $M \geqslant 3$ integrability of the original system (4.3) and (4.4) is no longer obvious. As a matter of fact, a

J. Stat. Mech. (2021) 114001

M-component hydrodynamic type system is generally *not integrable* for $M \geqslant 3$. Below we present the theorem, proved in [41], which summarises the mathematical properties of the hydrodynamic reductions (4.3) and (4.4) subject to the structure (4.9) of the interaction matrix G_{jk}.

Theorem [41]. *M-component reductions (4.3) and (4.4) of the generalised kinetic equation (4.1) with the interaction kernel satisfying (4.8) are hyperbolic, linearly degenerate integrable hydrodynamic type systems for any $M \in \mathbb{N}$.*

Specifically, it was shown in [41] that the following fundamental properties are satisfied for the system (4.3) and (4.4):

(a) *Riemann invariants.*
Let $u_j = a_j w_j$, where the symmetrising coefficients a_j are defined by (4.8) and (4.9). Then, the invertible point transformation $\boldsymbol{w} \to \boldsymbol{r}$ specified by

$$r_k = -\frac{1}{u_j}\left(1 + \sum_{m \neq k} u_m \epsilon_{mk}\right), \quad k = 1, 2, \cdots, M, \tag{4.12}$$

reduces the system (4.3) and (4.4) to the diagonal (Riemann invariant) form

$$\frac{\partial r_i}{\partial t} + V_i(\boldsymbol{r})\frac{\partial r_i}{\partial x} = 0, \quad i = 1, 2, \cdots, M, \tag{4.13}$$

where the characteristic velocities V_i are expressed in terms of the Riemann invariants $r_1, r_2, \cdots, r_N$ as

$$V_i(\boldsymbol{r}) = s_i(w_1(\boldsymbol{r}), w_2(\boldsymbol{r}), \cdots, w_M(\boldsymbol{r})), \quad i = 1, 2, \cdots, M. \tag{4.14}$$

Here, $s_i(w_1, \cdots, w_M)$ are solutions of the system (4.4),

(b) *Linear degeneracy.*
The characteristic velocities V_j of the diagonal system (4.13) satisfy

$$\partial_j V_j = 0, \quad j = 1, 2, \cdots, M, \text{ where } \partial_j \equiv \partial/\partial r_j, \tag{4.15}$$

so that system (4.3) and (4.4) is linearly degenerate in the Lax sense [133].

(c) *Semi-Hamiltonian property.*
In addition to (4.15), the characteristic velocities $V_i(\boldsymbol{r})$ satisfy the overdetermined system

$$\partial_j \frac{\partial_k V_i}{V_k - V_i} = \partial_k \frac{\partial_j V_i}{V_j - V_i}, \quad i \neq j \neq k \tag{4.16}$$

for each three distinct characteristic velocities ($\partial_k \equiv \partial/\partial r_k$). Diagonal hydrodynamic type systems satisfying (4.16) are called semi-Hamiltonian [66].

(d) *Generalised hodograph solution.*
A semi-Hamiltonian hydrodynamic type system can be locally integrated via the generalised hodograph transform due to Tsarev [66, 134]. Its general local solution

J. Stat. Mech. (2021) 114001

for $\partial_x r_i \neq 0$, $i = 1, \cdots, M$ is given by the formula

$$x - V_i(\boldsymbol{r})t = W_i(\boldsymbol{r}), \quad i = 1, 2, \cdots, M, \tag{4.17}$$

where functions $W_i(\boldsymbol{r})$ are found from the linear system of PDEs:

$$\frac{\partial_i W_j}{W_i - W_j} = \frac{\partial_i V_j}{V_i - V_j}, \quad i, j = 1, \cdots, N, \ i \neq j. \tag{4.18}$$

Properties of linearly degenerate semi-Hamiltonian (integrable) hydrodynamic type systems have been studied in [135, 136]. Using the results of [135, 136] it was shown in [41] that the general local solution of the hydrodynamic reductions (4.3) and (4.4) of the kinetic equation can be represented in the form

$$x - s_{0i}t = \int^{r_i} \xi \phi_i(\xi) \mathrm{d}\xi + \sum_{m \neq i} \epsilon_{im} \int^{r_m} \phi_m(\xi) \mathrm{d}\xi, \quad i = 1, 2, \cdots, M, \tag{4.19}$$

where $\phi_1(\xi), \cdots, \phi_M(\xi)$ are arbitrary functions. Some interesting particular solutions (self-similar, quasiperiodic) following from (4.19) can be found in [41]. The Hamiltonian structure of the hydrodynamic reductions (4.3) and (4.4) was investigated in [43]. The generalised hydrodynamic reductions arising if one allows the discrete spectral points ζ_j in (4.2) be functions of (x, t) were studied in [42].

In conclusion of this section we note that, somewhat counter-intuitively, the above results on the hyperbolic structure and integrability of hydrodynamic reductions of the kinetic equation for soliton gas apply to the multi-component soliton gas of the focusing NLS equation, whose Whitham modulation system is known to be elliptic for a generic set of modulation parameters and for any genus [122, 137]. This apparent paradox is resolved by noticing that the Whitham system for the focusing NLS equation exhibits real eigenvalues (characteristic speeds) in the soliton limit. For example, for the genus 1 case, the two pairs of complex conjugate eigenvalues of the modulation matrix collapse into a single, quadruply degenerate real eigenvalue, determining the velocity of the fundamental soliton, see e.g. [63].

5. Riemann problem for soliton gas

Having obtained the hydrodynamic description of multi-component soliton gas, it is natural to consider the Riemann problem that plays a fundamental role in classical gas and fluid dynamics [138]. The classical Riemann problem consists of finding solution to a system of hyperbolic conservation laws subject to piecewise constant initial conditions exhibiting discontinuity at $x = 0$. The distribution solution of the Riemann problem generally consists of a combination of constant states, simple (rarefaction) waves and strong discontinuities (shocks or contact discontinuities) [133]. The discontinuous solutions satisfy the Rankine–Hugoniot jump conditions. If a hyperbolic system is linearly degenerate, it does not support simple waves and classical shocks,

J. Stat. Mech. (2021) 114001

and the solution of Riemann problem contains only constant states and contact discontinuities [139]. Here, following [37, 75], we present such solutions for different types of soliton gases.

5.1. General solution

We consider the hyperbolic system (4.3),

$$(w_i)_t + (s_i(\boldsymbol{w})w_i)_x = 0, \quad i = 1, \cdots, n \tag{5.1}$$

subject to the initial data corresponding to two n-component unidirectional or bidirectional soliton gases prepared in the respective uniform states $\boldsymbol{w}^{\mathrm{L}} \in \mathbb{R}^n$ and $\boldsymbol{w}^{\mathrm{R}} \in \mathbb{R}^n$, that are initially separated:

$$\boldsymbol{w}(x,0) = \begin{cases} \boldsymbol{w}^{\mathrm{L}}, & \text{if } x < 0, \\ \boldsymbol{w}^{\mathrm{R}}, & \text{if } x \geqslant 0. \end{cases} \tag{5.2}$$

We emphasize here that the Riemann problem (5.1) and (5.2) is formulated for the kinetic equation (via the substitution (4.2)) but not for the original dispersive hydrodynamic system (1.1) or (1.2). For this reason, we shall call it the *spectral Riemann problem* as it essentially describes the spatiotemporal evolution of the spectral DOS of the soliton gas. The spectral Riemann problem for the KdV and focusing NLS two-component soliton gases ($n = 2$) was investigated in [36, 38, 75] and for rather general isotropic and anisotropic dispersive hydrodynamic soliton gases with an arbitrary number of spectral components in [37]. The Riemann problem of this type has also been considered in the context of GHD [55, 56, 140–143].

The spectral Riemann problem (5.1) and (5.2) corresponds to the dispersive hydrodynamic Riemann problem that can be viewed as a soliton gas shock tube problem, an analog of the shock tube problem of classical gas dynamics [33, 138]. The shock tube problem represents a good benchmark for the spectral kinetic theory of soliton gas, where one can investigate both overtaking and head-on collisions by choosing the appropriate components of solitonic spectra and then comparing the predictions of the kinetic theory with direct numerical simulations of dispersive hydrodynamics.

Following [37, 75], we consider the spectral Riemann problem (analytically) and the corresponding soliton gas shock tube problem (numerically) for n-component unidirectional and bidirectional soliton gases. Due to the scale invariance of the problem (the kinetic equation (5.1) and the initial condition (5.2) are both invariant with respect to the scaling transformation $x \to Cx$, $t \to Ct$), the spectral solution is a self-similar distribution $\boldsymbol{w}(x/t)$. Because of the linear degeneracy (4.15) of the hydrodynamic system (5.1) the only admissible similarity solutions are constant states separated by propagating contact discontinuities, cf, for instance [139]. Discontinuous, weak, solutions are physically acceptable here since the kinetic equation describes the conservation of the number of solitons within any given spectral interval, and the Rankine–Hugoniot type conditions can be imposed to ensure the conservation of the number of solitons across the discontinuities. As a result, the solution of the Riemann problem (4.3) and (5.2) for each component $w_i(x,t)$ is composed of $n+1$ constant states, or plateaus, separated by

J. Stat. Mech. (2021) 114001

n discontinuities (see e.g. [133]):

$$w_i(x,t) = \begin{cases} w_i^1 = w_i^{\mathrm{L}}, & x/t < z_1, \\ \cdots & \\ w_i^j, & z_{j-1} \leqslant x/t < z_j \\ \cdots & \\ w_i^{n+1} = w_i^{\mathrm{R}}, & z_n \leqslant x/t, \end{cases} \tag{5.3}$$

where the lower index i indicates the ith component of the vector $\boldsymbol{w}$, and the upper index j is the index of the plateau. For clarity we have labeled the superscripts $j = 1$ as 'L' (left boundary condition) and $j = n + 1$ as 'R' (right boundary condition). The contact discontinuities propagate at the characteristic velocities [133]:

$$z_j = s_j(w_1^j, \cdots, w_n^j) = s_j(w_1^{j+1}, \cdots, w_n^{j+1}), \tag{5.4}$$

where the plateaus' values w_i^j are found from the Rankine–Hugoniot jump conditions [33]:

$$-z_j \left[w_i^{j+1} - w_i^j\right] + \left[s_i(w_1^{j+1}, \cdots, w_n^{j+1}) w_i^{j+1} - s_i(w_1^j, \cdots, w_n^j) w_i^j\right] = 0, \tag{5.5}$$

where $i, j = 1, \cdots, n$. The Rankine–Hugoniot conditions with $i = j$ are trivially satisfied by the definition of contact discontinuity (5.4). We also note that conditions (5.4) are compatible with (5.5) for linearly degenerate systems of conservation laws.

Note that, if the solitons were not interacting, the initial step distribution $w_i(x, 0)$ for the component $\lambda = \zeta_i$ would have propagated at the free soliton velocity s_{0i}:

$$w_i^{\mathrm{free}}(x,t) = \begin{cases} w_i^{\mathrm{L}}, & x/t < s_{0i}, \\ w_i^{\mathrm{R}}, & s_{0i} \leqslant x/t, \end{cases} \quad i = 1 \cdots n, \tag{5.6}$$

which is very different compared to the solution (5.3).

5.2. Riemann problem: examples

5.2.1. KdV soliton gas. We now consider the simplest concrete Riemann problem for soliton gas. Namely, we shall study the collision of two single-component KdV soliton gases [75]. To be consistent with the notations of sections 2.1 and 3.2, we shall be using the spectral variable $\eta = \sqrt{-\lambda}$. Also, we simplify the general notation of the previous section to make the specific results more transparent.

We consider the two-component ansatz (4.2) for the DOS,

$$f(\eta; x, t) = w_1(x,t)\delta(\eta - \eta_1) \ + \ w_2(x,t)\delta(\eta - \eta_2), \tag{5.7}$$

where

$$0 < \eta_2 < \eta_1 < 1, \quad w_{1,2} \ \geqslant \ 0. \tag{5.8}$$

J. Stat. Mech. (2021) 114001

Substitution of (5.7) into the kinetic equations (2.10) and (2.11) for KdV soliton gas yields the system of two conservation laws

$$\partial_t w_1 \ + \ \partial_x(w_1 s_1) = 0, \qquad \partial_t w_2 \ + \ \partial_x(w_2 s_2) = 0, \tag{5.9}$$

where the transport velocities $s_{1,2} \equiv s(\eta_{1,2}, x, t)$ are given by (cf (4.7))

$$s_1 = 4\eta_1^2 + \frac{4(\eta_1^2 - \eta_2^2)\alpha_2 w_2}{1 - \alpha_1 w_1 - \alpha_2 w_2}, \qquad s_2 = 4\eta_2^2 - \frac{4(\eta_1^2 - \eta_2^2)\alpha_1 w_1}{1 - \alpha_1 w_1 - \alpha_2 w_2}, \tag{5.10}$$

where

$$\alpha_{1,2} = \frac{1}{\eta_{1,2}} \ln \left| \frac{\eta_1 \ + \ \eta_2}{\eta_1 \ - \ \eta_2} \right| \ > \ 0. \tag{5.11}$$

It is assumed that $w_1\alpha_1 + w_2\alpha_2 < 1$ (see the remark after equation (4.7)).

We now consider the system (5.9) and (5.10) subject to the Riemann data (5.2) with $\boldsymbol{w}^{\mathrm{L}} = (w_{10}, 0)$, $\boldsymbol{w}^{\mathrm{R}} = (0, w_{20})$, i.e.

$$\begin{cases} w_1(x,0) = w_{10}, & w_2(x,0) = 0, & x < 0, \\ w_2(x,0) = w_{20}, & w_1(x,0) = 0, & x \geqslant 0, \end{cases} \tag{5.12}$$

where $w_{10}, w_{20} > 0$ are some constants satisfying $w_{i0} \leqslant \eta_i/3$ (see (2.43)). Note that the initial velocities of the colliding soliton gases are fully determined, via equation (5.10), by the density distribution (5.12). An example of one realisation of direct numerical simulation of the collision of two single-component KdV soliton gases modelled by the spectral Riemann problem (5.9) and (5.12) is shown in figure 14. Details of the numerical implementation of the KdV soliton gas can be found in [75].

The required solution for each component w_i represents a combination of three constant states (plateaus) separated by two contact discontinuities given by equations (5.3)–(5.5) for $n = 2$. In the notations of this section,

$$w_i(x,t) = \begin{cases} w_{i0}\,\delta_{i,1}, & x/t < c^-, \\ w_{ic}, & c^- \leqslant x/t < c^+, \\ w_{i0}\,\delta_{i,2}, & c^+ \leqslant x/t, \end{cases} \tag{5.13}$$

where $i \in \{1, 2\}$ and δ_{ij} is the Kronecker delta. The values w_{1c} and w_{2c} of the component densities in the middle plateau region, where the interaction of soliton gases occurs, together with the velocities $c^{\pm}$ of the contact discontinuities, are found from the Rankine–Hugoniot jump conditions,

$$\begin{aligned} -c^-(w_{10} - w_{1c}) \ + \ (w_{10}s_{10} - w_{1c}s_{1c}) \ &= \ 0, \\ -c^-(0 - w_{2c}) \ + \ (0 - w_{2c}s_{2c}) \ &= \ 0\,; \end{aligned} \tag{5.14}$$

$$\begin{aligned} -c^+(w_{1c} - 0) \ + \ (w_{1c}s_{1c} - 0) \ &= \ 0, \\ -c^+(w_{2c} - w_{20}) \ + \ (w_{2c}s_{2c} - w_{20}s_{20}) \ &= \ 0, \end{aligned} \tag{5.15}$$

J. Stat. Mech. (2021) 114001

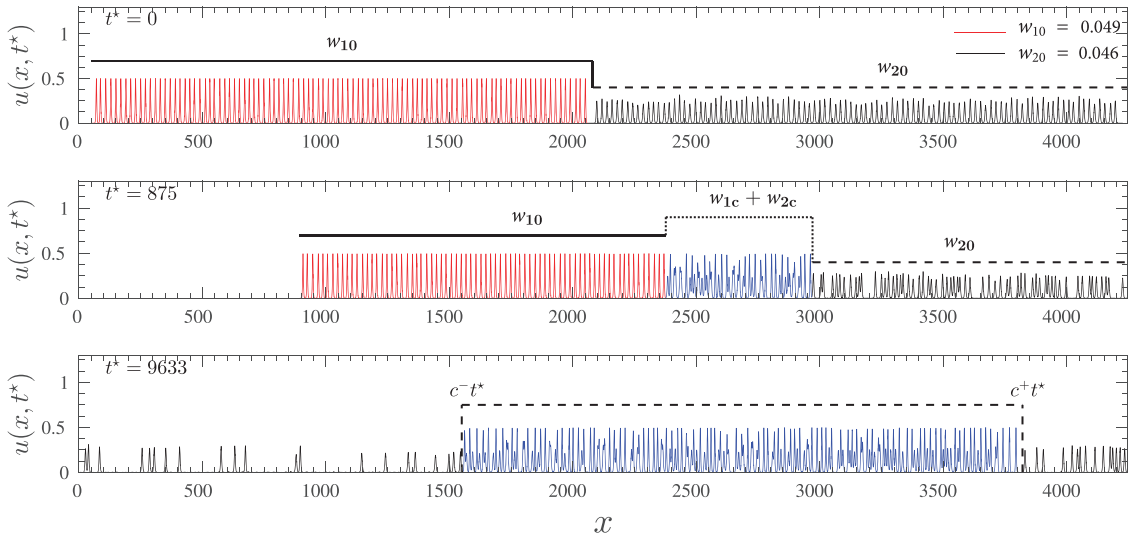

Figure 14. Soliton gas shock tube problem: numerical solution of the KdV equation for one typical realisation of the collision of two cold soliton gases. The expanding interaction region is shown in blue. The piece-wise constant solution for the total density of solitons β (5.18) is shown above the KdV solution plot. Reproduced from [75]. Copyright © EPLA, 2016. All rights reserved.

where the velocities $s_{1c} = s_1(w_{1c}, w_{2c})$ and $s_{2c} = s_2(w_{1c}, w_{2c})$ are determined by relations (5.10).

Solving (5.14) and (5.15), we obtain:

$$w_{1c} = \frac{w_{10}(1 - \alpha_2 w_{20})}{1 - \alpha_1\alpha_2 w_{10} w_{20}}, \qquad w_{2c} = \frac{w_{20}(1 - \alpha_1 w_{10})}{1 - \alpha_1\alpha_2 w_{10} w_{20}}. \tag{5.16}$$

$$c^- = 4\eta_2^2 - \frac{4(\eta_1^2 - \eta_2^2)\alpha_1 w_{1c}}{1 - \alpha_1 w_{1c} - \alpha_2 w_{2c}}, \qquad c^+ = 4\eta_1^2 + \frac{4(\eta_1^2 - \eta_2^2)\alpha_2 w_{2c}}{1 - \alpha_1 w_{1c} - \alpha_2 w_{2c}}. \tag{5.17}$$

One can see that velocities $c^\pm$ of the edges of the expansing interaction region coincide with the characteristic velocities (5.10), which is the basic property of contact discontinuities, cf (5.4).

The total density of solitons $\beta = \int_0^1 f(\eta)\mathrm{d}\eta = w_1 + w_2$ satisfies

$$\beta(x,t) = \begin{cases} w_{10}, & x < c^- t, \\ w_{1c} + w_{2c}, & c^- t \leqslant x < c^+ t, \\ w_{20}, & x \geqslant c^+ t. \end{cases} \tag{5.18}$$

The piece-wise constant solution for $\beta(x,t)$ is shown in figure 14 above the soliton gas plot. It is not difficult to show that the density of the two-component soliton gas in the interaction region, $\beta_c = w_{1c} + w_{2c} > w_{10}, w_{20}$ but $\beta_c < w_{10} + w_{20}$. We emphasize that, although the soliton gas is initially prepared in a rarefied regime where solitons are

J. Stat. Mech. (2021) 114001

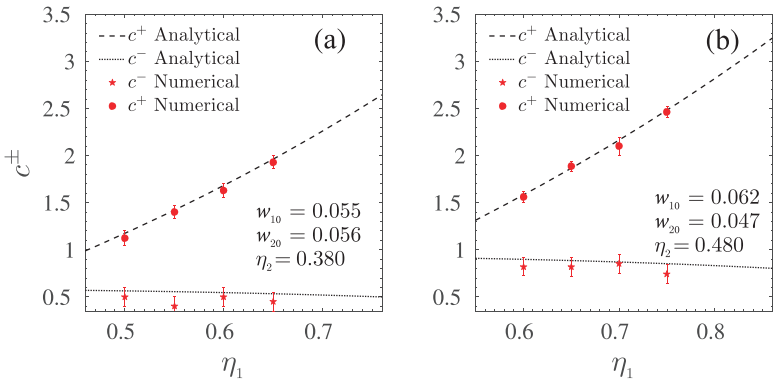

Figure 15. Comparisons for the shock tube problem for the KdV soliton gas: the speeds $c^{\pm}$ of the edges of the interaction region for two different sets of parameters. Reproduced from [75]. Copyright © EPLA, 2016. All rights reserved.

spatially well-separated, the total density of solitons increases in the interaction region, and a denser soliton gas is formed for which solitons exhibit significant overlap.

The expanding interaction region in the soliton gas Riemann problem can be viewed as a stochastic counterpart of the traditional, coherent dispersive shock wave forming due to a dispersive regularisation of the Riemann initial data in the KdV equation [18, 144].

Upon using the ansatz (5.7) the values of the two first moments (3.49) in the interaction region assume the form,

$$\langle u\rangle_c = 4(\eta_1 w_{1c} \ + \ \eta_2 w_{2c}), \qquad \langle u^2\rangle_c = \frac{16}{3}(\eta_1^3 w_{1c} \ + \ \eta_2^3 w_{2c}), \tag{5.19}$$

where w_{1c} and w_{2c} are determined in terms of the initial data by formulae (5.16).

Comparisons of the theoretical results (5.16), (5.17) and (5.19) for the soliton gas physical 'observables' $c^{\pm}, \beta, \langle u\rangle, \langle u^2\rangle$ with direct numerical simulations of the shock tube problem for the KdV soliton gas are presented in figures 15 and 16.

5.2.2. Solition gases for the defocusing and resonant NLS equations. The spectral Riemann problem (5.1) and (5.2) for bidirectional soliton gases for the defocusing and resonant NLS equations (see section 2.2) was considered in [37], where the spectral Riemann problem solution (5.3)–(5.5) was constructed for the collisions of two- and three-component gas and comparisons of some analytically obtained 'observables' (the speeds of the contact discontinuities and the spatial profiles of the mean density $\langle\rho\rangle$) with direct numerical simulations of the soliton gas collision have been made.

Figure 17 displays the numerically obtained $x-t$ diagrams extracted from a single realisation of the soliton gas collision and illustrating the difference between overtaking and head-on interactions in the anisotropic soliton gas of the resonant NLS equation.

In figure 18, comparisons are shown for the profiles of the ensemble average $\langle\rho\rangle$ of the wave field $\rho(x,t)$ associated with the spectral Riemann problem solution for the collision of three-component soliton gases for the defocusing and resonant NLS equations. The spectral data used for the numerical realisation of the soliton gases

J. Stat. Mech. (2021) 114001

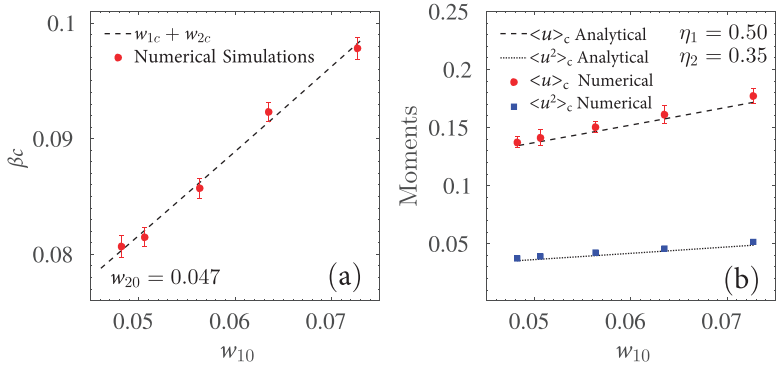

Figure 16. (a) Comparison for the KdV soliton gas shock tube problem. The equilibrium total density $\beta_c = w_{1c} + w_{2c}$ in the interaction region as a function of the density w_{10} of the 'left' gas. The density of the 'right' gas $w_{20} = 0.047$; (b) the moments $\langle u\rangle_c, \langle u^2\rangle_c$ of the random wave field in the interaction region. Reproduced from [75]. Copyright © EPLA, 2016. All rights reserved.

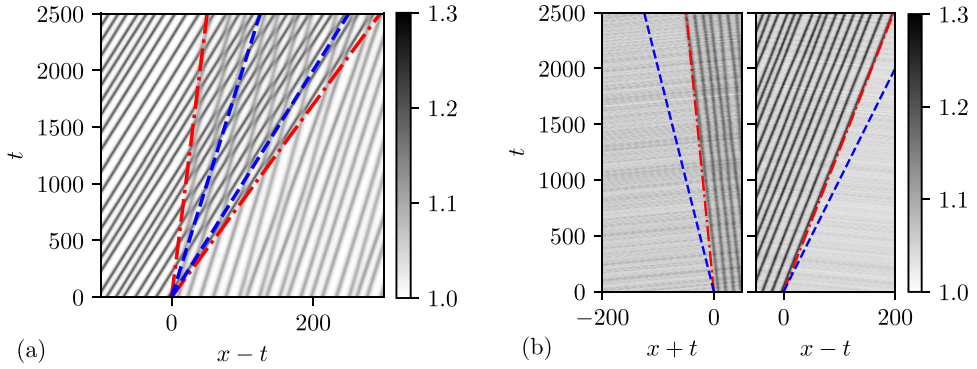

Figure 17. Spatiotemporal plots of the field $\rho(x,t)$ for one realization of the anisotropic soliton gas collision (the resonant NLS soliton gas). Trajectories of the solitons appear in solid lines. Red dash-dotted lines correspond to the trajectories of the contact discontinuities: $x = z_1 t$, $x = z_2 t$, cf (5.4), and blue dashed lines to the free soliton trajectories: $x = s_{01} t$, $x = s_{02} t$. (a) Overtaking collisions $(\zeta_1, \zeta_2) = (1.05, 1.10)$, cf initial condition (i) in table 1. (b) Head-on collisions $(\zeta_1, \zeta_2) = (-1.05, 1.10)$, cf initial condition (ii) in table 1. Reprinted figure with permission from [37], Copyright (2021) by the American Physical Society.

are collected in table 1. The numerical evaluation of the ensemble average $\langle\rho\rangle$ involves averaging over 100 realisations. As expected, the solution is composed of four plateaus, where regions II and III contain at least two distinct soliton components and are the regions of interactions. The comparison shows an excellent agreement confirming the efficacy of the developed spectral kinetic theory. Note that in figure 18 the discontinuities in $\langle\rho(x,t)\rangle$ have a finite slope which is an artefact of the statistical averaging procedure detailed in [37].

J. Stat. Mech. (2021) 114001

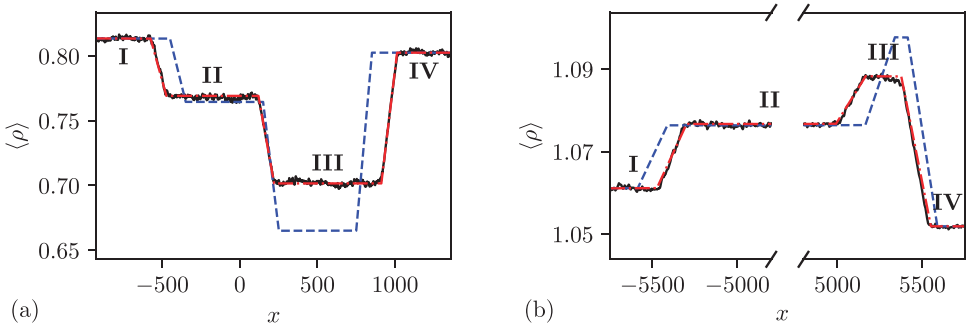

Figure 18. Comparison between the ensemble average $\langle \rho(x,t) \rangle$ obtained by averaging over 100 realisations of the numerical solution of the three-component soliton gas shock tube problem (solid line) for bidirectional dispersive hydrodynamics and the analytical solution obtained via the corresponding spectral Riemann problem (dash-dotted line). The dashed line corresponds to the average field density in the artificial soliton gas composed of non-interacting solitons with the spectral distribution given by (5.6). (a) Defocusing NLS soliton gas at $t = 2000$, case (iii) table 1. (b) Resonant NLS soliton gas at $t = 5000$, case (iv) in table 1. Reprinted figure with permission from [37], Copyright (2021) by the American Physical Society.

Table 1. Spectral Riemann problem data used in the numerical simulations for figures 17 and 18.

	Spectral parameters	Left boundary condition	Right boundary condition
(i)	$(\zeta_1 = 1.05, \zeta_2 \in [1.06, 1.10])$	$\boldsymbol{w}^{\mathrm{L}} = (0, 6.6) \times 10^{-2}$	$\boldsymbol{w}^{\mathrm{R}} = (6.6, 0) \times 10^{-2}$
(ii)	$(\zeta_1 = -1.05, \zeta_2 \in [1.06, 1.1])$	$\boldsymbol{w}^{\mathrm{L}} = (0, 6.6) \times 10^{-2}$	$\boldsymbol{w}^{\mathrm{R}} = (6.6, 0) \times 10^{-2}$
(iii)	$(\zeta_1, \zeta_2, \zeta_3) = (-0.2, 0.1, 0.4)$	$\boldsymbol{w}^{\mathrm{L}} = (2.5, 0, 7.5) \times 10^{-2}$	$\boldsymbol{w}^{\mathrm{R}} = (5, 5, 0) \times 10^{-2}$
(iv)	$(\zeta_1, \zeta_2, \zeta_3) = (-1.1, 1.05, 1.1)$	$\boldsymbol{w}^{\mathrm{L}} = (1.6, 0, 5) \times 10^{-2}$	$\boldsymbol{w}^{\mathrm{R}} = (3.3, 3.3, 0) \times 10^{-2}$

6. Summary and outlook

In this article, we have reviewed the results on the spectral theory of soliton gases obtained by the author and his collaborators over the last two decades, although many of the developments are relatively recent. The theory is inspired by Zakharov's 1971 paper [28], where the ideas of the spectral kinetic description of a weakly interacting, rarefied soliton gas for the KdV equation were introduced for the first time. It has transpired later that the perspective of dispersive hydrodynamics, particularly the Whitham theory of modulated spectral finite-gap solutions provides an appealing mathematical framework for the generalisation of Zakharov's kinetic equation to the case of strongly interacting, dense soliton gas [32, 36, 38]. It has also been realised that soliton gas represents a ubiquitous physical phenomenon, a kind of strongly nonlinear turbulent wave motion that can observed in the environmental conditions [21, 39] and realised in laboratory experiments [23, 24]. The recently discovered connections of the soliton gas dynamics and

J. Stat. Mech. (2021) 114001

statistics with the topical areas of modulational instability and rogue wave formation [10, 25, 26] have provided the soliton gas research with further relevance.

One can envisage many important and interesting mathematical and physical problems arising in connection with the developed spectral theory of soliton gas. Probably the most pertinent one is the determination of the statistical parameters of the integrable turbulence associated with a given spectral DOS of a soliton gas, in particular, obtaining the probability density function, the power spectrum and the autocorrelation function of the turbulent nonlinear wave field. This would provide a theoretical explanation of the intriguing statistical properties of integrable turbulence observed in the numerical simulations and physical experiments [8, 10, 25, 27, 145]. Further, the spectral hydrodynamics/kinetics of non-equilibrium soliton gas could provide the means for the manipulation of the integrable turbulence statistics, and therefore, control of the rogue wave emergence. in physical systems described at leading order by integrable equations.

Another pertinent question is the generation of soliton gas out of 'non-gas' initial or boundary conditions. This problem is important from both the theoretical and experimental points of view. One possibility is to use the spontaneous 'soliton fission' mechanism [31, 64] inspired by the original Zabusky–Kruskal work [12] and employed in the experiments on the creation of a shallow water bidirectional anisotropic soliton gas in [23]. In modulationally unstable media, a semiclassical scenario of the transition to integrable soliton turbulence via a chain of topological bifurcations of the finite-gap spectra was theoretically proposed in [63] and to some extent realised in an optics experiment reported in [54]. Of particular relevance is the IST based approach to the controlled (as opposed to the spontaneous) experimental realisation of soliton gas developed in [24]. This approach enables the generation of a soliton gas with a prescribed DOS, which is crucial for the verification and utilisation of the spectral kinetic theory.

Yet another prospective area of the further development of the soliton gas theory is the interaction of soliton gas with external potentials, either 'static' as in the soliton gas in trapped BECs [48, 146] or dynamic, as in the recently proposed hydrodynamic soliton tunnelling framework [17, 110, 147]. Related to this, the development of the theory of soliton gas in perturbed integrable systems is of particular importance for applications where the higher order, non-integrable corrections to the core integrable dynamics are always present and generally result in the slow evolution of the DOS, that is distinct from the spectral kinetic transport by the continuity equation, see [24].

Finally, the recently emerged intriguing parallels between the spectral theory of soliton gas and GHD [57, 78] provide yet another avenue for the novel cross-disciplinary research that could be of significant benefit for both fields of research.

Acknowledgments

This work was partially supported by EPSRC Grant EP/R00515X/2. I would like to express my gratitude to the late A L Krylov, who had suggested this topic to me many years ago. I am grateful to M Hoefer, A Kamchatnov, M Pavlov, S Randoux, P Suret and A Tovbis for the collaboration and many stimulating discussions over the years. I would like to thank T Congy and G Roberti for their more recent contributions and

J. Stat. Mech. (2021) 114001

for the help with preparing the figures. Special thanks to T Bonnemain for reading the manuscript and providing a number of helpful comments.

Appendix A. Nonlinear dispersion relations for the finite-gap solutions of the focusing NLS equation

We introduce the fundamental wavenumber and frequency vectors: $\boldsymbol{k} = (k_1, \cdots, k_N, \tilde{k}_1, \cdots, \tilde{k}_N)$ and $\boldsymbol{\omega} = (\omega_1, \cdots, \omega_N, \tilde{\omega}_1, \cdots, \tilde{\omega}_N)$, respectively, whose components are defined as follows

$$k_j = -\oint_{\alpha_j} \mathrm{d}p, \qquad \omega_j = \oint_{\alpha_j} \mathrm{d}q, \quad j = 1, \cdots, N, \tag{A.1}$$

$$\tilde{k}_j = \oint_{\beta_j} \mathrm{d}p, \qquad \tilde{\omega}_j = -\oint_{\beta_j} \mathrm{d}q, \quad j = 1, \cdots, N. \tag{A.2}$$

Here, $\mathrm{d}p(z)$ and $\mathrm{d}q(z)$ are the meromorphic quasimomentum and quasienergy differentials with the only poles at $z = \infty$ on both sheets of the Riemann surface (3.57) defined by (see e.g. [122, 124])

$$\mathrm{d}p = 1 + \mathcal{O}(z^{-2}), \qquad \mathrm{d}q = 4z + \mathcal{O}(z^{-2}) \tag{A.3}$$

near $z = \infty$ on the main sheet, respectively, and the normalisation conditions requiring that all of the periods of $\mathrm{d}p, \mathrm{d}q$ are real (real normalised differentials). The homology basis α_j, β_j is defined in section 3.3.1 (see figure 11). The signs of integrals in (A.1) and (A.2) will be opposite if we replace j by $-j$.

The wavenumbers and frequencies are symmetrically extended to negative indices by $k_{-j} = k_j, \omega_{-j} = \omega_j$, $j = 1, \cdots, N$, and similar equations for the 'tilded' quantities. They also satisfy the corresponding equations (A.1) and (A.2), but the signs of integrals in (A.1) and (A.2) will be opposite when we replace j by $-j$.

The proof that k_j, $\tilde{k}_j$, ω, $\tilde{\omega}$ defined by (A.1) and (A.2) are indeed the wavenumbers and frequencies of the finite-gap focusing NLS solution associated with the spectral surface $\mathcal{R}$ of (3.57) can be found in [38]. It was then shown in [38] that for the wavenumbers and frequencies (A.1) and (A.2) associated with the finite-gap focusing NLS solution the nonlinear dispersion relations are given by

$$\begin{aligned}
&\tilde{k}_j + \sum_{|m|=1}^{N} k_m \oint_{\beta_m} \frac{P_j(\zeta)\mathrm{d}\zeta}{R(\zeta)} = -\frac{1}{2}\oint_{\tilde{\gamma}} \frac{\zeta P_j(\zeta)\mathrm{d}\zeta}{R(\zeta)}, \\
&\tilde{\omega}_j + \sum_{|m|=1}^{N} \omega_m \oint_{\beta_m} \frac{P_j(\zeta)\mathrm{d}\zeta}{R(\zeta)} = -\oint_{\tilde{\gamma}} \frac{\zeta^2 P_j(\zeta)\mathrm{d}\zeta}{R(\zeta)}, \\
&|j| = 1, \cdots, N,
\end{aligned} \tag{A.4}$$

where $\tilde{\gamma}$ is a large clockwise oriented contour containing Γ, and $P_j(z)$ and w_j are defined in (3.62) and (3.63) Taking the real and imaginary parts of (A.4) and using the residues

J. Stat. Mech. (2021) 114001

in the right-hand side, we obtain separate systems for the solitonic components k_m, ω_m and the carrier components $\tilde{k}_m$, $\tilde{\omega}_m$.

References

[1] Nazarenko S 2011 *Wave Turbulence* (*Lecture Notes in Physics*) 1st edn (Berlin: Springer)
[2] Zakharov V E 1965 Weak turbulence in media with a decay spectrum *J. Appl. Mech. Tech. Phys.* **6** 22–4
[3] Zakharov V E 2009 Turbulence in integrable systems *Stud. Appl. Math.* **122** 219–34
[4] Novikov S P, Manakov S, Pitaevskii L P and Zakharov V 1984 *Theory of Solitons: The Inverse Scattering Method* (*Monographs in Contemporary Mathematics*) (Berlin: Springer)
[5] Belokolos E D, Bobenko A I, Enolski V Z, Its A R and Matveev V B 1994 *Algebro-Geometric Approach to Nonlinear Integrable Equations* (New York: Springer)
[6] Osborne A 2010 *Nonlinear Ocean Waves and the Inverse Scattering Transform* vol 97 (New York: Academic)
[7] Calogero F and Zakharov V E (ed) 1991 *What Is Integrability?* (*Springer Series in Nonlinear Dynamics*) 1st edn (Berlin: Springer)
[8] Agafontsev D S and Zakharov V E 2015 Integrable turbulence and formation of rogue waves *Nonlinearity* **28** 2791
[9] Agafontsev D S and Zakharov V E 2016 Integrable turbulence generated from modulational instability of cnoidal waves *Nonlinearity* **29** 3551
[10] Kraych A E, Agafontsev D, Randoux S and Suret P 2019 Statistical properties of the nonlinear stage of modulation instability in fiber optics *Phys. Rev. Lett.* **123** 093902
[11] Russell J S 1845 Report on waves *Technical Report* (London: British Association for the Advancement of Science)
[12] Zabusky N J and Kruskal M D 1965 Interaction of 'solitons' in a collisionless plasma and the recurrence of initial states *Phys. Rev. Lett.* **15** 240
[13] Ablowitz M J, Kaup D J, Newell A C and Segur H 1974 The inverse scattering transform-Fourier analysis for nonlinear problems *Stud. Appl. Math.* **53** 249–315
[14] Newell A 1985 *Solitons in Mathematics and Physics* (*CBMS-NSF Regional Conf. Series in Applied Mathematics*) (Philadelphia, PA: SIAM)
[15] Remoissenet M 2013 *Waves Called Solitons. Concepts and Experiments* 4th edn (Berlin: Springer)
[16] Gardner C S, Greene J M, Kruskal M D and Miura R M 1967 Method for solving the Korteweg–deVries equation *Phys. Rev. Lett.* **19** 1095–7
[17] Maiden M D, Anderson D V, Franco N A, El G A and Hoefer M A 2018 Solitonic dispersive hydrodynamics: theory and observation *Phys. Rev. Lett.* **120** 144101
[18] El G A and Hoefer M A 2016 Dispersive shock waves and modulation theory *Physica* D **333** 11–65
[19] Zakharov V, Pushkarev A, Shvets V and Yan'kov V V 1988 Soliton turbulence *JETP Lett.* **48** 83–7
[20] Kachulin D, Dyachenko A and Zakharov V 2020 Soliton turbulence in approximate and exact models for deep water waves *Fluids* **5** 67
[21] Costa A, Osborne A R, Resio D T, Alessio S, Chrivì E, Saggese E, Bellomo K and Long C E 2014 Soliton turbulence in shallow water ocean surface waves *Phys. Rev. Lett.* **113** 108501
[22] Slunyaev A 2021 Persistence of hydrodynamic envelope solitons: detection and rogue wave occurrence *Phys. Fluids* **33** 036606
[23] Redor I, Barthélemy E, Michallet H, Onorato M and Mordant N 2019 Experimental evidence of a hydrodynamic soliton gas *Phys. Rev. Lett.* **122** 214502
[24] Suret P *et al* 2020 Nonlinear spectral synthesis of soliton gas in deep-water surface gravity waves *Phys. Rev. Lett.* **125** 264101
[25] Gelash A, Agafontsev D, Zakharov V, El G, Randoux S and Suret P 2019 Bound state soliton gas dynamics underlying the spontaneous modulational instability *Phys. Rev. Lett.* **123** 234102
[26] Gelash A A and Agafontsev D S 2018 Strongly interacting soliton gas and formation of rogue waves *Phys. Rev.* E **98** 042210-1-042210-12
[27] Agafontsev D S and Gelash A A 2021 Rogue waves with rational profiles in unstable condensate and its solitonic model *Front. Phys.* **9** 610896
[28] Zakharov V 1971 Kinetic equation for solitons *J. Exp. Theor. Phys.* **33** 538–41
[29] Lowman N K and Hoefer M A 2013 Dispersive shock waves in viscously deformable media *J. Fluid Mech.* **718** 524–57

J. Stat. Mech. (2021) 114001

[30] Lowman N K, Hoefer M A and El G A 2014 Interactions of large amplitude solitary waves in viscous fluid conduits *J. Fluid Mech.* **750** 372–84
[31] Maiden M D, Franco N A, Webb E G, El G A and Hoefer M A 2020 Solitary wave fission of a large disturbance in a viscous fluid conduit *J. Fluid Mech.* **883** A10
[32] El G A 2003 The thermodynamic limit of the Whitham equations *Phys. Lett.* A **311** 374–83
[33] Whitham G B 1999 *Linear and Nonlinear Waves* (New York: Wiley)
[34] El G A, Krylov A L, Molchanov S A and Venakides S 2001 Soliton turbulence as a thermodynamic limit of stochastic soliton lattices *Physica* D **152–153** 653–64
[35] Flaschka H, Forest M G and McLaughlin D W 1980 Multiphase averaging and the inverse spectral solution of the Korteweg–de Vries equation *Commun. Pure Appl. Math.* **33** 739–84
[36] El G A and Kamchatnov A M 2005 Kinetic equation for a dense soliton gas *Phys. Rev. Lett.* **95** 204101
[37] Congy T, El G and Roberti G 2021 Soliton gas in bidirectional dispersive hydrodynamics *Phys. Rev.* E **103** 042201
[38] El G and Tovbis A 2020 Spectral theory of soliton and breather gases for the focusing nonlinear Schrödinger equation *Phys. Rev.* E **101** 052207
[39] Osborne A R, Resio D T, Costa A, Ponce de León S and Chirivì E 2019 Highly nonlinear wind waves in Currituck sound: dense breather turbulence in random ocean waves *Ocean Dynam.* **69** 187–219
[40] Roberti G, El G, Tovbis A, Copie F, Suret P and Randoux S 2021 Numerical spectral synthesis of breather gas for the focusing nonlinear Schrödinger equation *Phys. Rev.* E **103** 042205
[41] El G A, Kamchatnov A M, Pavlov M V and Zykov S A 2011 Kinetic equation for a soliton gas and its hydrodynamic reductions *J. Nonlinear Sci.* **21** 151–91
[42] Pavlov M V, Taranov V B and El G A 2012 Generalized hydrodynamic reductions of the kinetic equation for a soliton gas *Theor. Math. Phys.* **171** 675–82
[43] Bulchandani V B 2017 On classical integrability of the hydrodynamics of quantum integrable systems *J. Phys. A: Math. Theor.* **50** 435203
[44] Kuijlaars A and Tovbis A 2021 On minimal energy solutions to certain classes of integral equations related to soliton gases for integrable systems *Nonlinearity* **34** 7227
[45] Meiss J D and Horton W Jr 1982 Drift-wave turbulence from a soliton gas *Phys. Rev. Lett.* **48** 1362
[46] Schwache A and Mitschke F 1997 Properties of an optical soliton gas *Phys. Rev.* E **55** 7720–5
[47] Fratalocchi A, Armaroli A and Trillo S 2011 Time-reversal focusing of an expanding soliton gas in disordered replicas *Phys. Rev.* A **83** 053846
[48] Schmidt M, Erne S, Nowak B, Sexty D and Gasenzer T 2012 Non-thermal fixed points and solitons in a one-dimensional Bose gas *New J. Phys.* **14** 075005
[49] Turitsyna E G *et al* 2013 The laminar–turbulent transition in a fibre laser *Nat. Photon.* **7** 783–6
[50] Dutykh D and Pelinovsky E 2014 Numerical simulation of a solitonic gas in KdV and KdV-BBM equations *Phys. Lett.* A **378** 3102–10
[51] Soto-Crespo J M, Devine N and Akhmediev N 2016 Integrable turbulence and rogue waves: breathers or solitons? *Phys. Rev. Lett.* **116** 103901
[52] Giovanangeli J-P, Kharif C and Stepanyants Y A 2018 Soliton spectra of random water waves in shallow basins *Math. Modell. Nat. Phenom.* **13** 40
[53] Girotti M, Grava T, Jenkins R and McLaughlin K D T-R 2021 Rigorous asymptotics of a KdV soliton gas *Commun. Math. Phys.* **384** 733–84
[54] Marcucci G, Pierangeli D, Agranat A J, Lee R-K, DelRe E and Conti C 2019 Topological control of extreme waves *Nat. Commun.* **10** 5090
[55] Castro-Alvaredo O A, Doyon B and Yoshimura T 2016 Emergent hydrodynamics in integrable quantum systems out of equilibrium *Phys. Rev.* X **6** 041065
[56] Bertini B, Collura M, De Nardis J and Fagotti M 2016 Transport in out-of-equilibrium XXZ chains: exact profiles of charges and currents *Phys. Rev. Lett.* **117** 207201
[57] Doyon B 2020 Lecture notes on generalised hydrodynamics *SciPost Phys. Lect. Notes* 18
[58] Biondini G, El G A, Hoefer M A and Miller P D 2016 Dispersive hydrodynamics: preface *Physica* D **333** 1–5
[59] Kaup D J 1975 A higher-order water-wave equation and the method for solving it *Prog. Theor. Phys.* **54** 396–408
[60] Kamchatnov A M 2000 *Nonlinear Periodic Waves and Their Modulations: An Introductory Course* (Singapore: World Scientific)
[61] Abanov A G, Bettelheim E and Wiegmann P 2009 Integrable hydrodynamics of Calogero–Sutherland model: bidirectional Benjamin–Ono equation *J. Phys. A: Math. Theor.* **42** 135201

J. Stat. Mech. (2021) 114001

[62] Gurevich A V, Zybkin K P and Él' G A 1999 Development of stochastic oscillations in a one-dimensional dynamical system described by the Korteweg–de Vries equation *J. Exp. Theor. Phys.* **88** 182–95
[63] El G A, Khamis E G and Tovbis A 2016 Dam break problem for the focusing nonlinear Schrödinger equation and the generation of rogue waves *Nonlinearity* **29** 2798–836
[64] Trillo S, Deng G, Biondini G, Klein M, Clauss G F, Chabchoub A and Onorato M 2016 Experimental observation and theoretical description of multisoliton fission in shallow water *Phys. Rev. Lett.* **117** 144102
[65] Trillo S, Klein M, Clauss G F and Onorato M 2016 Observation of dispersive shock waves developing from initial depressions in shallow water *Physica* D **333** 276–84
[66] Tsarev S P 1985 Poisson brackets and one-dimensional Hamiltonian systems of hydrodynamic type *Sov. Math. - Dokl.* **31** 488–91
[67] Dubrovin B A and Novikov S P 1989 Hydrodynamics of weakly deformed soliton lattices. Differential geometry and Hamiltonian theory *Russ. Math. Surv.* **44** 35–124
[68] Lax P D and Levermore C D 1983 The small dispersion limit of the korteweg–de vries equation. ii *Commun. Pure Appl. Math.* **36** 571–93
[69] Lax P D 1991 The zero dispersion limit, a deterministic analogue of turbulence *Commun. Pure Appl. Math.* **44** 1047–56
[70] Monin A and Yaglom A 2013 *Statistical Fluid Mechanics: Mechanics of Turbulence* vol 1, 2 1st edn (New York: Dover)
[71] Venakides S 1989 The continuum limit of theta functions *Commun. Pure Appl. Math.* **42** 711–28
[72] Drazin P and Johnson R 1989 *Solitons: An Introduction* 2nd edn (Cambridge: Cambridge University Press)
[73] Lax P D 1968 Integrals of nonlinear equations of evolution and solitary waves *Commun. Pure Appl. Math.* **21** 467–90
[74] Pelinovsky E N, Shurgalina E G, Sergeeva A V, Talipova T G, El G A and Grimshaw R H J 2013 Two-soliton interaction as an elementary act of soliton turbulence in integrable systems *Phys. Lett.* A **377** 272–5
[75] Carbone F, Dutykh D and El G A 2016 Macroscopic dynamics of incoherent soliton ensembles: soliton gas kinetics and direct numerical modelling *Europhys. Lett.* **113** 30003
[76] Doyon B, Spohn H and Yoshimura T 2018 A geometric viewpoint on generalized hydrodynamics *Nucl. Phys.* B **926** 570–83
[77] Doyon B, Yoshimura T and Caux J-S 2018 Soliton gases and generalized hydrodynamics *Phys. Rev. Lett.* **120** 045301
[78] Spohn H 2021 Hydrodynamic equations for the Toda lattice (arXiv:2101.06528)
[79] Yang J 2010 *Nonlinear Waves in Integrable and Nonintegrable Systems* (Philadelphia, PA: SIAM)
[80] Pashaev O K and Lee J-H 2002 Resonance solitons as black holes in Madelung fluid *Mod. Phys. Lett.* A **17** 1601–19
[81] Lee J-H and Pashaev O K 2007 Solitons of the resonant nonlinear Schrödinger equation with nontrivial boundary conditions: Hirota bilinear method *Theor. Math. Phys.* **152** 991–1003
[82] Gurevich A V and Krylov A L 1988 The origin of a nondissipative shock wave *Dokl. Math.* **33** 603–5
[83] Zakharov V E and Shabat A B 1973 Interaction between solitons in a stable medium *J. Exp. Theor. Phys.* **37** 823–8
[84] Zakharov V E and Shabat A B 1972 Exact theory of two-dimensional self-focusing and one-dimensional self-modulation of waves in nonlinear media *J. Exp. Theor. Phys.* **34** 62–9
[85] Ablowitz M J and Segur H 1981 *Solitons and Inverse Scattering Transform* (Philadelphia, PA: SIAM)
[86] Faddeev L and Takhtajan L 2007 *Hamiltonian Methods in the Theory of Solitons* (*Classics in Mathematics*) 1st edn (Berlin: Springer)
[87] Kotani S 2008 KdV flow on generalised reflectionless potentials *J. Math. Phys., Anal. Geom.* **4** 490–528
[88] Dyachenko S, Zakharov D and Zakharov V 2016 Primitive potentials and bounded solutions of the KdV equation *Physica* D **333** 148–56
[89] Miura R M 1968 Korteweg–de Vries equation and generalizations. I. A remarkable explicit nonlinear transformation *J. Math. Phys.* **9** 1202–4
[90] Ablowitz M J 2011 *Nonlinear Dispersive Waves: Asymptotic Analysis and Solitons* (*Cambridge Texts in Applied Mathematics*) 1st edn (Cambridge: Cambridge University Press)
[91] El G A 2016 Critical density of a soliton gas *Chaos* **26** 023105
[92] Shurgalina E G and Pelinovsky E N 2016 Nonlinear dynamics of a soliton gas: modified Korteweg–de Vries equation framework *Phys. Lett.* A **380** 2049–53
[93] Whitham G B 1965 Non-linear dispersive waves *Proc. R. Soc.* A **283** 238–61
[94] Novikov S P 1974 The periodic problem for the Korteweg–de Vries equation *Funct. Anal. Appl.* **8** 236–46
[95] Lax P D 1975 Periodic solutions of the KdV equation *Commun. Pure Appl. Math.* **28** 141–88

J. Stat. Mech. (2021) 114001

[96] Its A R and Matveev V B 1975 Schrödinger operators with finite-gap spectrum and n-soliton solutions of the Korteweg–de Vries equation *Theor. Math. Phys.* **23** 51–68
[97] Dubrovin B A 1975 Periodic problem for the Korteweg–de Vries equation in the class of finite band potentials *Funct. Anal. Appl.* **9** 41–51
[98] Matveev V B 2008 30 years of finite-gap integration theory *Phil. Trans. R. Soc.* A **366** 837–75
[99] Pastur L and Figotin A 1992 *Spectra of Random and Almost Periodic Potentials* (Berlin: Springer)
[100] Abramowitz M and Stegun I 1972 *Handbook of Mathematical Functions with Formulas, Graphs, and Mathematical Tables* (New York: Dover)
[101] Osborne A R 1995 Solitons in the periodic Korteweg–de Vries equation, the FTHETA-function representation, and the analysis of nonlinear, stochastic wave trains *Phys. Rev.* E **52** 1105–22
[102] Congy T, El G A and Hoefer M A 2019 Interaction of linear modulated waves and unsteady dispersive hydrodynamic states with application to shallow water waves *J. Fluid Mech.* **875** 1145–74
[103] Weinstein M I and Keller J B 1987 Asymptotic behavior of stability regions for Hill's equation *SIAM J. Appl. Math.* **47** 941–58
[104] Osborne A R 1993 Behavior of solitons in random-function solutions of the periodic Korteweg–de Vries equation *Phys. Rev. Lett.* **71** 3115
[105] Bertola M, El G A and Tovbis A 2016 Rogue waves in multiphase solutions of the focusing nonlinear Schrödinger equation *Proc. R. Soc.* A **472** 20160340
[106] Osborne A 2019 Breather turbulence: exact spectral and stochastic solutions of the nonlinear schrödinger equation *Fluids* **4** 72
[107] Sinai Y 1977 *Introduction to Ergodic Theory* (Princeton, NJ: Princeton University Press)
[108] Dubrovin B A 1981 Theta functions and non-linear equations *Russ. Math. Surv.* **36** 11–92
[109] Lifshits I, Gredeskul S and Pastur L 1988 *Introduction to the Theory of Disordered Systems* (New York: Wiley)
[110] Sande K v d, El G A and Hoefer M A 2021 Dynamic soliton-mean flow interaction with nonconvex flux *J. Fluid Mech.* **928** A21
[111] Feller W 1968 *An Introduction to Probability Theory* vol 1 3rd edn (New York: Wiley)
[112] Tajiri M and Watanabe Y 1998 Breather solutions to the focusing nonlinear Schrödinger equation *Phys. Rev.* E **57** 3510–9
[113] Slunyaev A, Kharif C, Pelinovsky E and Talipova T 2002 Nonlinear wave focusing on water of finite depth *Physica* D **173** 77–96
[114] Gelash A A 2018 Formation of rogue waves from a locally perturbed condensate *Phys. Rev.* E **97** 022208-1–8
[115] Randoux S, Suret P and El G 2016 Inverse scattering transform analysis of rogue waves using local periodization procedure *Sci. Rep.* **6** 29238
[116] Akhmediev N, Ankiewicz A and Soto-Crespo J M 2009 Rogue waves and rational solutions of the nonlinear Schrödinger equation *Phys. Rev.* E **80**
[117] KharifC, PelinovskyÂ E N and Slunyaev A 2009 *Rogue Waves in the Ocean* (*Advances in Geophysical and Environmental Mechanics and Mathematics*) 1st edn (Berlin: Springer)
[118] Onorato M, Residori S, Bortolozzo U, Montina A and Arecchi F T 2013 Rogue waves and their generating mechanisms in different physical contexts *Phys. Rep.* **528** 47–89
[119] Onorato M, Residori S and Baronio F (ed) 2016 *Rogue and Shock Waves in Nonlinear Dispersive Media* (*Lecture Notes in Physics*) vol 926 (Berlin: Springer)
[120] Its A R and Kotlyarov V P 1976 Explicit formulas for solutions of the nonlinear Schrödinger equation *Dopov. Acad. Nauk Ukr. RSR* A **11** 965–8
[121] Chen J, Pelinovsky D E and White R E 2019 Rogue waves on the double-periodic background in the focusing nonlinear Schrödinger equation *Phys. Rev.* E **100** 052219
[122] Forest M G and Lee J-E 1986 Geometry and modulation theory for the periodic nonlinear Schrodinger equation *Oscillation Theory, Computation, and Methods of Compensated Compactness* ed C Dafermos, J L Ericksen, D Kinderlehrer and M Slemrod (New York: Springer) pp 35–69
[123] Tracy E R and Chen H H 1988 Nonlinear self-modulation: an exactly solvable model *Phys. Rev.* A **37** 815
[124] Tovbis A and El G A 2016 Semiclassical limit of the focusing NLS: Whitham equations and the Riemann–Hilbert Problem approach *Physica* D **333** 171–84
[125] Li S and Biondini G 2018 Soliton interactions and degenerate soliton complexes for the focusing nonlinear Schrödinger equation with nonzero background *Eur. Phys. J. Plus* **133** 400
[126] Tricomi F G 1951 On the finite Hilbert transformation *Q. J. Math.* **2** 199–211
[127] Okada S and Elliott D 1991 The finite Hilbert transform in $\mathscr{L}^2$ *Math. Nachr.* **153** 43–56
[128] Benjamin T B and Feir J E 1967 The disintegration of wave trains on deep water part 1. Theory *J. Fluid Mech.* **27** 417–30

J. Stat. Mech. (2021) 114001

[129] Zakharov V E and Ostrovsky L A 2009 Modulation instability: the beginning *Physica* D **238** 540–8
[130] Medenjak M, Policastro G and Yoshimura T 2021 $T\bar{T}$-deformed conformal field theories out of equilibrium *Phys. Rev. Lett.* **126** 121601
[131] Bento M C, Bertolami O and Sen A A 2002 Generalized Chaplygin gas, accelerated expansion, and dark-energy–matter unification *Phys. Rev.* D **66** 043507
[132] Born M and Infeld L 1934 Foundations of the new field theory *Proc. R. Soc.* A **144** 425–51
[133] Lax P D 1973 *Hyperbolic Systems of Conservation Laws and the Mathematical Theory of Shock Waves* (Philadelphia, PA: SIAM)
[134] Tsarëv S P 1991 The geometry of Hamiltonian systems of hydrodynamic type. the generalized hodograph method *Math. USSR-Izvestiya* **37** 397–419
[135] Pavlov M V 1987 Hamiltonian formalism of weakly nonlinear hydrodynamic systems *Theor. Math. Phys.* **73** 1242–5
[136] Ferapontov E V 1991 Integration of weakly nonlinear hydrodynamic systems in Riemann invariants *Phys. Lett.* A **158** 7
[137] Pavlov M V 1987 Nonlinear Schrödinger equation and the Bogolyubov–Whitham method of averaging *Theor. Math. Phys.* **71** 584–8
[138] Landau L and Lifshitz E 1987 *Fluid Mechanics* 2nd edn (Portsmouth, NH: Heinemann)
[139] Rozhdestvenskii B and Janenko N 1983 *Systems of Quasilinear Equations and Their Applications to Gas Dynamics* (Providence, RI: American Mathematical Society)
[140] Doyon B and Spohn H 2017 Dynamics of hard rods with initial domain wall state *J. Stat. Mech.* 073210
[141] Kuniba A, Misguich G and Pasquier V 2020 Generalized hydrodynamics in box-ball system *J. Phys. A: Math. Theor.* **53** 404001
[142] Croydon D A and Sasada M 2021 Generalized hydrodynamic limit for the box-ball system *Commun. Math. Phys.* **383** 427
[143] Alba V, Bertini B, Fagotti M, Piroli L and Ruggiero P 2021 Generalized-hydrodynamic approach to inhomogeneous quenches: correlations, entanglement and quantum effects (arXiv:2104.00656)
[144] Gurevich A V and Pitaevskii L P 1974 Nonstationary structure of a collisionless shock wave *Sov. Phys. - JETP* **38** 291–7
Gurevich A V and Pitaevskii L P 1973 *Zh. Eksp. Teor. Fiz.* **65** 590–604
[145] Agafontsev D S, Randoux S and Suret P 2021 Extreme rogue wave generation from narrowband partially coherent waves *Phys. Rev.* E **103** 032209
[146] Hamner C, Zhang Y, Chang J J, Zhang C and Engels P 2013 Phase winding a two-component Bose–Einstein condensate in an elongated trap: experimental observation of moving magnetic orders and dark-bright solitons *Phys. Rev. Lett.* **111** 264101
[147] Sprenger P, Hoefer M A and El G A 2018 Hydrodynamic optical soliton tunneling *Phys. Rev.* E **97** 032218

J. Stat. Mech. (2021) 114001